SMAC MIMETICS SENSITIZE HIV-INFECTED CELLS TO MG1-MEDIATED DEATH

BENGISU MOLYER YILDIRIR

Thesis submitted to the University of Ottawa in partial fulfillment of the requirements for the degree of Doctor of Philosophy in Microbiology and Immunology.

Department of Biochemistry, Microbiology and Immunology

Faculty of Medicine

University of Ottawa

Thesis supervisor: Dr. Jonathan B. Angel

Declaration

I, Bengisu Molyer Yildirir, confirm that the work presented in this thesis is my own. Where information has been derived from other sources, I confirm that this has been indicated in the thesis.

Date: September 9, 2024

Abstract

The main challenge in finding an HIV cure is the targeting and elimination of the HIV reservoir of latently infected CD4+ T-cells and persistently infected macrophages. While these cells are phenotypically indistinguishable from their healthy counterparts, they display impairments in their interferon (IFN) signaling. This makes them susceptible to killing by the interferon sensitive oncolytic rhabdovirus virus MG1. Although MG1 has affinity for latently/persistently HIV-infected cells, its effectiveness and selectivity can be enhanced.

To enhance killing, MG1 was combined with the pro-apoptotic molecules, second mitochondria derived activator of caspases (SMAC) mimetic (AEG 40730, LCL-161, birinapant) to kill the latently HIV-infected lymphocytic cell line J1.1 and myelocytic cell line OM10.1. In HIV-infected cell lines, it was shown that the order of administration of MG1 and SMAC mimetics is important to optimize killing. Moreover, increased caspase-3/7 and caspase-1 expression followed cell death, and cell death could not be blocked by the pan-caspase inhibitor ZVAD-fmk or the necroptosis inhibitor necrostatin1-s, alone or in combination, indicating that cell death does not occur via a single pathway. SMAC mimetics have shown to activate the non-canonical NFκB pathway and cause TNFα-dependent or independent death in different models of HIV-infected cells. Here, it was also shown that although there was increased activation of the non-canonical NFκB pathway, this did not result in TNFα production, and no straightforward relationship could be found between TNFα and cell death.

In HIV-infected monocyte derived macrophages, there was a significant increase in cell death when MG1 was combined with SMAC mimetics compared to either treatment alone. This increase in cell death was also accompanied by a decrease in proviral HIV DNA. MG1 infection or combination treatment with MG1 and SMAC mimetics resulted in TNFα production, which

may be one of the contributors of increased cell death. It was previously shown that VSVΔ51 does not kill latently HIV-infected cells. To see if combination treatment would sensitize cells to VSVΔ51 mediated cell death, OM10.1 cells and HIV-infected macrophages were treated with the combination of VSVΔ51 and SMAC mimetics. This resulted in significantly increased cell death compared to either treatment alone, and was accompanied by a decrease in proviral HIV DNA.

To increase MG1's specificity to target cells of HIV, MG1 plasmids containing full length or modified versions of HIV envelope gp160 were produced. These pseudotyped viral constructs would have restricted tropism and would only be expected to infect the target cells of HIV. Unfortunately, these viral constructs were unable to be rescued and the clones require further optimization.

This is the first study to employ combination therapy with oncolytic virus and SMAC mimetics with the goal of eliminating latently HIV-infected cells. These findings that SMAC mimetic treatment and MG1 infection might synergize to specifically kill HIV-infected cells highlights the significant potential of this therapy as an innovative cure approach.

Dedication

This thesis is dedicated to my amazing husband, Dr. Gökalp Yıldırır, my source of strength, my beacon of hope, and my partner in all things. Watch out world, Dr.Dr.Bengalp is here!

Acknowledgements

I would like to thank my supervisor, Dr. Jonathan B. Angel, who believed in me and pushed me to be a better scientist in every step of the way. His mentorship has been invaluable throughout this journey. I would also like to thank all the past and present members of the Angel lab. They were always there for me with advice, jokes, and understanding. Thank you to Ana Vera-Cruz, Megan Magro, and Brittany Haas for all the vent and brainstorming sessions. Without them, I would not have been able to push through graduate school. A special thanks to Stephanie Burke-Schinkel, who was there for me from day one, when I was just a young undergraduate student volunteering in the lab.

Thank you to my thesis advisory committee members, Dr. Marceline Côté, Dr. Tommy Alain, and Dr. Robin Parks for their guidance, thoughtful discussions, and their belief in me.

I would like to thank my parents, for showing me the value of higher education and never doubting me. I would like to especially thank my mom, Filiz Molyer, who has always been there for me, laughed and cried with me, always listened to the latest updates on my project even though at times what I am talking about must have sounded like gibberish. We did it mom! Thank you to my husband, who sang musical songs with me, read my favorite books, discussed science with me, and held my hand and did not think I was super weird when I cried at the My Chemical Romance concert. Thank you to my wonderful cat Yoshi, who is always the best dressed and smells like warm dust.

Finally, I would like to thank the Clinical Investigative Unit nurses and volunteers who have helped me get the necessary samples for my project. Without them, this work would not have been possible.

Table of Contents

List of Abbreviations

AIDS Acquired Immunodeficiency Syndrome

AM Alveolar Macrophage

Apaf1 apoptotic protease-activating factor 1

APC Allophycocyanin

APOBEC3 Apolipoprotein B mRNA Editing Enzyme, Catalytic Polypeptidelike 3

AZT 3'-Azido-3'-deoxythymidine

BAF BRG1- or HBRM-Associated Factors

BAL Bronchoalveolar Lavage

BCL2 B-cell lymphoma protein 2

BET Bromodomain and Extraterminal (proteins)

BIRC2 Baculoviral IAP Repeat Containing 2

BLT Bone Marrow, Liver, and Thymus

BSA Bovine Serum Albumin

CA HIV Capsid Protein

cART Combination Antiretroviral Therapy

CCL19 Chemokine (C-C Motif) Ligand 19

CCR5 CC-Chemokine Receptor Type 5

CD Cluster of Differentiation

cDNA Complementary DNA

cFLIP CASP8 and FADD-like Apoptosis Regulator

cIAP Cellular Inhibitor of Apoptosis

CNS Central Nervous System

CRISPR Clustered Regularly Interspaced Short Palindromic Repeats

CXCR4 CXC-chemokine receptor type 4

DAMPs Danger Associated Molecular Patterns

DC Dendritic Cell

dCA didehydro-cortistatin A

ddPCR Digital Droplet PCR

DISC Death Inducing Signaling Complex

DMEM Dulbecco's Modified Eagle's medium

dNTP Deoxynucleotide Triphosphate

DR4 TRAIL receptor 1

DR5 TRAIL receptor 2

dsRNA Double-Stranded RNA

EDTA Ethylenediaminetetraacetic Acid

EIF4E Eukaryotic Initiation Factor 4E

ELISA Enzyme-Linked Immunosorbent Assay

Env HIV Envelope Protein

ER Endoplasmic Reticulum

FADD Fas-Associated Protein with Death Domain

FasL Fas Ligand

FBS Fetal Bovine Serum

FLICA Fluorochrome Inhibitor of Caspases

FLICE FADD-like ICE

G Rhabdoviridae Glycoprotein

GALT Gut Associated Lymphoid Tissue

GFP Green Fluorescent Protein

GO Gene Ontology

GSDMD GasderminD

HAND HIV-Associated Neurodegenerative Disorder

HDAC Histone Deacetylase

HDACi Histone Deacetylase Inhibitor

HEK Cells Human Embryonic Kidney Cells

HIV Human Immunodeficiency Virus

HLA Human Leukocyte Antigen

HSA Heat Stable Antigen

HSV Herpes Simplex Virus

IAPs Inhibitors of Apoptosis

IFN Interferon

IFN1 Type I Interferon

IFNAR IFNα/β receptor

IFNAR1 IFNα/β receptor subunit 1

IL Interleukin

INT HIV Integrase

IP intraperitoneal

IRES Internal Ribosome Entry Site

ISG IFN-stimulated Gene

ISG15 Interferon-stimulated Gene 15

ISRE Interferon Response Element

IV intravenous

JAK Janus Kinase

LDL-R Low Density Lipoprotein Receptor

LMW-Poly(I:C) Low Molecular Weight Polyinosinic-Polycytidylic Acid

LRA Latency Reversal Agent

LTR Long Terminal Repeat

LUBAC Linear Ubiquitin Chain Assembly Complex

M Rhabdoviridae Matrix Protein

mCMV Murine Cytomegalovirus

MCSF Macrophage Colony Stimulating Factor

MA HIV Matrix Protein

MDM Monocyte Derived Macrophage

MG1 Recombinant Maraba Virus

MHC I Major Histocompatibility Complex I

MLKL Mixed Lineage Kinase Domain Like Pseudokinase

MOI Multiplicity of Infection

NFkB Nuclear Factor Kappa-light-chain-enhancer of Activated B Cells

NGS Normal Goat Serum

NHP Non-Human Primate\

NIK NFκB Inducing Kinase

NK Cell Natural Killer Cell

NKG2D Natural Killer Group 2D

NLR Nucleotide-binding Oligomerization Domain-like Receptor

NOD-SCID-IL2Rgnull NSG

NP HIV Nucleoprotein

OV Oncolytic Virus

PAMP Pathogen Associated Molecular Pattern

PBMC Peripheral Blood Mononuclear Cells

PBS Phosphate Buffered Saline

PCR Polymerase Chain Reaction

PD-1 Programmed Cell Death Protein 1

PD-L1 Programmed Cell Death Protein 1

PE Phycoerythrin

Pen/Strep Penicillin, streptomycin

PFA Paraformaldehyde

PKC Protein Kinase C

PKR Protein Kinase R

PLHIV Person(s) Living with HIV

PR HIV Protease

PRR Pattern Recognition Receptor

PVDF Polyvinylidene Fluoride

qPCR Quantitative PCR

R5-tropic CCR5 Tropic

RhIV rhabdo immunodeficiency virus

RIG-I Retinoic Acid Inducible Gene I

RIPK1 Receptor-Interacting Serine/Threonine-Protein Kinase 1

RIPK3 Receptor-Interacting Serine/Threonine-Protein Kinase 3

RPMI-1640 Roswell Park Memorial Institute 1640 medium

RT HIV Reverse Transcriptase

SAHA Suberoylanilide Hydroxamic Acid

SAMHD1 Sterile Alpha Motif Domain and HD Domain-containing Protein 1

SDS Sodium Dodecyl Sulfate

SHIV SIV/HIV Chimeric Virus

SIV Simian Immunodeficiency Virus

SMAC Second Mitochondrial Activator of Caspase

ss Single Stranded

ssRNA Single-Stranded RNA

STAT Signal Transducer and Activator of Transcription

TGFβ Transforming Growth Factor Beta

TLR Toll-Like Receptor

TRADD Tumor Necrosis Factor Receptor Type 1-associated DEATH Domain Protein

TRAIL TNF-Related Apoptosis-Inducing Ligand

TNFα tumor necrosis factor α

TNFR1 tumor necrosis factor receptor-1

UPR Unfolded Protein Response

UV Ultra-Violet

VSV Vesicular Stomatitis Virus

VSVΔ51 Recombinant Vesicular Stomatitis Virus

VV Vaccinia Virus

WPH weeks post humanization

WT Wildt Type

X4-tropic CXCR4 Tropic

XIAP X-linked Inhibitor of Apoptosis

ZBP1 Z-DNA Binding Protein 1

List of Figures

List of Tables

Chapter 1: Introduction

1.1 HIV infection and pathogenesis

In 1981, several research groups published articles describing unusual cases of patients who presented with rare infections and cancers, such as *Pneumocytists cariini* pneumonia, a lung infection, and Kaposi's sarcoma, an aggressive cancer, accompanied by other opportunistic infections[1]. A year later, the term Acquired Immunodeficiency Syndrome (AIDS) was used for the first time, to describe the illness these heavily immunocompromised patients have[2]. The etiological agent for AIDS, human immunodeficiency virus (HIV) is discovered in 1983, by two independent research groups[3,4], and the development of antiretroviral agents to treat HIV infection began. As of 2022, 39 million people live with HIV, and there are 630,000 annual deaths from HIV-related causes[5].

HIV belongs in the genus *Lentivurus* and in the *Retroviridae* family[6]. It can further be classified as HIV-1, which evolved from non-human primate immunodeficiency virus from Central African Chimpanzees[7], and HIV-2, which evolved from West African sooty mangabeys[8]. HIV-1 can be further classified into distinct lineages, M, N, O and P, where M is the most prevalent and has infected millions of people worldwide[6], and P, which is the least prevalent and has only been detected in a single person from Cameroon[9]. For the purpose of this thesis, whenever HIV is mentioned, it refers to HIV-1 unless otherwise stated.

- Viral characteristics and replication cycle

HIV contains two copies of single stranded positive sense RNA per virion. The RNA codes for 16 viral proteins:

- Group-specific antigen (gag), which consists of the structural proteins p24 (capsid), p6, p7 (nucleocapsid protein which bind RNA to protect it from degradation), and p17 (matrix protein),
- Polymerase (Pol), which consists of protease (PR, cleaves gag and pol to their functional proteins), reverse transcriptase (RT, transcribes RNA into DNA) and integrase (IN, integrates the double stranded DNA transcribed by the reverse transcriptase into host genome),
- Envelope (env) gp160, which is cleaved to gp120 and gp41 in mature virions,
- Vif, which counters the cellular restriction factor Apolipoprotein B Editing Complex 3G (APOBEC3G),
- Vpr, which induces cell cycle arrest,
- Vpu, which reduces cell surface expression of CD4 and inhibits NFκB activation, and overcomes the inhibition of viral release mediated by tetherin,
- Nef, which reduces cell surface expression of CD4, and major histocompatibility complex (MHC) class 1,
- Rev, which exports viral RNAs into the cytoplasm,
- Tat, which recruits viral transcription factors to the promoter[10–12].

The viral lifecycle begins by HIV attaching itself to a susceptible host cell, such as $CD4^+$ T-cells, macrophages, or dendritic cells. Upon binding of gp120 to the main receptor CD4, conformational changes occur, which result in HIV binding to a co-receptor, either CCR5 or CXCR4. Binding to the co-receptor results in another conformational change, which allows the N terminal of gp41to insert itself into the cell membrane, and the fusion of the viral envelope and host membrane. This triggers the release of the viral nucleocapsid into the host cell, where in the cytoplasm, the error-prone RT starts transcribing RNA into double stranded cDNA with flanking

long terminal repeats (LTR) at its 5' and 3' sites, called the proviral DNA. The intact capsid containing the viral DNA enters the nucleus, where transcription is completed, and uncoating occurs. The proviral DNA forms a pre-integration complex with integrase and other host proteins and is then inserted into the host genome[13]. The embedded proviral DNA then serves as a template for the viral mRNA, producing the viral HIV proteins and the full length viral RNA. Upon assembly of the immature virion on the plasma membrane, the Gag-Pol protein is cleaved to its mature form by the HIV protease, resulting in the formation of mature HIV virion, ready for another round of the infection cycle[14].

- Pathogenesis and disease progression

HIV is transmitted through viral exposure at mucosal surfaces such as the anogenital mucosa via sexual contact, percutaneous inoculation, or from mother to infant[15]. Primary infection occurs in monocytes/macrophages, dendritic cells and $CD4^+$ T-cells which results in the primary amplification of the virus. These cells or cell-free virions migrate via the bloodstream to gastrointestinal tract, bone marrow, spleen, and lymph nodes, where the secondary amplification takes place. This results in massive depletion of $CD4^+$ T-cells, particularly in the gut associated lymphoid tissue (GALT)[16], where up to 80% of $CD4^+$ T-cells die[17]. Within two weeks after infection, HIV can be detected throughout the body[10].

The HIV infection stages can be separated into 3: The acute phase, the chronic phase, and AIDS. The acute phase begins with the eclipse period, which is the first two weeks of infection where HIV RNA remains undetectable. The following stages in the acute phase can be further divided into Fiebig stages I-V, which describe what diagnostic tests can be used in the detection of HIV (Figure 1). In the acute phase, HIV infection starts to present as flu-like symptoms such as

fatigue, fever, headache, weight loss, nausea and diarrhea[18]. Peak viremia, e.g. $10^6/10^7$ copies of HIV RNA per mL in the peripheral blood, is reached in the acute phase[14] and is correlated with the severity of disease symptoms[19]. In the absence of treatment, 12-20 weeks after peak viremia, viral load decreases steadily to reach a set point, due to the host immune response consisting of high levels of IFNα and soluble IL-2R[20], HIV specific adaptive immune responses such as $CD8^+$ T-cells that kill HIV-infected cells[21,22] and broadly neutralizing antibodies[23,24]. This attempt at controlling the infection results in the appearance of mutations in the virus due to selective pressure[25]. Mutations also occur due to the error-prone nature of HIV reverse transcriptase[26]. The viral load at set-point stays stable for years and is accompanied by transient and spontaneous restoration of $CD4^+$ T-cell counts[27]. Importantly, the viral set point correlates with disease outcome, where individuals with higher viral set points progress faster to AIDS compared to those with lower viral set points. Furthermore, a subset of people called 'elite controllers' are able to keep the set point below 50 copies/mL in the blood and do not progress to AIDS even with no treatment[28]. Following the viral set point HIV infection moves to its chronic phase, which can last 10 years or more. Although viral replication and the effort to control said replication continues, this stage is mostly asymptomatic[29]. Ultimately, the immune system becomes unable to control the infection, and the disease progresses to AIDS, where $CD4^+$ T-cell counts fall below 200 cells/mm^3 of blood[30].

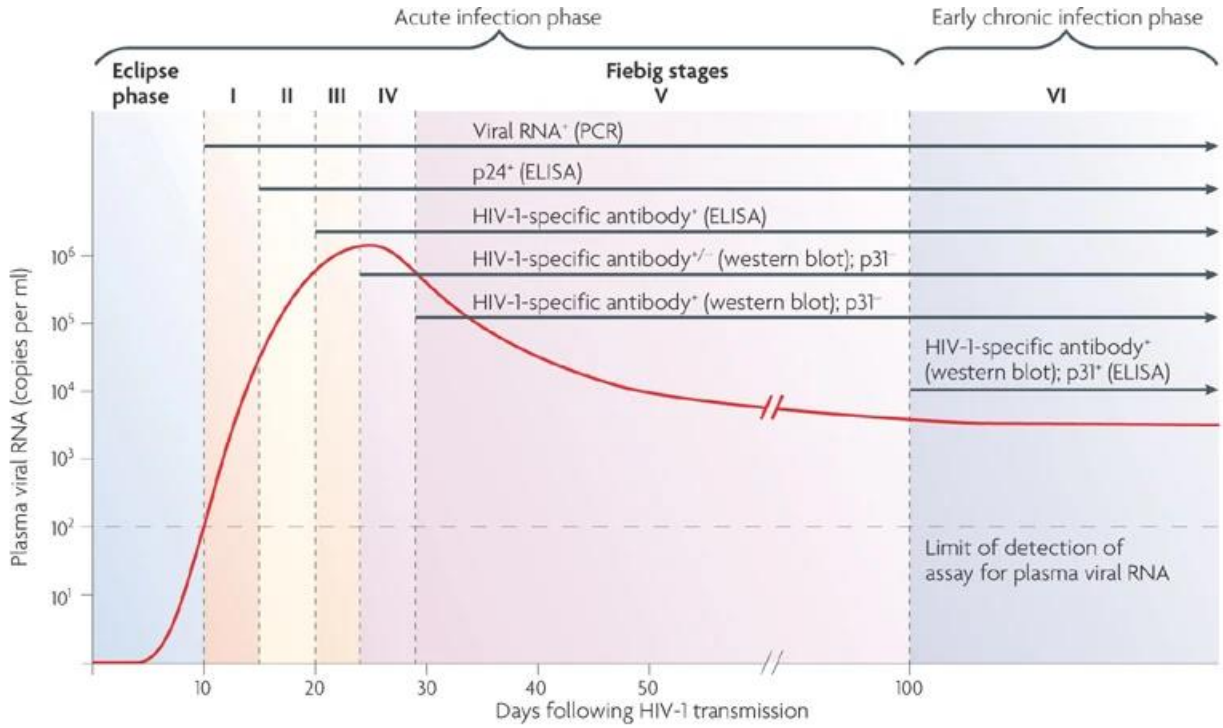
Acute infection phase
Early chronic infection phase
Eclipse phase
Fiebig stages
I
II
III
IV
V
VI
Viral RNA+ (PCR)
p24+ (ELISA)
HIV-1-specific antibody+ (ELISA)
HIV-1-specific antibody+/− (western blot); p31−
HIV-1-specific antibody+ (western blot); p31−
HIV-1-specific antibody+ (western blot); p31+ (ELISA)
Limit of detection of assay for plasma viral RNA
Plasma viral RNA (copies per ml)
10^6
10^5
10^4
10^3
10^2
10^1
10
20
30
40
50
100
Days following HIV-1 transmission

Figure 1, phases of HIV infection. Figure adapted from McMichael et al., (2010)[31], reprinted from Nature Reviews Immunology, McMichael, A. J., Borrow, P., Tomaras, G. D., Goonetilleke, N. & Haynes, B. F. The immune response during acute HIV-1 infection: clues for vaccine development. Nat. Rev. Immunol. 10, 11–23 (2010), copyright 2024 with permission from Springer Nature.

- HIV latency and viral reservoirs

In the field of HIV research, latency is defined as a nonproductive state of infection, where cells harboring proviral HIV DNA are transcriptionally silent in making infectious virions, but can be stimulated to do so[32]. However, most latently infected cells carry defective HIV proviruses that are replication defective[32,33]. On the other hand, viral reservoir is defined as cell types or anatomical sites which are permissive to HIV replication and accumulation despite effective cART, such as the brain, GALT, and lymph nodes[34].

a) $CD4^+$ T-cells

$CD4^+$ T-cells make up the best characterized viral reservoirs for HIV. Although activated $CD4^+$ T-cells are the main target of HIV, they quickly succumb to the cytopathic effects of the infection, or are killed by other immune cells[35]. However, some of these infected cells go back to a resting state and differentiate into memory $CD4^+$ T-cells, harboring proviral HIV DNA. The central (T_{CM}), transitional (T_{TM}) and effector memory (T_{EM}) T-cells are the main reservoir for HIV but each are affected to a different extent[36]. The sequestration of transcription factors, chromatin modifications, and DNA methylation prevent transcription of HIV[32]. The persistence of the viral reservoir in the memory $CD4^+$ T-cells is driven by homeostatic proliferation[37], as evidenced by the specific HIV integration sites being linked to clonal expansion[38,39]. Although the frequency of memory $CD4^+$ T-cells carrying HIV provirus is estimated to be $300/10^6$, only a small ratio are thought to be able to produce infectious virions[33,40].

b) Macrophages

Even though once controversial and overlooked, it has been established that myeloid lineage cells, particularly macrophages can be persistently infected and can serve as reservoirs for HIV. Although monocytes, the progenitors for macrophages are highly resistant to HIV infection with a recent study finding less than 6.6 copies per million monocytes intact HIV proviral DNA in virologically suppressed PLHIV[41–43], macrophages are one of the main targets of HIV. HIV DNA found in macrophages in the lamina propria of vaginal, penile urethral, and intestinal mucosa are some of the suggestions that macrophages play a role in early HIV infection[44–47]. Unlike $CD4^+$ T-cells, macrophages are more resistant to the cytopathic effects of HIV[48,49], and in some cases HIV proteins have been shown to protect macrophages from apoptosis[50,51]. Macrophages can harbor infectious viral particles in cytoplasmic vesicles and thus they aid in spreading of HIV into other tissues such as brain[52], gut[53,54], gut-associated lymphoid tissues[55,56], and semen[57,58]. They are long-lived, with HIV-infected macrophages having a half-life of 2-4 weeks[59,60], and can reside in tissues where there is low penetration of cART which supports viral persistence[61,62]. HIV has been found in tissue resident macrophages such as Kupffer cells[63], microglial cells and perivascular macrophages in the brain[64–66], and alveolar macrophages, even during effective cART[67,68].

c) Viral reservoirs in the body

Viral reservoirs are established in the body, particularly where there is poor cART penetration. GALT contains the most latently infected cells[69,70], followed by lymph nodes. However lymph nodes appear to have the greatest contribution to viral rebound upon cART cessation where GALT and blood follow as second and third[71]. The central nervous system (CNS) is another HIV reservoir, where microglia are the main contributors. Furthermore, HIV compartmentalization can

be seen in the brain, which could result in drug resistance mutations[72]. Other tissues that carry HIV proviral DNA include but are not limited to the lung, bone marrow, genital tract, kidney, and the liver[73].

- Mechanisms of HIV latency

Mechanisms of HIV latency can be broadly divided into pre-integration latency and post-integration latency. Pre-integration latency refers to the state when viral replication cycle is interrupted or fully blocked before viral DNA can integrate into the host cell genome. This type of latency can be seen in both $CD4^+$ T-cells and macrophages and primarily occurs when the infected cells return to quiescent state prior to viral integration[74]. The pre-integration complex (PIC) can stay stable for several weeks in the cytoplasm of the host cell, and still holds the capacity to integrate upon cell activation[75]. In macrophages, host restriction factors contribute to pre-integration latency. These include APOBEC3G and APOBEC3A, which introduces G to A hypermutation in the viral genome[76–78], sterile α-motif/histidine-aspartate domain-containing protein 1 (SAMHD1) which reduces the dNTP pool in the cytoplasm by hydrolyzing dNTPS which in turn limits the reverse transcriptase activity of HIV[79], RNA polymerase II-associated factor 1 (PAF1) family members which interact with the viral RNA and interferes with its stability[80], and Myxovirus-resistance protein 2 (MX2), which suppresses nuclear accumulation of viral DNA[81].

Post-integration latency is a more stable form of latency. The bulk of the latently infected memory $CD4^+$ T-cell population display post-integration latency, where HIV transcription is silenced. The reasons for post-integration latency include HIV integration into transcriptionally silenced heterochromatin, not having reached the Tat protein threshold for viral transcription,

mutations that prevent the formation of replication-competent virion, and reduced host transcription factors[74,82]

1.2 HIV treatment

Combination antiretroviral therapy (cART), is the current gold standard for treatment of HIV. The first drug approved to combat HIV infection, a nucleoside analogue called 3′-azido-3′-deoxythymidine (AZT), which inhibited reverse transcription of HIV, came out in 1987[83,84]. However, it soon became apparent that despite early promising results, drug resistance developed after continued usage[85]. In 1996, highly active antiretroviral therapy (HAART, also known as combination antiretroviral therapy cART) was introduced which consisted of two nucleoside reverse transcriptase inhibitors (NRTI) along with a protease inhibitor or non-nucleoside reverse transcriptase inhibitor (NNRTI)[86,87]. Soon, cART evolved to include other classes of drugs, such as integrase inhibitors, CCR5 agonists, and fusion inhibitors, attachment inhibitors, reviewed in detail by Menéndez-Arias et al[88]. The complex scheduling of drugs, toxicity and quickly developing drug resistance made adhering to the treatment difficult with the first generation of cART. Today, a daily fixed dose combination of 3 different drugs against two different targets is the standard of care[89]. However, advances are continuously being made to lower the burden of pills, such as with long-acting therapies[90].

With treatment adherence, cART is able to lower the viral levels in the blood to undetectable (20–50 copies HIV-1 RNA/mL), turning HIV infection to be a chronic illness and allowing persons living with HIV (PLHIV) to have near normal life expectancy[91]. Furthermore, it has been shown that people who do not have detectable viral loads are unable to sexually transmit

HIV to their HIV negative partners[92,93]. This finding, popularized as Undetectable = Untransmittable (U=U) has helped immensely in fighting the stigma against HIV infection[94].

Although cART is excellent at suppressing viremia, it has its limitations. It needs to be a lifelong therapy, as treatment interruption results in plasma viral rebound which occurs after 2-3 weeks due to the latent HIV reservoirs established early on in the infection[95,96]. Mathematical modelling as well as long-term follow-up studies have shown that due to the long half-life of the reservoir, under best circumstances, eradication would take at least 60 years, which makes it highly unlikely[97,98]. Moreover, there are other issues to address such as access to treatment, long-term side effects, poor drug penetration, and viral persistence[99] resulting in the need to find better treatment options or an HIV cure.

1.3 HIV cure strategies

Unfortunately, cART is not a cure. Currently, there are only five patients who have been cured of HIV. 4 of them have received allogeneic CCR5Δ32/Δ32 hematopoietic stem cell transplantation (HSCT) and one of them has received allogeneic haplo-cord CCR5Δ32/Δ32 stem cell transplantation[100]. However, this approach is not feasible for the broader population. Thus, the search for an HIV cure is ongoing. Current strategies to cure HIV include shock and kill, block and lock, therapeutic vaccines, gene editing, and novel strategies such as oncolytic virus therapy.

- Shock and kill

This strategy aims to activate and hence "shock" the virus in the latently infected cells, and then eradicate the virus via immune clearance or drug therapy, thus the "kill". To achieve this, a class of drugs called latency reversal agents (LRAs) to activate the latent virus have been tested

extensively. The first clinical trial was with IL-2 and antibodies against CD3, the T-cell receptor which not only did not result in a decrease in latently infected $CD4^+$ T-cells, but also caused severe side-effects, such as patients developing a cytokine storm condition[101,102]. Today, LRAs can be broadly classified in 5 categories:

1. Histone post-translational modification modulators: These class of drugs modulate the tails of the histone proteins, thus conferring chromatin a more open conformation. Main examples are histone methyltransferases (HMTi) such as chaetocin[103] and histone deacetylation inhibitors (HDACi) such as vorinostat[104,105] and romidepsin[106].
2. Non-histone chromatin modulators: These drugs affect other elements in the chromatin that modulate transcription, such as transcription factors, interactions of DNA with RNA pol II, and DNA methylation. Notable examples include the BET bromodomain inhibitor JQ1[107] . HODHBt[108], and (BRG-/BRM-associated factor) BAF inhibitors[109].
3. NFκB stimulators: These drugs lead to the activation of NFκB, one of the main transcription factors for HIV. Examples are protein kinase C (PKC) agonists[110] and phorbol myristate acetate (PMA)[111].
4. TLR agonists: Engaging the toll like receptors (TLRs) that recognize double stranded RNA, or guanosine or uridine rich viral RNAs, these drugs include CL413, GS-986, GS-9840, and are reviewed in detail by Rozman and colleagues[112].
5. Extracellular stimulators: These drugs engage extracellular receptors on the cells, resulting in downstream signaling which ends in transcription of HIV. Most common examples include TNFα[113] and phytohemagglutinin (PHA)[114].

Due to their inability to activate all of the HIV reservoir and their reported toxicities, LRA use alone will most likely be not enough to cure HIV. Therefore, other approaches such as using more than one LRA or combining LRAs with other cytotoxic agents will almost certainly be required for this strategy to advance into the clinic[115].

Getting the "kill" part in "shock and kill" can potentially be achieved via immune cell clearance, using pro-apoptotic compounds such as Bcl-2 antagonists, PI3K/Akt inhibitors, RIG-I inducers, and SMAC mimetics[116]. or therapeutic vaccination.

Therapeutic HIV vaccines aim to enhance the acquired immune response against HIV and thereby prevent or significantly diminish viral rebound upon cART cessation.. Such vaccines include those based on HIV protein targets such as Gag[117] or Tat[118] to elicit a cytotoxic T-cell response, dendritic cell (DC) based vaccines in which DCs primed with inactivated HIV or that produce viral proteins are used to stimulate T cell responses[119,120], or those that are designed to induce broadly neutralizing antibodies against HIV[121]. However, currently these vaccines have resulted in limited success.

- Block and lock

Instead of activating latent HIV and then the eradication of the virus, the block and lock strategy aims to keep latent HIV in a transcriptionally silent form by reinforcing latency. Latency promoting agents (LPAs) include but are not limited to didehydro-cortistatin A (dCA) which inhibits HIV Tat[122], LEDGINs which inhibit HIV integrase activity and result in HIV provirus with an affinity to integrate to transcriptionally silent sites[123] and siRNAs for epigenetic silencing[124].

- Gene editing

The gene editing tool CRISPR/Cas9, can be used to alter the proviral HIV DNA embedded into latently infected cells or to generate cells that lack the co-receptor for HIV that are later used in adoptive transfer., Studies that have used gene editing to alter proviral HIV DNA show that CRISPR/Cas9 was able to successfully target the 3' LTR region and silence HIV transcription in latently infected promonocytes, microglial cells and T-cells[125]. *In vivo* studies in mice also showed reduction in of *gag* and *env* RNA[126], and successful proviral DNA excision[127]. Furthermore, in an simian immunodeficiency (SIV) infected non-human primate model, CRISPR/Cas9 editing was able to reduce the proviral DNA in blood and tissues such as the lung and lymph nodes[128]. The limitations for gene editing latently HIV-infected cells include delivery, cost of generating vectors if a technique such as zinc-finger nucleases are used, possible off-target effects, and the mutation rate of HIV.

CRISPR/Cas9 has also be used to generate CCR5 knockout hematopoietic stem cells (HSPC) from a donor and then adoptively transfer them to a patient that suffered from HIV infection and acute lymphoblastic leukemia. The CCR5 ablated cells lasted more than 19 months in the peripheral blood with no negative side effects from gene editing (NCT03164135)[129]. Other studies are trying to improve this approach by combining the CCR5 knockout with cell membrane anchored HIV fusion inhibitor to prevent re-infection by both CCR5 and CXCR4 tropic viruses[130].

1.4 Oncolytic viruses and their potential as an HIV therapy

- Oncolytic viruses and cancer

Oncolytic viruses (OVs) are viruses that have innate selectivity or have been engineered to have selectivity to kill cancer cells. OVs can kill cancer cells by inducing direct oncolysis of the

tumor cells. In some cases, due to the release of antigens[131] and virus-specific pathogen-associated molecular patterns (PAMPs)[132,133] from the dying cells, immunogenic cell death (ICD) can occur. This type of cell death stimulates immune responses and can turn previously "cold" tumors to "hot"[134]. Moreover, cell killing by OVs can result in collapse of the tumor vasculature, which transiently shuts down the blood flow to the tumors, depriving them of oxygen and nutrients[135]. Lastly, OVs can be engineered to deliver other therapeutic agents to the tumor, such as cytokines, microRNAs, suicide genes, and antibody-based therapies[136].

The first approved OV therapy in the United States is called T-VEC, a GM-CSF expressing HSV-1 virus against metastatic stage III-IV melanoma. T-VEC selectively replicates in tumor tissue and kills tumor cells, while the secretion of GM-CSF aids in the recruitment of dendritic cells, which is key to start an anti-tumor immune response. T-VEC is delivered via intralesional injection[137]. When used as a monotherapy in phase II clinical trials, it was able to significantly decrease tumor burden which was maintained for 3 years, and increased overall survival by 52% at 24 months. In line with this, in the OPTIM study, a phase III clinical trial with T-VEC, it was found that among patients with complete response, 5 year survival rate was 88.5%, with minor adverse effects such as flu-like symptoms, chills, fatigue, and pyrexia[138]. Currently, the oncolytic viruses approved for therapy can be seen in the following table (Table 1).

Commercial name	Virus	Approved for	Location and date
H101	Adenovirus	Nasopharyngeal carcinoma	China – 2005
T-VEC	HSV-1	Metastatic stage III-IV melanoma	USA – 2015 Europe – 2015 Australia – 2016 Israel - 2017
ECHO-7[a]	Echovirus	Stage I-II melanoma	Latvia – 2004 Georgia – 2015 Armenia - 2016
Teserpaturev	HSV-1	Residual or recurrent gliblastoma following radiotherapy and chemotherapy	Japan - 2021
Nadofaragene firadenovec	Adenovirus	Bacillus Calmette-Guerin (BCG) unresponsive invasive bladder cancer	USA - 2022

Table 1, currently approved oncolytic virus therapies in the world. Adapted from Shalhout et al., 2023[139].

Oncolytic viruses that are not approved for the clinic yet but are being actively researched include vaccinia virus (VV)[140], reovirus[141], measles virus[142], vesicular stomatitis virus (VSV)[143], and Maraba virus[144].

- Interferon sensitive oncolytic viruses VSV and MG1

VSV and Maraba are two closely related viruses, classified in the *Rhabdoviridae* family, genus *Vesiculovirus*. They are similar in gene structure, tropism, and lifecycle. They are both enveloped, non-segmented negative strand RNA viruses, containing five genes in their genome: 3' nucleocapsid protein N, phosphoprotein P, matrix protein M, glycoprotein G, and RNA-dependent-RNA-polymerase (RdRp) L 5'. Both have wide tropism as they mainly use the low density lipoprotein receptor (LDL-R)[145,146] as their cellular receptor, which is expressed in many tissues[147]. Their lifecycle entirely takes place in the cytoplasm. Infection begins by the attachment of G glycoprotein to the LDL receptor, and the virus is endocytosed via actin and clathrin mediated endocytosis[145]. Upon entry, the acidification of the endosome results in the viral membrane fusing with the endosome membrane (which is mediated by the glycoprotein G), and the release of the ribonucleoprotein (RNP) into the cytoplasm. In the cytoplasm, a complex composed of the N, P, and L proteins start to transcribe the viral genome into positive sense RNA, from 3' to 5'. The negative sense RNA genome is used as a template to produce mRNA for the N, P, M, G, and L, along with the full-length viral genome. The transcription of mRNA transcripts occurs via "stuttering" meaning the RdRp pauses at each intergenic region. This results in a gradient in viral transcription accumulation, where N>P>M>G>L. For VSV, replication is quick and assembly of progeny virion can be seen 2-3 hours post infection. The M protein of both viruses can impair host

nuclear mRNA export via interacting with the Rae1 and Nup98 proteins[148]. This interference also impairs the interferon response of the host cell against the infection.

Both VSV and Maraba virus have been attenuated via genetic engineering. For VSV, a deletion was made in the 51st amino acid of the M protein resulting in VSVΔM51, which inhibits the WT M protein's function of blocking nuclear transport. For Maraba, mutations identified in VSV that enhanced viral replication and reduced toxicity were mapped, and two amino acids, L123W in the M gene and Q242R in the G gene were mutated resulting in the attenuated Maraba virus, MG1[146]. The modifications to VSV and Maraba make them highly sensitive to IFN1.

Both VSV and MG1 have been popular oncolytic viruses to be used in cancer studies[143,144,149–152]. Their small genome, ease of engineering, quick replication cycle, and wide tissue tropism make them attractive candidates for oncolytic virus based therapies.

- Pre-clinical and clinical studies with MG1

MG1 has been shown to be safely delivered intravenously to immunocompetent mice in doses up to 10^9 pfu. In disease models of mice bearing syngeneic subcutaneous CT26, a colon cancer cell line, MG1 infection resulted in complete tumor regression when delivered intravenously[146]. MG1 has also been used as a vaccine vector alongside replication incompetent adenovirus (Ad prime: MG1 boost strategy) to deliver tumor antigens. In a study done in cats, the Ad:MG1 strategy was used to deliver the human placenta-specific 1 (hPLAC1) antigen. Twenty-one days following the Ad:hPLAC1 delivery, the cats were immunized with MG1-hPLAC1 at $2.5x10^{11}$ pfu. No shedding of the virus nor viremia could be detected, but the MG1 genome could be detected in plasma, urine, and fecal samples a week after inoculation. Post-mortem analysis also showed the presence of MG1 genomes in the spleen, heart, and lungs with the absence of

replicative virus. These results confirm that systemic delivery of MG1 can result in MG1 being dispersed in various anatomical sites[153]. In another study done in cynomolgus macaques, the Ad:MG1 strategy was used to deliver the MAGE-A3 cancer antigen expressed in melanoma. After priming with ad-MAGE-A3, the MG1-MAGE-A3 infusion was done twice with three days in between at the dose $1x10^{11}$ pfu. MG1 genomes were detected in the blood, urine, feces, spleen, and lymph nodes. No replicative particles were obtained.

In a phase I/II clinical trial using Ad:MG1-MAGEA3 in patients with MAGE-A3 positive solid tumors (NCT02285816) patients were treated with two infusions of MG1-MAGE-A3 at $1x10^{11}$ pfu, a single dose of intramuscular Ad-MAGE-A3 or intramuscular Ad-AMGE-A3 followed by systemic delivery of MG1-MAGE-A3. Pro-inflammatory cytokines such as IL-6 and TNFα were found to be upregulated whereas the immunosuppressive TGFβ was downregulated. Furthermore, over 1% of $CD8^+$ T-cells were shown to be specific for MAGE-A3 in one patient[154]. In another phase 1b clinical trial (NCT03773744), the safety and tolerability of intravenous and intratumoral injection of Ad:MG1-MAGE-A3 with pembrolizumab is being evaluated in patients with metastatic melanoma or previously treated cutaneous squamous cell carcinoma with results to come.

These pre-clinical and clinical studies confirm that MG1 is well tolerated, dispersed in anatomically distinct sites, can be used to induce an antibody response against a specific antigen when systemically delivered in humans, making it a good candidate to study as a potential HIV therapy.

- Oncolytic viruses as a potential HIV treatment

Disruption of type I IFN signaling in chronic HIV infection, such as impairment of pattern recognition receptors (PRR) signaling, impairment of innate viral sensing, and defects in IFN mediated antiviral responses are well documented and reviewed in detail by Sandstrom et al[155]. Our research group has shown that some of these defects persist in latently HIV-infected cells, and can be used to distinguish them from their uninfected counterparts. Ranganath et al., has shown that baseline expression of interferon α/β receptor subunit 1 (IFNAR1) and major histocompatibility complex-I (MHC-I) are lower in latently HIV-infected monocytic U1 cells and myelocytic OM10.1 cells, compared to their uninfected parental cells, U937 cells and HL-60 cells. Furthermore, this impairment is also observed in the induction of interferon stimulated gene (ISG). When the latently HIV-infected cell lines and their uninfected counterparts were treated with exogenous IFNα, the upregulation of MHC-I, protein kinase R (PKR), and ISG15 in latently infected cells were significantly lower than the uninfected cells. Response to Poly(I:C) as measured by IFNα/β secretion was significantly lower in U1 cells compared to U937 cells as well[156].

In light of these defects, our research group hypothesized that latently infected cells would be more permissible to interferon sensitive oncolytic virus infection, namely MG1 and VSVΔ51. When HIV-infected cell lines U1 and OM10.1 were infected with MG1, a significantly higher proportion of cells were infected as measured by GFP expression, and killed as compared to the uninfected parental cells. This observation also held true for latently infected $CD4^+$ T-cells that have been infected with HIV *ex vivo*, as demonstrated by a significant decrease in proviral HIV DNA as measured by qPCR and p24 as measured by ELISA.

MG1 killing and infection was measured in persistently HIV-infected monocyte derived macrophages as well. Since the infection rates are usually very low in *in vitro* infection models of macrophages [157,158], a reporter CCR5 tropic HIV, namely HIV NL4.3 BAL-IRES-HSA was used. In this model, cells that are persistently infected with HIV express mouse heat stable antigen (HSA) on their cell surface, allowing the differentiation of HIV-infected cells (HSA+) from bystander cells (HSA-)[158]. Using this model, our group was able to show that MG1 has a higher infection rate in HSA+ cells compared to HSA- cells. Moreover, upon MG1 infection, there was more cell death in the HSA+ fraction, indicating that MG1 preferentially infects and kills HIV-infected MDM. Similar to what was done in latently infected $CD4^+$ T-cells, this was further confirmed by measuring proviral HIV DNA and the p24 capsid protein, where the qPCR assay and ELISA showed a significant decrease in both. It was also confirmed that an infectious MG1 virus is necessary to achieve killing, as UV inactivated MG1 or supernatants taken from infected cells where MG1 was filtered out were not able to induce killing of either latently infected $CD4^+$ T-cells or persistently infected MDM[159–162].

To assess MG1's possible clinical applications, alveolar macrophages (AM) obtained from bronchoalveolar lavage of PLHIV on cART were infected with MG1 and proviral HIV DNA was measured with digital droplet PCR (ddPCR). It was seen that there is a significant reduction of proviral HIV DNA 48h post MG1 infection, providing us insights about the clinical relevance of MG1 as a potential HIV therapeutic.

In contrast to what was seen with MG1, VSVΔ51 was unable to induce significant killing of HIV-infected cell lines or primary HIV infection models[159–162].

To increase the efficiency of MG1 therapy, killing by MG1 and selectivity of MG1 can be enhanced. To do this, this project aims to use pro-apoptotic small molecules called second

mitochondria derived activators of caspases (SMAC) mimetics as viral sensitizers, and pseudotyping MG1 with HIV envelope protein gp160 to optimize MG1-mediated killing.

1.5 Cell death pathways and their role in viral infection

Cell death can be broadly categorized into two: programmed cell death and necrosis. Necrosis occurs due to irreversible trauma, where the cell goes through an unprogrammed explosion[163]. Programmed cell death can be further divided into caspase dependent (e.g. apoptosis, pyroptosis), and caspase independent (e.g. necroptosis). In the following sections, three programmed cell death mechanisms that pertain to this project will be discussed.

- Pyroptosis

Pyroptosis or "fiery cell death" is an inflammatory form of cell death. It can be initiated canonically and non-canonically. In the canonical pathway, PAMPs and DAMPs are recognized via PRRs such as TLRs or NOD-like receptors (NLRs). PRRs then assemble with Inflammasome Adaptor Protein Apoptosis-Associated Speck-Like Protein Containing CARD (ASC) and pro-caspase-1, forming the inflammasome. Depending on what PRR is associated with the inflammasome, the inflammasome can have different names such as NLRP3 inflammasome or NRLC4 inflammasome. The caspase-recruitment domain (CARD) of ASC interacts with pro-caspase-1 to initiate its processing and activation[164]. Caspase-1 then cleaves Gasdermin D (GSDMD) into two, which then opens pores on the cell membrane, causing cell swelling and death. Furthermore, caspase-1 also cleaves IL-1β and IL-18 to their mature forms, which get released from the pores opened by GSDMD, causing inflammation[165]. In the non-canonical pathway, caspase-1 is bypassed and instead caspase-4/5/11 are activated in response to LPS stimulation.

GSDMD is cleaved by caspase-4/5, but IL-1β and IL-18 still need to be cleaved by caspase-1[166]. Chemical inhibitors of pyroptosis include but are not limited to the pan-caspase inhibitor ZVAD-fmk, and inflammasome inhibitors C172, glyburide, dapagliflozin[166].

- Apoptosis

Apoptosis is a tightly regulated, non-inflammatory form of cell death that not only occurs because of external stress factors or damage, but also naturally during development[167]. Apoptosis can happen through two main mechanisms: Intrinsic and extrinsic. Extrinsic apoptosis pathway requires engagement of death receptors with their respective death signal ligands. These receptors usually involve tumor necrosis factor (TNF) receptor superfamily. The best characterized ligand/receptor pairs are TNFα/ tumor necrosis factor receptor-1(TNFR1), Fas ligand (FasL)/Fas receptor (FasR), tumor necrosis factor-related apoptosis-inducing ligand (TRAIL)/TRAIL Receptor-1 (DR4) and TRAIL Receptor-2 (DR5)[168]. Upon the interaction of TNFα with its receptor, a complex containing TNF, TNFR-1, TNF Receptor-Associated Death Domain (TRADD), receptor-interacting serine/threonine-protein kinase 1 (RIPK1), TNF receptor associated factor 2 (TRAF2), and Fas-associated protein with death domain (FADD) forms and is called complex 2a. This complex aids in the maturation of caspase-8, which in turn activates caspases-3/7[169,170]. Signaling through FasL/FasR or TRAIL/DR4-5 results in recruitment of Fas-associated protein with death domain (FADD), and the cellular FLICE inhibitory proteins (c-FLIPs), and the formation of death-inducing signaling complex (DISC). This complex, similar to complex 2a, cleaves pro-caspase 8/10 into their active forms which then cleave caspase-3/7[171–173].

Intrinsic apoptosis pathway, also called the mitochondrial death pathway, is triggered when the cell is subjected to cytotoxic drugs, irradiation, and oxidative stress and is not receptor

mediated. These factors affect the mitochondrial membrane and result in the opening of mitochondrial permeability transition pores, where pro-apoptotic proteins are released into the cytosol[174]. The first proteins released are cytochrome *c*, SMAC and HtrA2/Omi[175,176]. Cytochrome *c* then binds apoptotic protease-activating factor 1 (Apaf1) and pro-caspase-9, forming the apoptosome. This complex formation triggers the cleavage of caspase-9, which in turn cleaves pro-caspase-3 and -7 to their mature forms, resulting in apoptosis[177]. Apoptosis can be inhibited by using pan-caspase inhibitors such as ZVAD-fmk, but this inhibition may switch cell death signaling to necroptosis[178].

Important protein families in the apoptosis pathway include Bcl-2 family proteins, inhibitors of apoptosis (IAP) proteins and SMAC. Bcl-2 family proteins contain both pro- (Bax, Bak, and Bid) and anti-apoptotic (Bcl-2, Bcl-X_L, and Mcl-1) members. Extrinsic apoptosis pathway can converge with the intrinsic pathway when Bid is cleaved by caspase-8 to form tBid, which subsequently locates to the mitochondrial membrane to kickstart the downstream events[179].

The anti-apoptotic IAPs are characterized by having a Baculovirus IAP repeat (BIR) domain in their N-terminus[180]. Currently, there are 8 identified IAP family members: cellular inhibitor of apoptosis protein-1 (cIAP1), cellular inhibitor of apoptosis protein-2 (cIAP2), X-linked inhibitor of apoptosis protein (XIAP,) neuronal apoptosis inhibitory protein (NAIP), survivin, Apollon, Livin, and inhibitor of apoptosis protein-related-like protein-2 (ILP-2)[181]. The best characterized of these proteins are cIAP1. cIAP2, and. XIAP. All three of these proteins contain a really interesting gene (RING) domain, which contributes to their ubiquitin (E3) ligase activity and Ub-associated domain (UBA). cIAP1 and cIAP2 also contain a caspase-recruitment domain (CARD)[182,183]. XIAP can bind to pro-caspase-9 with its BIR3 domain or to caspase-3/7 with its BIR2 domain, effectively preventing them from dimerization and subsequent activation[184,185]. On

the other hand, cIAP1 and cIAP2 can bind to TRAF2 with their BIR1 domain, and using their ubiquitin ligase activity, block the formation of complex 2a, and switch death ligand/death receptor signaling to the canonical NFκB pathway[186]. Moreover, cIAP1 and cIAP2 negatively regulate the non-canonical NFκB pathway by ubiquitinating and therefore causing the degradation of NF-κB-inducing kinase (NIK)[168].

SMAC are the best characterized inhibitors of the IAP family. The N-terminus of SMAC get cleaved upon their exit from the mitochondria, revealing an Ala-Val-Pro-Ile (AVPI) motif, which allows SMAC to bind to BIR3 domain of cIAP1, cIAP2, resulting in their autoubiquitination and degradation, and to the BIR 2 and BIR 3 domains of XIAP, preventing XIAP's interaction with caspase-9[187,188].

- Necroptosis

Necroptosis can be induced due to extracellular stress such as death ligand/death receptor, interferon gamma (IFN-γ)/IFNAR, dsRNA/Toll-like receptor-3 (TLR3) and dsDNA/Z-DNA binding protein-1 (ZBP1) signaling, and osmotic stress[189]. Necroptosis initiated through all these different signaling pathways converge at the point where Receptor Interacting Protein Kinases 1 (RIPK1) and Receptor Interacting Protein Kinases 3 (RIPK3) are recruited to the signaling cascade. When the signaling is initiated through TNFα/TNFR1, complex 1 consisting of TNFα, TNFR1, TRADD, TNFR-associated factor 2 (TRAF2), RIPK1, cIAP1and cIAP2, and linear ubiquitin chain assembly complex (LUBAC) forms on the cell membrane[190]. From here, the cell can undergo cell death via apoptosis or necroptosis depending on the presence of caspase-8[191], or persist to activate cell survival mechanisms. If the cell commits to the necroptosis pathway, downstream of the formation of complex 1, RIPK1/3 and mixed-lineage kinase domain–like

(MLKL) form the necrosome where RIPK3 mediated the phosphorylation of MLKL which results in MLKL oligomerization. Following this, MLKL translocates to the plasma membrane, where it binds to phosphatidylinositol phosphates, resulting in membrane pore opening and calcium efflux[192] which ends in the death of the cell. Unlike apoptosis, necroptosis is an inflammatory type of cell death, as DAMPs are released from the cell upon death[193]. Necroptosis can be blocked by the inhibition of RIPK1 via necrostatin-1[194].

- An intricate game of cell death

Most programmed cell death pathways are somewhat interconnected. As described previously, apoptosis can switch to necroptosis depending on the availability of caspase-8, FADD and caspase-8 can contribute to the activation of caspase-1 and IL-1β maturation[195], Influenza A virus (IAV) can induce RIPK3/caspase-8/NLRP3 dependent cell death[196], chemotherapy drugs can cause caspase-8 to cleave GSDMD, causing pyroptosis in breast cancer cells[197], caspase 1 can cleave pro-caspase-3 to initiate apoptosis in the absence of GSDMD[198], and in macrophages, independent of caspase-8, absent in melanoma-2 (AIM2) inflammasome can result in the cleavage of caspase-3 and therefore apoptosis[199]. All of this to say, in this intricate game of death, cell death mechanisms can be difficult to untangle from each other and that scientific discoveries can change our perspective on the exact way a cell undergoes death.

- HIV and cell death pathways

While cell death during HIV infection occurs mainly through apoptosis[200], both necroptosis and pyroptosis can occur in HIV-infected $CD4^+$ T-cells, when apoptosis is blocked[201,202].

Interestingly, most HIV proteins act as a double-edged sword, with most of them carrying both pro- and anti-apoptotic properties.

HIV Tat has been shown to upregulate caspase-8, FADD-like ICE (FLICE) [203], and CD178[204] in HIV-infected $CD4^+$ T-cell cultures. Moreover, Tat can cause bystander cell death, as monocytes treated with exogenous Tat have been shown to secrete the death ligand TRAIL, activating apoptosis pathways in bystander $CD4^+$ T-cells[205], and that internalization of the secreted Tat via vacuole can activate the pro-apoptotic protein Bim, triggering the intrinsic apoptosis pathway[206]. Conversely, anti-apoptotic effects of Tat include $CD4^+$ T-cells transfected with Tat upregulating anti-apoptotic proteins such as cFLIP and Bcl-2 and downregulating caspase-10 and being more resistant to FasL mediated apoptosis[207].

Vpr accumulation during HIV infection results in G2 phase cell cycle arrest and apoptosis[208]. Vpr can also upregulate the stress ligand natural killer group 2D (NKG2D) on $CD4^+$ T-cells, triggering natural killer (NK) cell mediated apoptosis[209]. Conversely, in early HIV infection, low concentrations of Vpr upregulates Bcl-2 and downregulates Bax, favoring anti-apoptotic pathways[210]. Moreover, Vpr has also been shown to upregulate survivin, an anti-apoptotic factor that increases the stability of XIAP[211].

Membrane bound and soluble versions of gp120, the HIV envelope glycoprotein, have been shown to bind to CD4 receptor, resulting in the death of HIV-infected and bystander cells[212,213]. Conversely, gp120 has been shown to upregulate cIAP1, cIAP2, and XIAP in HIV-infected macrophages[50].

1.6 Enhancing MG1-mediated killing – using SMAC mimetics as viral sensitizers

- Oncolytic viruses and viral sensitizers in cancer

Combining oncolytic viruses with small molecules to enhance their effectiveness has been of increasing interest in the cancer field. These small molecules aim to inhibit antiviral signaling pathways thereby increasing viral propagation and/or infection and activate pro-apoptotic pathways of the host cell to enhance the efficiency of killing target cells. Viral sensitizers such as ruxolitinib[214] and vorinostat[215] target JAK/STAT signaling, bortezomib[216] and sunitinib[217] target the NFκB pathway, and rapamycin[218] and torin1[219] target the PI3K/Akt/mTOR pathway to dampen IFN 1 response and thus increase oncolytic virus infection. Other viral sensitizers can target the apoptosis pathway to increase cell death, such as SMAC mimetics.

- SMAC mimetics

SMAC mimetics are small pro-apoptotic molecules that mimic NH_2-AVPI binding motif of endogenous SMAC proteins. Similar to SMAC proteins, SMAC mimetics can efficiently bind to the BIR domains of cIAP1, cIAP2 and XIAP proteins to antagonize them by either (1) preventing their binding to caspases or (2) activating their E3 ligase activity, resulting in their subsequent degradation[168,220]. Due to the roles of cIAP1, cIAP2 and XIAP proteins, SMAC mimetics can promote TNFα dependent or independent apoptosis[221–223], or TNFα dependent necroptosis[224]. SMAC mimetics can be broadly classified as monovalent, i.e. having one -AVPI binding motif such as LCL-161 (Novartis) and Debio-1143 (Ascenta Therapeutics) or bivalent, i.e. having two -AVPI binding motifs such as AEG-40730 (Aegara Therapeutics) and birinapant (Tetralogic Pharmaceuticals).

- Cancer and SMAC mimetics

As evasion of apoptosis is one of the hallmarks of cancer, using SMAC mimetics are an attractive candidate for cancer therapy[225]. Different SMAC mimetics have been used in a variety of cancer cell lines to induce cell death, as several cancers such as liver and pancreatic cancer have upregulated expression of IAPs[170,226,227]. Currently, there are 6 completed clinical trials with SMAC mimetics, 3 of them with the monovalent SMAC mimetic LCL-161 against relapsed or refractory myeloma (Phase II, NCT01955434), primary myelofibrosis (Phase II, NCT02098161), and multiple myeloma (Phase I/II, NCT03111992), 3 of them with the monovalent SMAC mimetic Debio 1143 for tolerability (Phase I, NCT01078649,Phase Ib/II, NCT04122625,) and against advanced solid malignancies (Phase Ib,NCT03270176). Both LCL-161 and Debio 1143 have shown good tolerability and improved control of the disease.

- HIV and SMAC mimetics

SMAC mimetics are explored as a potential therapeutic agent in HIV due to the dysregulation of apoptosis pathways in HIV-infected cells. In HIV-infected cells, SMAC mimetics can either a) reverse latency via the activation of non-canonical NFκB pathway or b) kill HIV-infected cells (Figure 2).

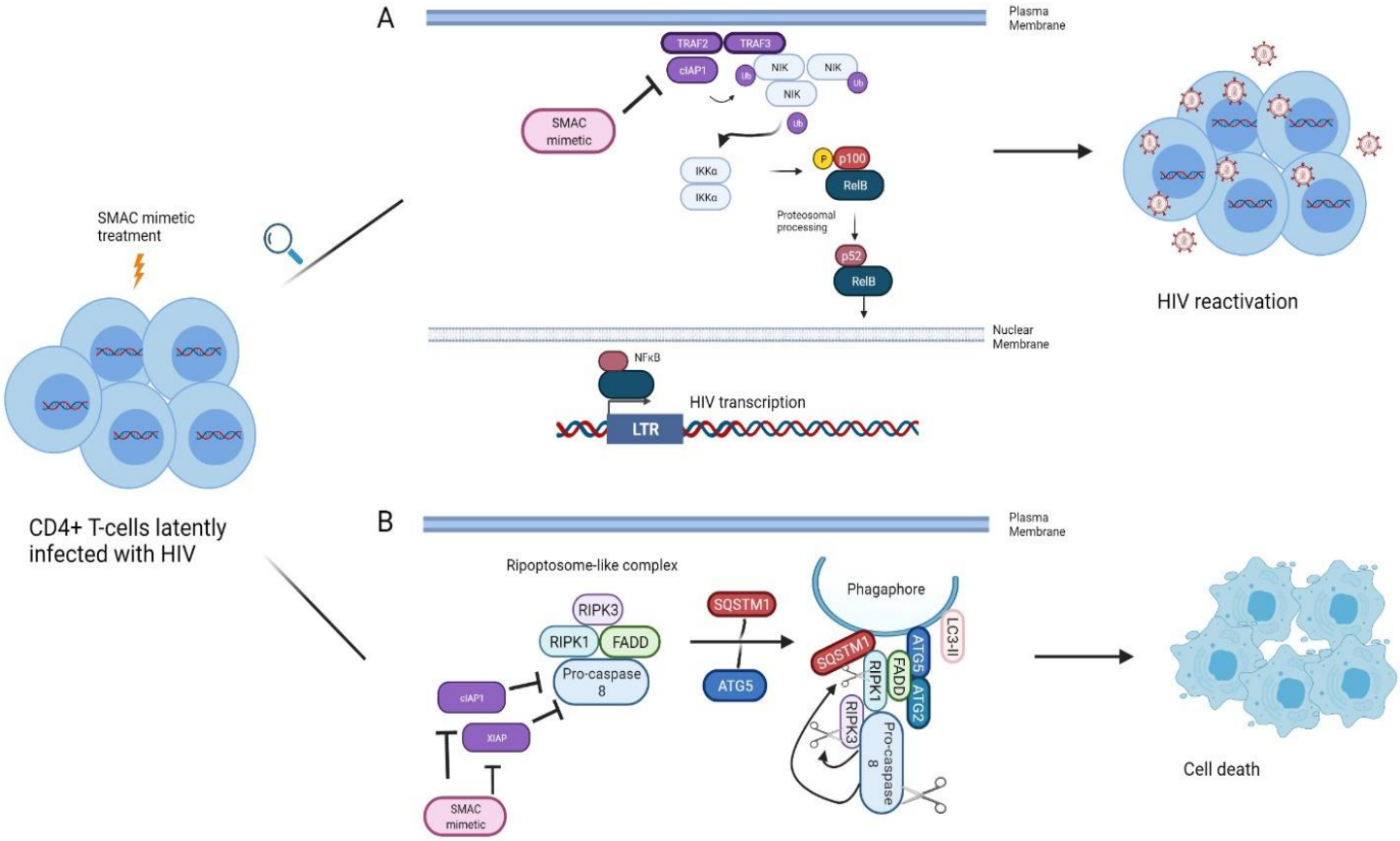
A
Plasma Membrane
TRAF2
TRAF3
cIAP1
NIK
NIK
NIK
Ub
SMAC mimetic
IKKα
IKKα
P
p100
RelB
Proteosomal processing
p52
RelB
Nuclear Membrane
NFκB
HIV transcription
LTR
HIV reactivation
SMAC mimetic treatment
CD4+ T-cells latently infected with HIV
B
Plasma Membrane
Ripoptosome-like complex
RIPK3
RIPK1
FADD
Pro-caspase 8
cIAP1
XIAP
SMAC mimetic
SQSTM1
ATG5
Phagaphore
SQSTM1
LC3-II
ATG5
ATG2
FADD
RIPK1
RIPK3
Pro-caspase 8
Cell death

Figure 2, Effect of SMAC mimetics on latently HIV-infected cells. Upon SMAC mimetic treatment, latently HIV-infected cells have been shown to undergo A) Latency reversal due to degradation of cIAP1 and cIAP2 via SMAC mimetics and subsequent activation of the non-canonical NFκB pathway. Or B) Cell death that utilizes apoptosis and autophagy machinery. Adapted from Molyer et al., 2021

a) SMAC mimetics as latency reversal agents

The SMAC mimetic SBI-0637142 has been used in the latently infected cell line J-lat 10.6 and increased HIV expression as measured by GFP expression following treatment was observed. This effect was increased when SBI-0637142 was used in combination with the HDACi panobinostat. Furthermore, when resting $CD4^+$ T-cells isolated from PLHIV were treated with SBI-0637142, latency reversal comparable to the degree of stimulation with CD3 and CD28 was observed[228]. Furthermore, Ciapavir, the second generation design of the SMAC mimetic SBI-0637142 with increased potency, proved more potent than SBI-0637142 in reversing latency both in the J-lat 2D10 cells as measured by GFP expression, and humanized HIV-infected bone-liver-thymus (BLT) mouse model as measured by HIV *gag* mRNA expression, without causing significant toxicity or activation of T-cells.[229]

The bivalent SMAC mimetic AZD5582 has also shown to induce HIV replication in resting $CD4^+$ T-cells from PLHIV on cART, and was able to increase SIV production to more than 60 copies/mL in cART suppressed SIV infected rhesus macaques, without inducing global T-cell activation[230]. AZD5582 has also been used in combination with dual affinity targeting (DART) with bispecific CD3 and HIV envelope targeting. The aim of this study was to reverse latency with the AZD5582, and then target $CD8^+$ T-cells to HIV envelope expressing cells (achieved by latency reversal) in simian/human immunodeficiency virus (SHIV) infected, cART treated rhesus macaques. However, no significant increase in SHIV RNA was observed, and the DART targeting did not result in a significant decrease in SHIV DNA in the $CD4^+$ T-cells of the peripheral blood, lymph node, or bone marrow[231].

b) SMAC mimetics to kill latently infected cells

The bivalent SMAC mimetic birinapant has been shown to kill latently HIV-infected promonocytic cell line U1 and lymphocytic cell line ACH2. A stronger killing affect was observed when birinapant was combined with PKC activator PEP0005 due to the increased production of TNFα upon PEP0005 treatment, resulting in TNFα-dependent apoptosis[232].

HIV infection upregulates cIAP1 and XIAP in *in vitro* infected central memory $CD4^+$ T-cells (T_{CM})[233,234]. The SMAC mimetics birinapant and GDC-1052 was able to successfully degrade these IAPs and cause TNFα independent death of HIV-infected T_{CM} via a mixture of autophagy and apoptosis pathways. The proposed mechanism of this cell death pathway is autophagy machinery serving as a scaffold on which DISC can form to induce cell death[234] (Figure 2, B).

Similar to HIV-infected T_{CM}, XIAP and cIAP1 expression is significantly higher in *in vitro* HIV-infected MDM[223]. The SMAC mimetics birinapant, LCL-161, and Debio 1143 were each able to induce killing in a TNFα dependent manner, again with a mixture of autophagy and apoptosis[223]. In another study, LCL-161 and the bivalent SMAC mimetic AEG-40730 was able to kill the HIV-infected cell line U1 significantly greater than its uninfected parental cell U937, and specifically kill persistently HIV-infected MDM while leaving bystander cells relatively unharmed (as measured by cell death in HSA+ and HSA- populations), possibly through a RIPK1 mediated mechanism. This killing was TNFα dependent in U1 cells but TNFα independent in HIV-infected macrophages. Cell death of HIV-infected macrophages was increased when LCL-161 was combined with the RIPK1 inhibitor necrostatin-1, showing that RIPK1 may also be a key mediator in cell death of HIV-infected MDM[235].

Taken together, of these results show that the effect of SMAC mimetics on HIV-infected cells depend heavily on the SMAC mimetic and cell line/HIV infection model used.

- Combination treatment with SMAC mimetics and oncolytic viruses

As can be seen in the examples in the previous section, the effect of SMAC mimetics can enhance the activity of a number of other agents. Especially in the cancer field, SMAC mimetics have been used with oncolytic viruses to enhance the effect of OV therapy. LCL-161 has been used with the oncolytic alphavirus M1 on refractory hepatocellular and colorectal cancer cell lines to induce ER stress mediated apoptosis. The usage of LCL-161 increased bystander killing affect and increased replication of M1 virus[236]. When EMT6, a syngeneic breast carcinoma tumor, bearing mice were treated with a combination of LCL-161 and VSVΔ51, there was significant increase in mouse survival and slowed tumor growth rate. Treatment with TNFα blocking antibodies abrogated this affect, showing TNFα dependency[237]. In another study, combination of LCL-161 and VSVΔ51 in EMT6 tumor bearing mice, promoted $CD8^+$ T-cell accumulation in the tumor, polarized tumor-associated macrophages into M1 state, and worked as a nonspecific adjuvant to increase tumor cell killing. Interestingly, this study has pointed out that the administration order of SMAC mimetic and oncolytic virus is of importance, as in this model pre-treatment with LCL-161 demonstrated no therapeutic synergy[238]. In other studies, LCL-161 combination with VSVΔ51 armed with TNFα in EMT6 tumor bearing mice have led to vascular shutdown, tumor cell death, and durable cures[239]. Furthermore, in a study that directly armed VSV with a SMAC mimetic called VSV-S showed that VSV-S induces apoptosis in breast cancer cells via the intrinsic apoptosis pathway, and that when mice bearing the highly aggressive 4TI breast cancer tumors were treated VSV-S, a decrease in tumor weight and tumor volume could be observed[240].

Considering the individual effects of the oncolytic virus MG1 and SMAC mimetics on HIV-infected cells, these studies suggest combining SMAC mimetics with MG1 may increase MG1-mediated killing of HIV-infected cells.

1.7 Enhancing the selectivity of MG1-mediated killing - pseudotyping MG1 with HIV envelope protein

Pseudotyping viruses refers to partially or completely changing the native glycoprotein of a virus to that of another. This strategy can be employed to study viral entry mechanisms of high containment level viruses in biosafety level 2 conditions such as for Ebola Virus[241] and coronavirus[242,243], for vaccine development[244,245], study of neutralizing antibodies[246,247], or to limit or change tropism of virus[248]. Pseudotyping can be transient, i.e. limited to one cycle of replication or permanent, i.e. permanently changing the viral glycoprotein.

Although no work has been done with pseudotyping Maraba virus yet, there are many studies that have employed VSV to pseudotype it with the HIV envelope protein. These approaches range from using the full length HIV envelope gp160[249], to using truncated versions of gp160[250], to fusing HIV gp120 with the CT-tail of the VSV-G glycoprotein[245,251]. All of these approaches have succeeded in limiting the tropism of VSV to cells that express the receptor/co-receptors for HIV which resulted in the specific infection of target cells of HIV

Given the success with VSV, pseudotyping MG1 with HIV envelope protein can also be successful in limiting MG1's tropism to CD4 and CCR5 expressing cells, effectively limiting MG1's tropism to target cells of HIV, and thus enhancing the specificity of MG1 (Figure 3).

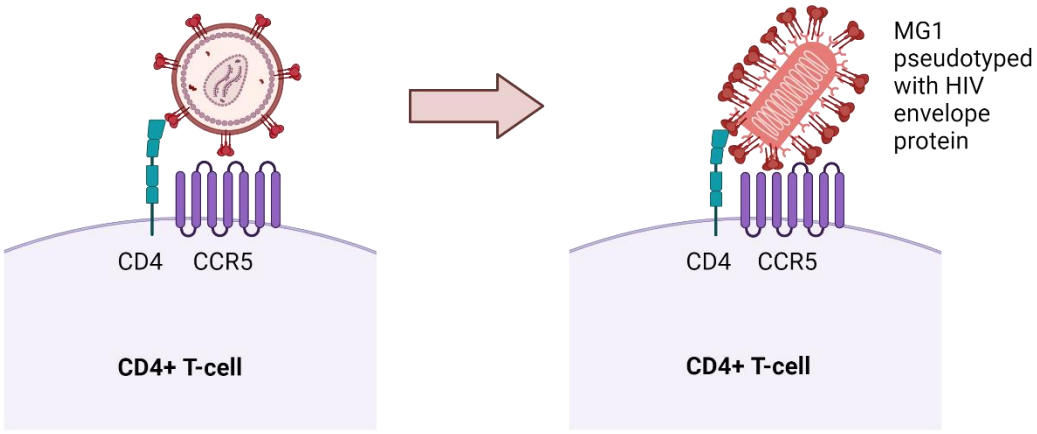
CD4
CCR5
CD4+ T-cell
MG1
pseudotyped
with HIV
envelope
protein
CD4
CCR5
CD4+ T-cell

Figure 3, MG1 pseudotpyed with HIV envelope would have limited tropism, only being able to infect cells that express CD4 and CCR5, the receptor and co-receptor for HIV. Made with BioRender.

1.8 Rationale

MG1 has been shown to selectively target and kill cell lines latently infected with HIV, $CD4^+$ T-cell latent HIV infection models, *ex vivo* infected persistently infected monocyte derived macrophage models and alveolar macrophages obtained from people living with HIV. For MG1 to be used in the clinic, its killing and specificity can be enhanced. To enhance MG1-mediated killing, small pro-apoptotic molecules called SMAC mimetics can potentially be used. SMAC mimetics have been shown to selectively kill HIV-infected cells, and have been shown to sensitize cancer cells to oncolytic virus mediated death. To increase the specificity of MG1, MG1 can be pseudotyped with HIV envelope protein gp160, to limit its targets to that of HIV.

1.9 Hypothesis

`

It is hypothesized that combination of MG1and modified versions of MG1 with SMAC mimetics (AEG 40730, LCL 161 and birinapant) can be used to enhance MG1 infection and killing

1.10 Project Aims

The first aim of this project is to determine if SMAC mimetics sensitize HIV-infected cell lines and *ex vivo* HIV-infected monocyte derived macrophages to MG1-mediated death. The second aim of this project is to pseudotype MG1 with HIV envelope protein gp160 to reduce MG1's tropism and increase its specificity to target cells of HIV.

Overall, this project aims to enhance the killing and specificity of MG1 to HIV-infected cells.

Chapter 2

Methodology

2.1 Reagents

2.1.1 Media

Gibco® Roswell Park Memorial Institute 1640 medium (RPMI-1640) with phenol red indicator, Gibco® Dulbecco's Modified Eagle's medium (DMEM), and Gibco® phosphate buffered saline (PBS) powder, ands OPTI-MEM were purchased from Thermosphere Scientific (Ottawa, ON). Endotoxin-free Dulbecco's PBS, pH 7.4 was purchased from Millipore-Sigma. Reagents to supplement the media are heat-inactivated fetal bovine serum (FBS), penicillin (100units(U)/mL) and streptomycin (10 go/mL) (PenStrep), puromycin (1ug/mL), zeocin, plasticising and L-glutamine (ThermoFisher Scientific), heat-inactivated human AB serum (Valley Biomedical, Winchester, Virginia).

2.1.2 Cloning Reagents

The restriction enzyme Acc651 (Cat# R0599), T4 DNA ligase (Cat# M020), Q5 site directed mutagenesis kit (Cat# E0554S), Gibson Assembly® Cloning Kit (Cat# E5510S), and NEB® 10-beta Competent E. coli (High Efficiency) (Cat# C3019H) were obtained from New England Biolabs (Whitby, ON). FastAP dephosphorylase (Cat# EF0651) was obtained from ThermoFisher Scientific.

2.1.3 Transfection Reagents

Lipofectamine® 2000 Transfection Reagent was purchased from Invitrogen (Burlington, ON). Gibco™ Opti-MEM™ Reduced Serum Media was purchased from ThermoFisher Scientific. FuGENE® HD Transfection Reagent (Cat# E2311) and FuGENE® 4K Transfection Reagent (Cat# E5911) was purchased from Promega. GeneJuice® Transfection Reagent (Cat# 70967-5) was purchased from Millipore Sigma.

2.1.4 Cell stimulation and SMAC mimetics

Recombinant human M-CSF (carrier-free) (Cat # 574802) was purchased from Biolegend. Human TNF-alpha recombinant protein (Cat# PHC3015) was purchased from ThermoFisher Scientific. Low molecular weight Poly(I:C) (Cat# TLRL-PICW) was purchased from Cederlane. Cell activation cocktail (without Brefeldin A) (Cat# 89CHF) was purchased from Biolegend, The SMAC mimetic AEG-40730 (Cat# 5330) was purchased rom Tocris Bioscience, LCL-161 (Cat# S7009) and birinapant (Cat# S7015) and camptothecin solution (Cat#S1288) were purchased from Selleck chemicals (Burlington, ON). Staurosporine solution (Cat# S6942) was purchased from Millipore. Pan-caspase inhibitor Z-VAD-FMK (Cat#2163) was purchased from Biotechne and Necrostatin1-s (Cat#17802) was purchased from Cell Signaling Technology.

2.2 Ethics statement

Experiments relying on the participation of healthy volunteers were approved by The Ottawa Health Science Network Research Ethics Board. Healthy volunteers provided written informed consent to partake in the study.

2.3 Cell culture

2.3.1 Cell lines

Vero (CCL-81), Jurkat, and HEK-293T (CRL-3216) cells were obtained from (American Type Culture Collection (ATCC, Manassas, VA). TREx ™-293 cells expressing VSV G were a gift from Dr. Carolina Ilkow. GHOST (ARP-3944) cells were obtained through the NIH HIV Reagent Program, Division of AIDS, NIAID, NIH contributed by Dr. Vineet N. Kewal Ramani and Dr. Dan R. Littman. J1.1 (ARP-1340) cells were obtained through the NIH HIV Reagent Program, Division of AIDS, NIAID, NIH contributed by Dr. Thomas Folks[252], OM10.1 (ARP-

1319) cells were obtained through the NIH HIV Reagent Program, Division of AIDS, NIAID, NIH contributed by Dr. Salvatore Butera[253].

Vero and 293T cells were cultured in DMEM with 10% FBS and PenStrep in T75 cell culture flasks (FalconTM, Fisher Scientific), GHOST cells were cultured in DMEM with 10% FBS, 1 ug/mL puromycin and PenStrep in T75 culture flasks and TRex-293 cells were cultured in DMEM with 10% FBS and PenStrep in T75 cell culture flasks with the addition of blasticidin (300 µg/mL) and zeocin (5 µg/mL) every other day. Cells were routinely split every 2-3 days to maintain the cell monolayer by detachment via TrypLE (GibcoTM, ThermoFisher Scientific) in a total volume of 10 mL. J1.1 and OM10.1 cells were cultured in RPMI-1640 medium, supplemented with 10% FBS, PenStrep, and L-Glutamine (2mM), in T75 flasks. Cells were maintained at $0.2x10^5$ to $1x10^6$ cells/ml by passaging every 2-3 days.

2.3.2 Isolation of peripheral blood mononuclear cells (PBMC)

Peripheral blood was drawn from healthy donors into sterile 60 ml syringes, containing 100U/ml filter-sterilized Heparin Sodium (LEO Pharma Inc., Thornhill, ON). Following collection, 30 ml of whole blood was layered over 15 ml of Lymphoprep™ density gradient medium (Stemcell Technologies, Vancouver, BC) and centrifuged at 400 x g for 30 minutes (Megafuge 1.0, Heraeus Instruments, Germany) without braking. The buffy coats from individual donors were then collected into 50 ml Falcon tubes and topped up with PBS to 50 ml. Cells were pelleted by centrifugation at 300 x g for 20 minutes. Cell pellets from individual donors were then pooled in one 50ml Falcon tube, and cells were washed twice with PBS at 400 x g for 10 minutes. Following the final wash, peripheral blood mononuclear cells (PBMC) were counted by trypan blue exclusion and resuspended at an appropriate concentration and plated on an appropriate dish for further experiments.

2.3.3 *in vitro* generation of monocyte-derived macrophages

Following PBMC isolation, cells were resuspended at $6.25x10^6$/ml in warm, serum-free RMPI-1640 supplemented with PenStrep in 100 cm^2 untreated round culture plates (Sarstedt, Nümbrecht, Germany) and left to adhere for 2 hours at 37°C. Plates were washed 3 times with endotoxin-free PBS (pH 7.4, GibcoTM) to remove non-adherent lymphocytes, and 10ml of warmed RPMI-1640, supplemented with PenStrep and 10% heat-inactivated human AB serum (MDM media), and M-CSF (25u/ml) was added to the plate. Adherent cells were incubated at 37°C with 5% CO2 for a total of 7 days. At 3 days post-plating, cells were washed twice with warmed endotoxin-free PBS, and 20ml of MDM media was added to the plate. On day 8, adherent MDM were washed twice with endotoxin-free PBS, detached using 5 mL prewarmed accutase (Millipore-Sigma) and gentle pipetting, and counted by trypan blue exclusion. MDM were then pelleted by centrifugation (300 x g for 10min), resuspended at $2.5x10^5$ cells/ml in MDM media, and plated in 24 well non-treated culture plates (Sarstedt, Nümbrecht, Germany) for further experiments.

2.4 Production of virus stocks

2.4.1 HIV Amplification

The HIV NL4.3 BAL-IRES-HSA plasmid, encoding the CCR5-tropic (R5-tropic) virus, was obtained from Dr. Michel J. Tremblay at Université Laval, and was amplified on HEK-293T cells, as follows. Cells were seeded at $2x10^6$ cells/T75 flask and grown until confluent. Once confluent, the cells were transfected with 20 μg of purified plasmid using Lipofectamine™ 2000 and Opti-MEM™ Reduced Serum media, according to the manufacturer's protocol. Mock-infected stocks were made in parallel where an equivalent volume of PBS was added to the

Lipofectamine™/Opti-MEM™ instead of the HIV plasmid. Transfected cells were incubated at 37°C for 48 hours, after which culture media was collected, centrifuged (460 x g, for 10min), and filtered sequentially through 0.45µm and 0.22µm polyvinylidene fluoride (PVDF) filters (UltiDent Scientific, St. Laurent, QC) suing 50 mL syringes. Virus stocks were aliquoted at 1 mL and stored at -80 °C. HIV p24 antigen concentration was measured after one freeze/thaw cycle using the HIV-1 p24 Antigen Capture Kit (Frederick National Laboratory for Cancer Research, Frederick, MD; NIH AIDS Reagent Program), as per manufacturer protocol.

2.4.2 Oncolytic Virus Amplification

MG1- eGFP recombinant oncolytic virus was obtained from Dr. John and propagated on Vero cells. Briefly, Vero cells were grown to confluence in T75 tissue culture flasks 37°C. Cells were then infected at MOI 0.01with MG1 in 1ml of serum-free DMEM (containing PenStrep) at 37°C for 1hr. Following the incubation, 9 mL DMEM containing PenStrep and 2% FBS were added per flask, and the cells were incubated at 37°C for 24 hours. After the incubation, culture supernatants were collected and spun down at 300 x g for 10 minutes and filtered through a 0.2µm pore Nalgene bottle top filter (Nalgene Nunc, Rochester, NY). The filtered supernatants were then centrifuged at 22000 x g (Avanti JXN-26, Beckman Coulter, Brea, CA) for 1.5 hours at 4°C, after which the viral pellet was resuspended in PBS, aliquoted, and stored at -80°C.

2.4.3 MG1 titration by standard plaque assay

The MG1 stocks were titered in duplicate by 10-fold serial dilution, starting at a dilution factor of $1x10^7$ and ending at a dilution factor of $0.5x10^9$. Briefly, Vero cells were infected with 100 ul of appropriate dilution of MG1 stock at 37ºC for 1h, after which the cells were overlaid with a mixture of 1:1 1% agarose in ddH_2O and 2X DMEM. At 24 hours post-infection, plaques were visualized by crystal violet staining and viral titer was determined by counting the plaques.

For viral titering of MG1 from MG1 and birinapant treated cells, J1.1 cells were infected with MG1 and concurrently treated with birinapant as explained below. 48hpi, supernatant was collected and centrifuged to get rid of dead cells. Following this, Vero cells were infected with the supernatant that was diluted 10 fold as described above. 48hpi, plaques were visualized by crystal violet staining.

2.4.4 Rescue of wildtype MG1 and MG1 clones

A VSV rescue protocol was used to rescue WT MG1 and the MG1 clones. Briefly, Vero cells were infected with T7 polymerase expressing Vaccinia virus (T7 VV, gifted by Dr. Carolina Ilkow) at MOI 1. After infection, the cells were transfected with MG1 single gene plasmids containing MG1 N (1 µg), MG1 P (1.25 µg) MG1 L (0.25 µg) and MG1 backbone (2 µg) using Lipofectamine 2000. After 48h post incubation, VV was filtered out using 0.22 µm filter, and the remaining supernatant was used to amplify the rescued virus. The optimizations made to this protocol are discussed in detail in chapter 5.

2.5 Molecular biology

2.5.1 Cloning

Full length HIV envelope gp160 insert was generated from C clade p96zm651 HIV envelope expression vector (ARP-8662 obtained through the NIH HIV Reagent Program, Division of AIDS, NIAID, NIH, contributed by Drs. Yingying Li, Feng Gao and Beatrice H. Hahn) by adding the cut-sites of the Acc651 restriction enzyme and artificial start and stop codons by PCR. Both the insert and the backbone vector were cut by Acc65, and the backbone was dephosphorylated using FastAP dephosphorylase. The insert was ligated between the M and eGFP genes in the MG1 G-less backbone (gifted by Dr. Carolina Ilkow) using T4 ligase, and the ligation

mixture was transformed into *E.coli* NEB beta-10. The transformed bacteria were screened for the insert with colony PCR, using directional primers.

The modified MG1 clone containing a truncated version of gp160 (MTM_4aa), was generated by truncating the HIV envelope until 4 amino acids after the transmembrane region. Following this, MG1 G-less backbone was linearized by inverse PCR, and overlapping regions were added to both the insert and the backbone. The truncated clone was generated by Gibson Assembly.

The truncated insert used to generate MTM_4aa was cloned into the MG1 backbone, between the M and the CT region of MG1 G glycoprotein using Gibson Assembly to generate the MCT clone.

Maraba virus specific start/stop signal (5' TGTATGAAAAAAACTCATCAACAGCCATC 3')[254] was later added between gp160 and eGFP using Q5 site directed mutagenesis kit. Briefly, two back-to-back primers, each containing half of the start/stop signal were designed. Inverse PCR was done using these primers on the MGp160 clone plasmid, and the PCR product was ligated back together using the Kinase-Ligase-Dpn1 enzyme mix. This mixture was then transformed into *E.coli* NEB beta-10.

All of the clones were confirmed by full plasmid sequencing done by Plasmidsaurus.

2.5.2 Integrated HIV DNA PCR

Prior to the PCR, cells were lysed in appropriate volume of lysis buffer containing 0.1M Tris-HCl (pH: 8) (final concentration 10 mM), 0.5M KCl (final concentration 50 nM), 10mg/mL Proteinase K (final concentration 400 µg/mL), and incubated overnight in a heated shaker at 55ºC.

The following morning, the proteinase K was inactivated at 95ºC for 5 minutes, and the lysed cells were directly used for PCR.

Two-step nested PCR targeting CD3 and integrated HIV DNA was performed with previously described primer-probe sets. In step 1 preamplification, both CD3 and HIV proviral DNA was amplified in triplicate with 7.5 µl of lysate, 12.5µl of iQTM Supermix (BioRad), 0.75µl of the HCD3OUT3', HCD3OUT5', ALU1, and ALU2 primers (300nM each), 0.375µl of the ULF1 primer (150nM), and 1.625µl DNase-free/RNase-free H_2O (Sigma-Aldrich). A standard curve of 10 fold diluted ACH-2 cells (30000 to 3 cells) was run in parallel to quantify HIV proviral DNA copy number. The amplification conditions were as follows: 95ºC, 3 minutes for denaturation, 95 ºC for 1 minute, 55ºC for 1 minute, 72ºC for 10 minutes (for 12 cycles) and 72 ºC for 15 minutes for elongation.

Step 1 PCR products were diluted 1:5 in ddH_2O to be run in Step 2. In Step 2, proviral HIV DNA and CD3 were amplified separately in a 20µl reaction mix containing 6.4µl of the diluted Step 1 PCR products, 10µl of SsoAdvancedTM Universal Probes Supermix (BioRad), 3.6µl DNase-free/RNase-free H2O, and either: 0.25µl of HCD3IN5' and HCD3IN3' (1250nM each) and 0.5µl of CD3 FamZen Probe (200nM) for the CD3 reaction, or 0.25µl of LambdaT and UR2 (1250nM each) and UHIV FamZen Probe (200nM) for the proviral HIV DNA reaction. The amplification conditions were as follows: 95ºC, 4 minutes for denaturation, 95ºC, 3 seconds, 60ºC for 10 seconds (single acquisition for FAM) (for 40 cycles). All PCRs were run using the CFX ConnectTM Real-Time PCR Detection System (BioRad).

Primer and probe sequences used in cloning and PCR can be found in Table 2.

Target	Primer or probe name	Sequence (5' to 3')
CD3	HCD3OUT5	ACT GAC ATG GAA CAG GGG AAG
	HCD3OUT3	CCA GCT CTG AAG TAG GGA ACA TAT
	HCD3IN5	GGC TAT CAT TCT TCT TCA AGG T
	HCD3IN3	CCT CTC TTC AGC CAT TTA AGT A
	CD3 FAMZEN probe	56-FAM/AG CAG AGA A/ZEN/C AGT TAA GAG CCT CCA T/3IABkFQ
HIV	ULF1	ATG CCA CGT AAG CGA AAC TCT GGG TCT CTC TDG TTA GAC
	ALU1	TCC CAG CTA CTG GGG AGG CTG AGG
	ALU2	GCC TCC CAA AGT GCT GGG ATT ACA G
	LambdaT	TG CCA CGT AAG CGA AAC T
	UR2	CTG AGG GAT CTC TAG TTA CC-
	UHIV FAMZEN probe	/56-FAM/CA CTC AAG G/ZEN/C AAG CTT TAT TGA GGC /3IABkFQ/
gp160 insert generation	gp160_F	TAT GGT ACC ATG CGC GTG CGC GAG AT
	gp160_R	AAA GGT ACC TTA CAG CAG GGC GGT CTC GA
generation of MTM_4aa	Vector_f	TCG TGA ACC GCG TGC GCT AAG GTA CCC AGT TAT ATT TGT TAC AAC AAT GG
	Vector_R	AGG ATC TCG CGC ACG CGC ATT TAG TTT TTT TCA TAG TCT GCC CAT CAC C
	Fragment_F	CAG ACT ATG AAA AAA ACT AAA TGC GCG TGC GCG
	Fragment_R	AAC AAA TAT AAC TGG GTA CCT TAG CGC ACG CGG TTC AC
	vector_CT tail_F	GCA TCG TGA ACC GCG TGC GCG TTG CGA TTC GCT ATA AAT ACA AGG G

Generation of Mct	vector_CT tail_R	AGG ATC TCG CGC ACG CGC ATT GTT GTA ACA AAT ATA ACT GGG TAC CTC GA
	fragment_CT tail_F	CAG TTA TAT TTG TTA CAA CAA TGC GCG TGC GCG AG
	fragment_CT tail_R	TAT TTA TAG CGA ATC GCA ACG CGC ACG CGG TTC ACG
insertion of conserved VSV sequence in Mgp160	KLD_F	CAT CAA CAG CCA TCA CCC AGT TAT ATT TGT TAC AAC AAT GGT G
	KLD_R	AGT TTT TTT CAT ACA CCT TAC AGC AGG GCG GTC

Table 2, primer and probe sequences used in PCR and cloning reactions.

2.5.3 RNA isolation and RNA sequencing

J1.1 cells were either left untreated, infected with MG1 MOI $1x10^{-3}$, treated with 1 µM birinapant or concurrently treated with MG1 and birinapant for 48 hours. RNA was extracted using Qiagen RNeasy Mini Kit (Cat# 74104).

RNA sample quality assessment was performed with the Fragment Analyzer (Agilent) and concentration measured with the Qubit 3.0 (Thermo). NGS libraries were prepared with the Stranded mRNA library prep kit (Illumina) using 500 ng of RNA input. Sequencing was performed with the Nextseq 2000 P3 100 cycle flow cell (Illumina). We would like to acknowledge the assistance of StemCore Laboratories Genomics Core Facility (OHRI, uOttawa), RRID:SCR_012601.

Analysis was performed using GENCODE[255] v46 annotations and the GRCh38 genome assembly. The nf-core/rnaseq[256] version 3.14.0 was used to generate the quality assessment and read pseudocounts table. Fold change analysis was performed using the R bioconductor library DESeq2[257] with fold change shrinkage performed using the apeglm library[258] Enrichment analysis on the above generated fold change tables was performed using g:Profiler with GO biological term database with term size between 2-500. We would like to acknowledge the assistance of the Ottawa Bioinformatics Core Facility (uOttawa/OHRI), RRID:SCR_022466.

2.6 SMAC mimetic treatment

J1.1 cells and OM10,1 cells were plated at $1x10^6$ cells/mL in 500 µl in 24 well plates. Cells were then treated with different doses of SMAC mimetics AEG-40730 (Tocris Bioscience) (2µM – 6µM), LCL-161(Selleckchem) (2µM – 20µM) or birinapant (Selleckchem) (1µM – 2µM) in a total volume of 1 mL in R10 media. Cell viability and surface receptor expression was measured

48h post treatment by flow cytometry. Cell-free supernatants were collected to asses p24 and cytokine production.

HIV-infected MDM were plated at $2x10^5$ cells/mL in untreated 24 well plates, and treated with the SMAC mimetics AEG-40730, LCL-161 or birinapant with doses 2µM – 8µM in a total volume of 1 mL in MDM media. Frequency of HSA expressing cells, cell surface marker expression and cell viability were determined by flow cytometry.

2.7 Viral infection

2.7.1 *in vitro* HIV infection of monocyte derived macrophages

On day 9 of generation, MDM were washed once with prewarmed endotoxin-free PBS. HIV- NL4.3 BAL-IRES-HSA was added to cells at a ratio of 100ng of p24 per $1x10^6$ MDM in 500 µl. After an overnight incubation at 37°C with 5% CO2, the cell media volume was doubled to 1 mL using MDM media. Cells were then incubated for 6 days at 37°C with 5% CO2, with a 1/2 media change performed at 3dpi. At 6dpi, cells were prepared for other experiments.

2.7.2 MG1 infection

J1.1 and OM1.1 cells were plated at $1x10^6$ cells/mL in 200 µl. In 24 well plates, and infected with MG1 doses MOI 1- $1x10^{-5}$ in 300 µl R10 media for 2 hours after which the media was topped up to 1 mL/well. Cell viability was assessed using flow cytometry via PI staining.

HIV-infected MDM were infected with MOI 1 of MG1 in 250 µl for 2 hours after which the media was topped up to 1 mL/well with MDM media. Frequency of HSA expressing cells and cell viability were determined by flow cytometry.

2.8 Combination treatment with MG1 and SMAC mimetics

2.8.1 MG1 infection and concurrent SMAC mimetic treatment

J1.1 cells and OM10.1 cells were plated at $1x10^6$ cells/mL and were infected with MG1 (MOI $1x10^{-1}$ to $1x10^{-4}$) for two hours in 300 µl in R10 media. Following the infection, cells were topped up to 1 mL/well with appropriate concentration of each SMAC mimetic (AEG 40730, LCL 161 or birinapant at a concentration range 1µM – 20 µM). At 24h and 48h post infection, cell death, infection and casp3/7 activation were measured by flow cytometry.

HIV-infected MDM were infected at MG1 MOI 1 in 250 µl for 2 hours in MDM media. . Following the infection, cells were topped up to 1 mL/well with appropriate concentration of each SMAC mimetic (LCL 161 or birinapant at concentrations 2µM – 4µM). At 48h post infection, HSA frequency, cell death infection was measured via flow cytometry.

2.8.2 MG1 infection followed by SMAC mimetic treatment

J1.1 and OM10.1 cells were plated at $1x10^6$ cells/mL and were infected with MG1 (MOI $1x10^{-1}$ to $1x10^{-4}$) for two hours in 300 µl in R10 media. Following the infection, cells were topped up to 900 µL/well and 24h later appropriate concentration of each SMAC mimetic (AEG 40730, LCL 161, or birinapant at a concentration range 1µM – 20 µM) was added to the wells. At 48h post infection, cell death, casp3/7 activation and infection was measured by flow cytometry.

2.8.3 SMAC mimetic treatment followed by MG1 infection

J1.1 and OM10.1 cells were plated at $1x10^6$ cells/mL in 500 µl and treated with the appropriate concentration of SMAC mimetic (AEG-40730 or LCL-161, at 2µM - 10µM) for 24h. Following treatment, cells were spun down and re-plated, then infected with MG1 (MOI $1x10^{-1}$ to

$1x10^{-4}$) for two hours in 300 µl in R10 media for 2 hours. After the 2 hours, the cells were topped up to 1 mL with the appropriate SMAC mimetic containing supernatant. At 24h post infection, cell death, caspase 3/7 activation and infection as measured by a flow cytometry.

2.8.4 Concurrent TNFα and SMAC mimetic treatment

J1.1 cells were plated at $1x10^6$ cells/mL and were treated with 10 ng TNFα for two hours in 300 µl in R10 media. Following the treatment, cells were topped up to 1 mL/well with 1µM birinapant. 48h post treatment, cell death was measured by flow cytometry.

2.9 Cell death inhibitor treatment

J1.1 cells were plated at $1x10^6$ cells/mL and were treated with 50 µM ZVAD-fmk, 50 µM necrostatin-1s, a combination or 50 µM ZVAD-fmk and 50 µM necrostatin-1s, or left untreated in 200 µL for 1 hour at 37ºC. Following this, the cells were infected with MG1 (MOI $1x10^{-3}$) for two hours in 300 µl in R10 media. Following the infection, cells were topped up to 1 mL/well with 1 µM birinapant. 48h post infection, cell death was measured by flow cytometry.

2.10 Flow cytometry

All flow cytometric analysis was performed using the CytoFLEX Beckman Coulter Flow Cytometer (Beckman Coulter) FlowJo (BD Biosicences). Prior to staining, MDM were detached using accutase (60 min incubation at 37°C) and gentle pipetting. For the assessment of surface and intracellular markers, detached MDM were washed with PBS 1% BSA (460 x g for 5min). All antibodies used in the below experiments are listed in Table 3

Target	Reactivity	Host Species	Product number	Company	Clone	Conjugate	µg/test
CD24 (HSA)	Mouse	Rat	138505	Biolegend	30-F1	APC	0.4ug
CD24 (HSA)	Mouse	Rat	138503	Biolegend	30-F1	PE	0.6 ug
LDL-R	Human	Mouse	FAB2148P	R&D Systems	472413	PE	0.4 µg
PD-L1	Human	Mouse	393610	BioLegend	MIH2	APC	0.4 µg
AnnexinV	Human, mouse, rat	Escherichia coli	640908	Biolegend	N/A	PE	0.006µg
PI	Human	N/A	421301	Biolegend	N/A	Read on ECD	0.05µg
Caspase-3/7	Human	N/A	9125	Immunochemistry technologies	N/A	APC	Conc. Unavailable, 1:60 dilution
Caspase 1	Human	N/A	9122	Immunochemistry technologies	N/A	APC	Conc. Unavailable, 1:60 dilution

Table 3, antibodies used in flow cytometry analysis

2.11 ELISA and cytokine analysis

2.11.1 p24 ELISA

HIV p24 antigen concentration for SMAC mimetic treated cell lines 24h post treatment and 48h post treatment for MG1 and SMAC mimetic treated HIV-infected MDM. p24 ELISA was also used to measure the concentration of HIV stocks after one freeze/thaw cycle. Briefly, cell-free supernatants were lysed for 1 hour at 37°C with 1% Triton-X and p24 antigen expression was quantified by HIV-1 p24 Antigen Capture Kit (Frederick National Laboratory for Cancer Research, Frederick, MD; NIH AIDS Reagent Program) following the manufacturer's protocol. Absorbance was read at 450nm wavelength with a reference wavelength of 650 nm using the Multiskan Ascent Plate Reader.

2.11.2 TNFα and IFNα measurement

TNFα and IFNα from J1.1, OM10.1, HIV-infected MDMsupernatants were measured using TNF alpha Human ELISA kit (Cat# KHC3011, ThermoFisher Scientific). Cell activation cocktail stimulated (2 µl/mL for 48h) cells was used as a positive control. IFNα from HIV-infected MDM supernatants was measured by VeriKine Human Interferon Alpha ELISA Kit (Cat# 411100-1) from Cederlane. Poly(I:C) transfected cells (10µg/ 48h) was used as a positive control. All kits were used following the manufacturer's protocol.

2.11.3 Non-canonical NFkB activation assay

Prior to Non-canonical NFκB activation assay, nuclear extraction of cells were performed using nuclear extraction kit (Cat#0010, Active Motif) and the non-canonical NFκB activation was

measured by TransAM NFκB p52 Activation Assay (cat#48196 Active Motif). All kits were used following the manufacturer's protocol

Chapter 3

SMAC mimetics sensitize HIV-infected cell lines to MG1-mediated death

3.1 Introduction and Rationale

MG1 has been shown to induce greater killing in latently HIV-infected cell lines compared to their uninfected counterparts[159,160]. Pro-apoptotic small molecules SMAC mimetics have also been shown to selectively kill HIV-infected cells, in part due to the upregulation of anti-apoptotic proteins caused by HIV infection[232,235,259]. Cell death induced by MG1 of HIV-infected cells have been shown to be not fully dependent on apoptosis or necroptosis[161], while cell death induced by SMAC mimetic treatment of HIV-infected cells was shown to be via a mixture of apoptosis and autophagy, and that it could be TNFα-dependent or -independent[223,234].

Studies in the field of cancer has shown that SMAC mimetics enhance oncolytic virus-mediated killing, which may in part be because of the TNFα feedback loop due to the inflammation caused by the oncolytic virus[237–239].

The objective of this chapter was to investigate the effect of combination treatment of MG1 and SMAC mimetics (AEG 40730, LCL-161 and birinapant) on the latently HIV-infected lymphocytic cell line J1.1 and myelocytic cell line OM10.1 to see if a greater killing effect is induced compared to either treatment alone. Furthermore, the cell death pathways induced upon combination treatment, and infection, cytokine production and cell surface receptor expression following SMAC mimetic treatment was assessed.

3.2 Results

3.2.1 Combination treatment of MG1 and SMAC mimetics kill latently HIV-infected cells, depending on treatment administration order

The latently infected J1. cells were treated with a combination of SMAC mimetics and MG1. J1.1 cells were either (a) concurrently treated with MG1 and SMAC mimetics, (b) were infected with MG1 and treated with SMAC mimetics 24h post infection and (c) were treated with SMAC mimetics and infected with MG1 24h after treatment as previous studies in cancer has shown treatment order may abrogate the effect of oncolytic virus infection[238]. Three different SMAC mimetic combinations with MG1 were tested: MG1 with the bivalent SMAC mimetic AEG 40730, with the monovalent SMAC mimetic LCL-161 or with the bivalent SMAC mimetic birinapant. Cell death was measured by propidium iodide (PI) staining via flow cytometry, and cell viability was defined as %PI negative 48h following initial treatment.

There was a significant increase in cell death with increasing SMAC mimetic dose in concurrent treatment for all three SMAC mimetics. Similarly, in the conditions were J1.1 cells are infected with MG1 first and treated with AEG 40730 after, and where the cells are pre-treated with AEG 40730 and LCL 161, an increase in cell death was observed (Figure 4).

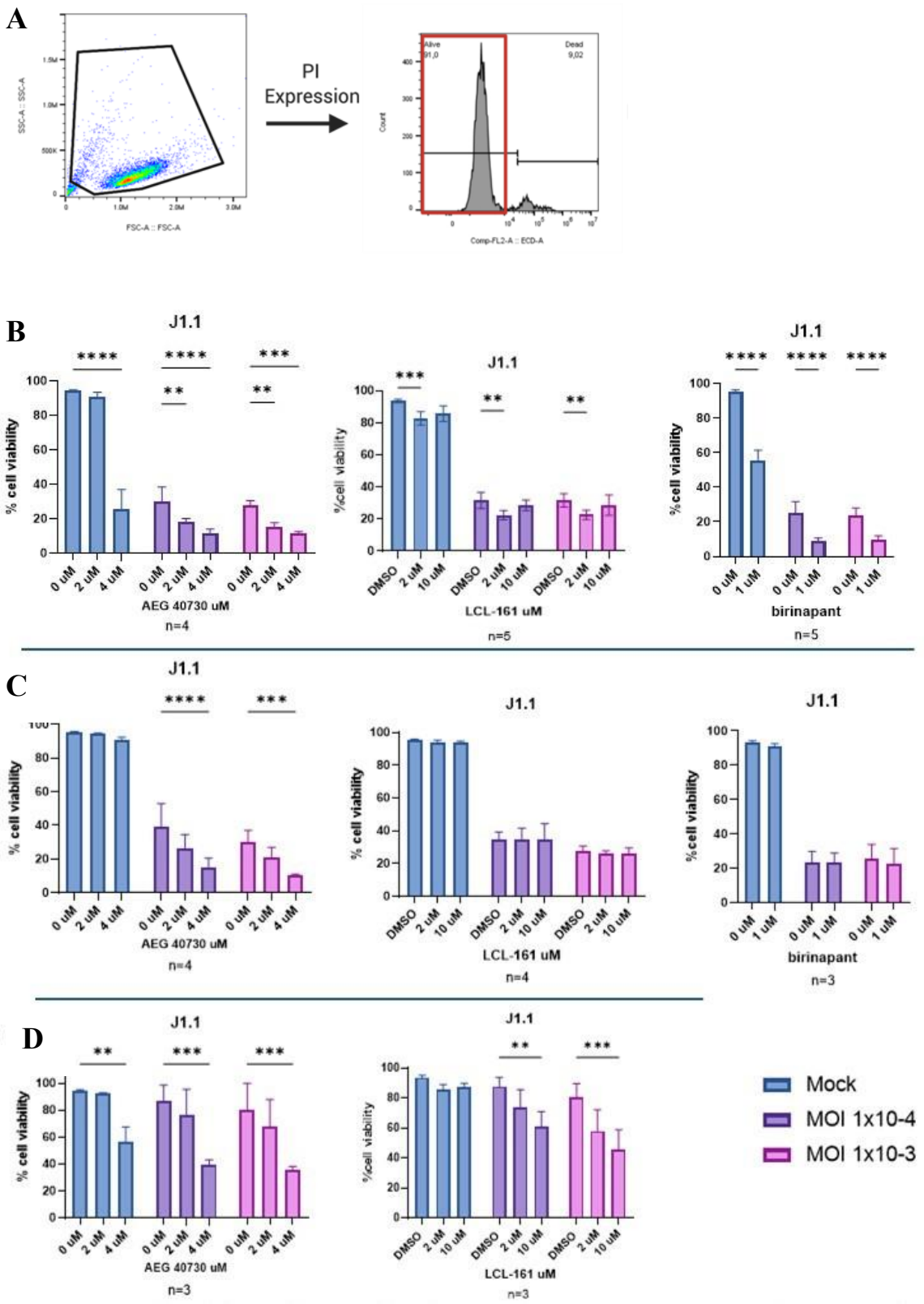
A
PI
Expression
Alive
91,0
Dead
9,02
Count
SSC-A :: SSC-A
FSC-A :: FSC-A
Comp-FL2-A :: ECD-A
B
J1.1
% cell viability
AEG 40730 uM
n=4
%cell viability
LCL-161 uM
n=5
birinapant
n=5
C
n=4
n=4
n=3
D
n=3
n=3
Mock
MOI 1x10-4
MOI 1x10-3

Figure 4, combination treatment with MG1 and SMAC mimetics increase cell death in J1.1 cells depending on administration order J1.1 cells were infected with MG1 MOI range $1x10^{-3}$ - $1x10^{-4}$ and treated with SMAC mimetics AEG 40730 (2 μM, and 4 μM.), LCL 161 (2 μM and 10 μM) and birinapant (1 μM). Cell death was measured by flow cytometry via PI staining. **A)** Gating strategy used to determine cell viability following PI staining **Row B)** Cell viability of J1.1 cells following 48hpi concurrent treatment **Row C)** Cell viability of J1.1 cells 48hpi that were infected with MG1 first and treated with SMAC mimetics 24h after and **Row D)** Cell viability of J1.1 cells 24hpi that were pre-treated with SMAC mimetics and then infected with MG1 24h after. (**P < .01, ***P<.001, ****P<.0001, by 2-way analysis of variance with the Dunnet post hoc test for multiple comparisons between different SMAC mimetic doses. Data represent mean values ± standard deviation of the mean; n values represent separate biological replicates.)

Next, similar to J1.1 cells, latently infected OM10.1 cells treated with a combination of SMAC mimetics and MG1. J1.1 cells were either (a) concurrently treated with MG1 and SMAC mimetics, (b) were infected with MG1 and treated with SMAC mimetics 24h post infection and (c) were treated with SMAC mimetics and infected with MG1 24h after treatment. Only AEG 40730 pre-treatment following MG1 infection significantly increased cell death, whereas other SMAC mimetics and treatment orders did not have a specific effect. These findings were consistent with the studies of SMAC mimetic killing of HIV-infected cells, showing that the effect of the SMAC mimetic is cell line and SMAC mimetic-dependent. Furthermore, these results confirmed the administration order of MG1 and SMAC mimetic is indeed important, as different administration orders resulted in different outcomes in terms of cell death (Figure 5).

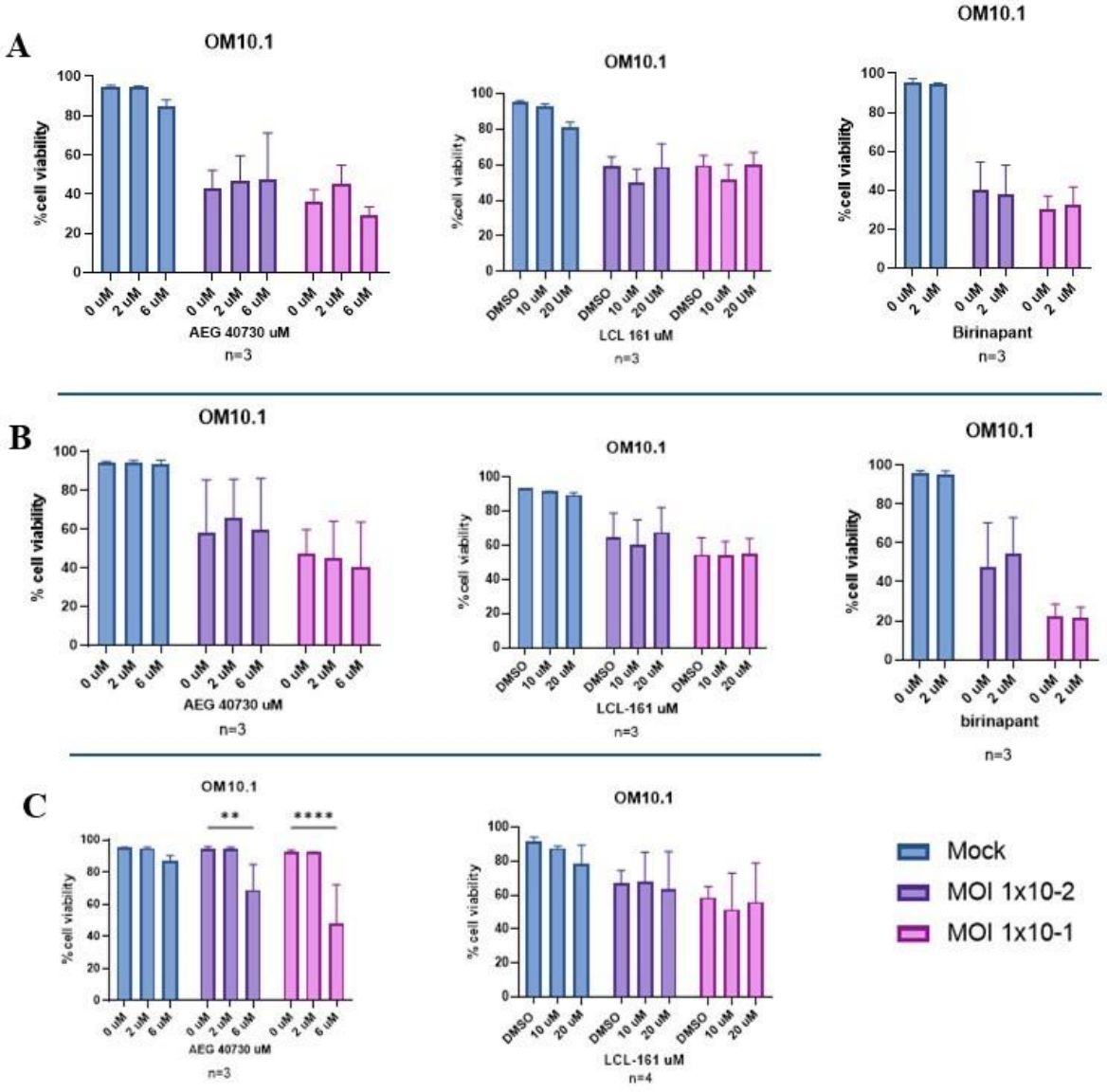
A
OM10.1
%cell viability
0 uM
2 uM
6 uM
AEG 40730 uM
n=3
OM10.1
%cell viability
DMSO
10 uM
20 uM
LCL 161 uM
n=3
OM10.1
%cell viability
Birinapant
n=3
B
OM10.1
% cell viability
AEG 40730 uM
n=3
OM10.1
%cell viability
LCL-161 uM
n=3
OM10.1
%cell viability
birinapant
n=3
C
OM10.1
**
****
% cell viability
AEG 40730 uM
n=3
OM10.1
% cell viability
LCL-161 uM
n=4
Mock
MOI 1x10-2
MOI 1x10-1

Figure 5, combination therapy with MG1 and SMAC mimetics increase cell death in OM10.1 cells only when SMAC mimetics are administered prior to MG1 infection, OM10.1 cells were infected with MG1 MOI range $1x10^{-2}$ - $1x10^{-1}$ and treated with SMAC mimetics AEG 40730 (2 μM, and 6 μM.), LCL 161 (10 μM and 20 μM) and birinapant (2 μM). Cell death was measured by flow cytometry via PI staining. **Row A)** Cell viability of OM10.1 cells following 48hpi concurrent treatment **Row B)** Cell viability of OM10.1 cells 48hpi that were infected with MG1 first and treated with SMAC mimetics 24h after and **Row C)** Cell viability of OM10.1 cells 24hpi that were pre-treated with SMAC mimetics and then infected with MG1 24h after. (**P < .01, ****P<.0001, by 2-way analysis of variance with the Dunnet post hoc test for multiple comparisons between different SMAC mimetic doses. Data represent mean values ± standard deviation of the mean; n values represent separate biological replicates.)

3.2.2 Caspase-3/7 and caspase-1 get activated following combination therapy, but cell death cannot be blocked by caspase or RIPK1 necroptosis inhibitors

Although the cell death mechanism by which MG1 kills HIV-infected cells is not fully elucidated[161,260], studies done on VSV show that apoptosis, pyroptosis, and necroptosis pathways must be inhibited to block cell death[261,262]. Hence, concurrently MG1 and SMAC mimetic treated J1.1 cells were stained with caspase 3/7 and caspase 1 FLICA 660 stain 48h post infection and caspase activation was measured by flow cytometry (Figure 6). Increase in both caspase-3/7 and caspase-1 was observed with the increase in cell death, confirming that more than one cell death pathway gets activated following treatment with SMAC mimetics and MG1.

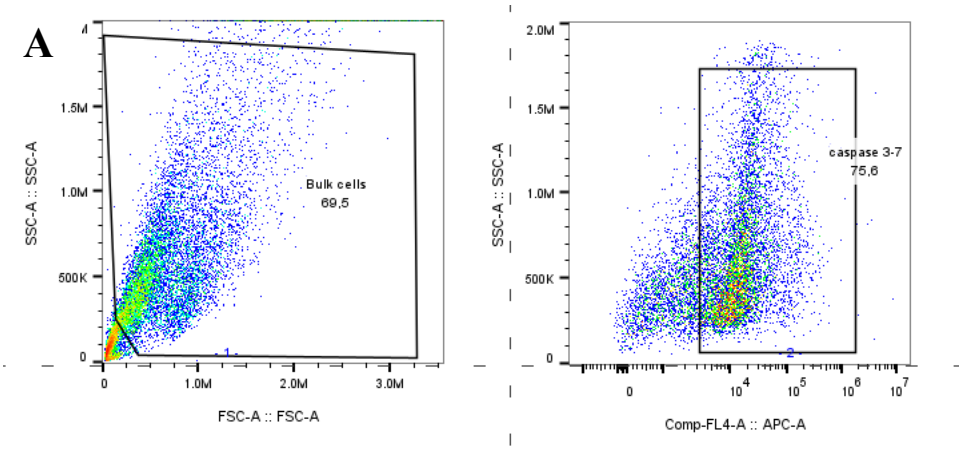
A
SSC-A :: SSC-A
FSC-A :: FSC-A
Bulk cells
69,5
caspase 3-7
75,6
Comp-FL4-A :: APC-A

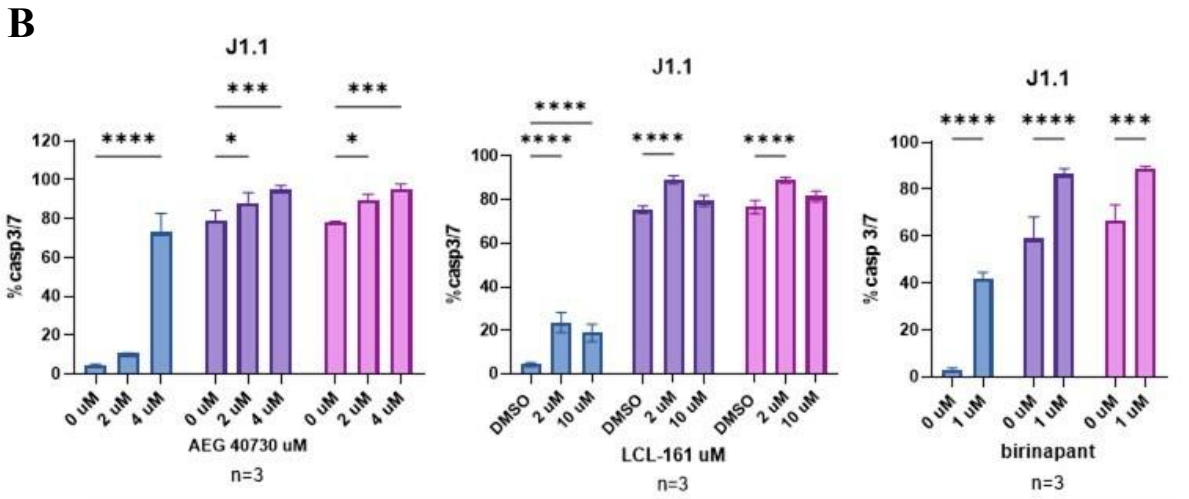
B
J1.1
% casp3/7
AEG 40730 uM
n=3
LCL-161 uM
n=3
birinapant
n=3

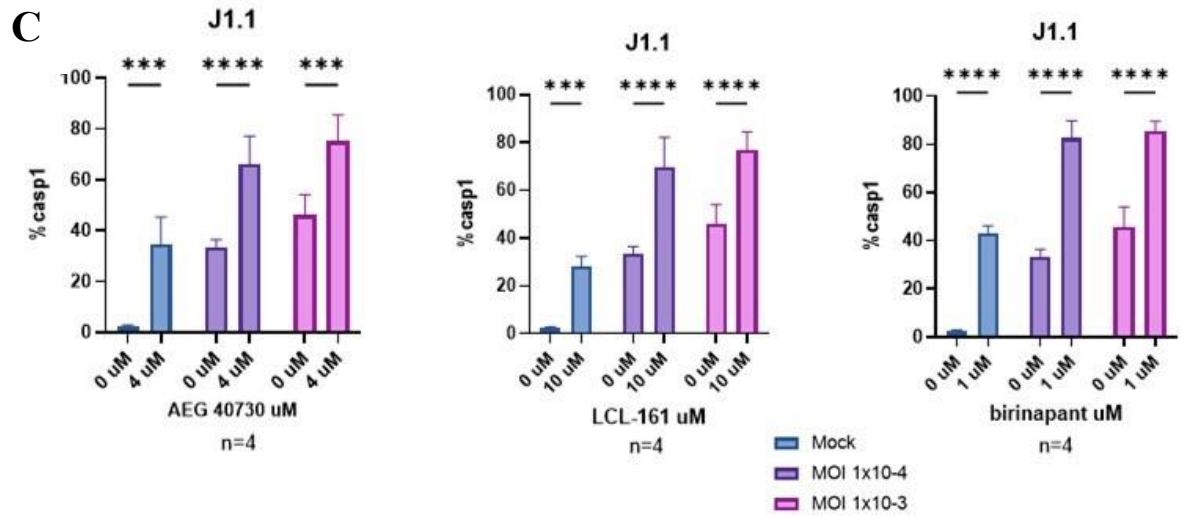
C
J1.1
% casp1
AEG 40730 uM
n=4
LCL-161 uM
n=4
birinapant uM
n=4
Mock
MOI 1x10-4
MOI 1x10-3

Figure 6, Caspase -3/7 and caspase-1 activation follows the increase in cell death in J1.1 cells after concurrent treatment with MG1 and SMAC mimetics. J1.1 cells were infected with MG1 MOI range $1x10^{-3}$ - $1x10^{-4}$ and treated with SMAC mimetics AEG 40730 (2 μM, and 4 μM.), LCL 161 (2 μM and 10 μM) and birinapant (1 μM). Caspase activity was measured by FLICA 660 staining flow cytometry **Row A)** Gating strategy employed to measure caspase 3/7 activity. **Row B)** Caspase 3/7 activity in of J1.1 cells following 48hpi concurrent treatment with MG1 and SMAC mimetics **Row C)** Caspase 1 activity in of J1.1 cells following 48hpi concurrent treatment with MG1 and SMAC mimetics (*P<.05 **P < .01, ***P<.001, ****P<.0001, by 2-way analysis of variance with the Dunnet post hoc test for multiple comparisons between different SMAC mimetic doses. Data represent mean values ± standard deviation of the mean; n values represent separate biological replicates.)

Next, J1.1 cells were pre-treated with 50 uM ZVAD-fmk, 50 uM necrostatin 1-s or a combination of both for 1 hour after which the cells underwent combination treatment with MG1 and the bivalent SMAC mimetic birinapant to investigate if cell death can be blocked via the use of caspase and necroptosis inhibitors. Cells were stained with PI 48h post treatment and cell death was determined via flow cytometry. Neither ZVAD-fmk or necrostatin 1-s alone were able to fully mitigate cell death induced by birinapant or MG1. However, combination of ZVAD-fmk and necrostatin 1-s pre-treatment successfully blocked cell death in birinapant treated cells, but cell death was still observed in MG1 infected or MG1 infected and birinapant treated cells, suggesting that MG1 killing of HIV-infected cells does not fully depend on caspases or RIPK-1 (Figure 7).

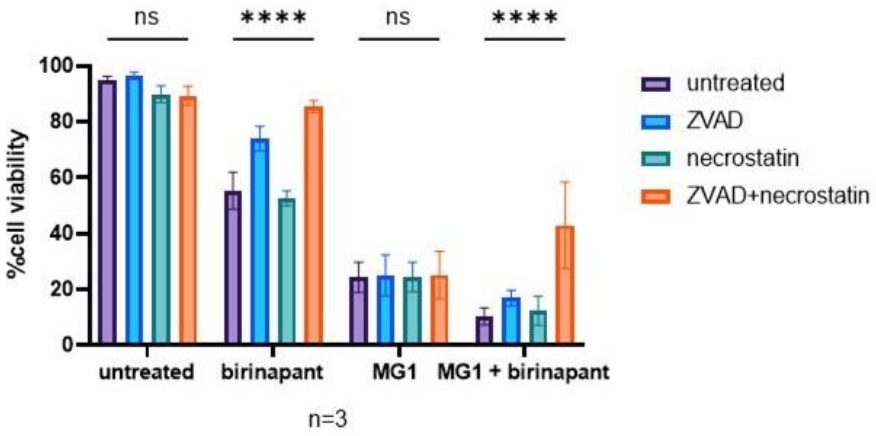
ns
****
ns
****
100
80
60
40
20
0
%cell viability
untreated
birinapant
MG1
MG1 + birinapant
n=3
untreated
ZVAD
necrostatin
ZVAD+necrostatin

Figure 7, cell death of J1.1 cells is not completely blocked following pre-treatment with cell with cell death inhibitors ZVAD-fmk and necrostatin 1-s prior to MG1 and/or SMAC mimetic treatment. J1.1 cells were left untreated or pre-treated with 50 μM ZVAD-fmk, 50 μM necrostatin 1-s or with both 1h prior to MG1 infection, birinapant (1 μM) treatment or a combination of both.. Cell death was measured by flow cytometry via PI staining. (****P<.0001, by 2-way analysis of variance with the Dunnet post hoc test for multiple comparisons between different SMAC mimetic doses. Data represent mean values ± standard deviation of the mean; n values represent separate biological replicates.)

3.2.3 MG1 infection percentage does not correlate with increased cell death of HIV-infected cells

MG1 used in this project is a GFP reporter virus, making it possible to see the percentage of infected cells via flow cytometry. In this context, infected cells were defined as PI negative, GFP positive cells (Figure 3.7, gating strategy). In J1.1 cells, an increase in GFP% did not follow the increase in cell death. An increase in GFP could only be seen in OM10.1 cells pre-treated with AEG 40730 (Figure 8).

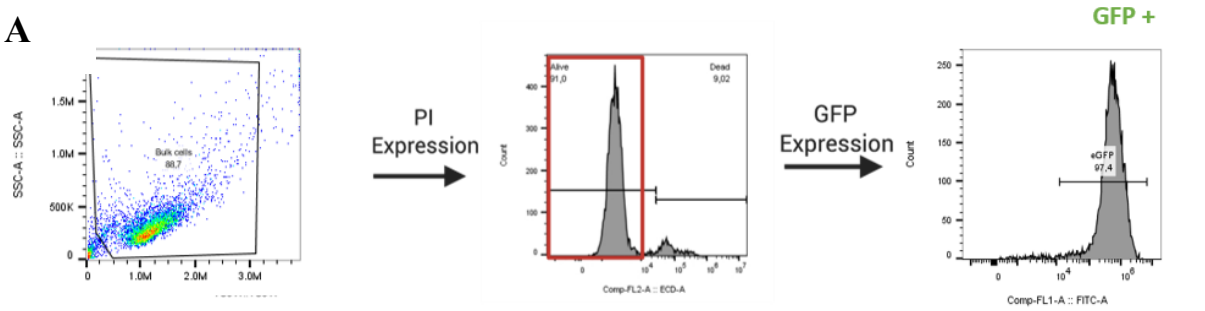
A
GFP +
SSC-A :: SSC-A
Bulk cells
80,7
PI
Expression
Alive
91,0
Dead
9,02
Count
Comp-FL2-A :: ECD-A
GFP
Expression
eGFP
97,4
Comp-FL1-A :: FITC-A

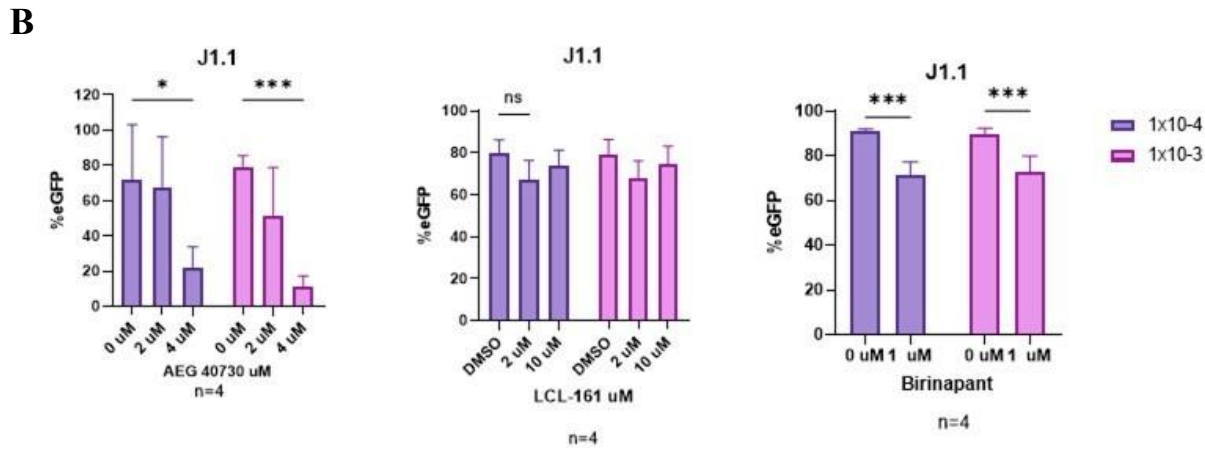
B
J1.1
%eGFP
AEG 40730 uM
n=4
J1.1
LCL-161 uM
n=4
J1.1
Birinapant
n=4
1x10-4
1x10-3

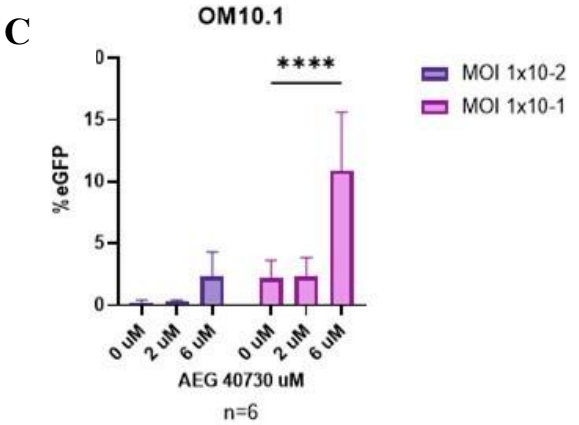
C
OM10.1
%eGFP
AEG 40730 uM
n=6
MOI 1x10-2
MOI 1x10-1

Figure 8, an increase in infection% of J1.1 cells is not observed following combination treatment with MG1 and SMAC mimetics while an increase in infection% of OM10.1 cells accompanies decreased cell viability. A) Gating strategy used to determine GFP percentage **Row B)** J1.1 cells were infected with MG1 MOI range $1x10^{-3}$ - $1x10^{-4}$ and concurrently treated with SMAC mimetics AEG 40730 (2 μM, and 4 μM.), LCL 161 (2 μM and 10 μM) and birinapant (1 μM). Infection was measured 48hpi by flow cytometry via GFP expression. **C)** OM10.1 cells were pre-treated with AEG 40730 (2 μM, and 6 μM) infected with MG1 MOI range $1x10^{-2}$ - $1x10^{-1}$ 24h after. Infection was measured 24hpi by flow cytometry via GFP expression. (**P*<.05, ****P*<.001, *****P*<.0001, by 2-way analysis of variance with the Dunnet post hoc test for multiple comparisons between different SMAC mimetic doses. Data represent mean values ± standard deviation of the mean; n values represent separate biological replicates.)

To further validate there is no increase in MG1 infection, viral production following combination treatment with MG1 and SMAC mimetics was measured by plaque assays. Supernatants from MG1 infected or MG1infected and birinapant treated J1.1 cells were collected, and used to infect Vero cells to perform a plaque assay. There were less plaques in wells which were infected with supernatant collected from J1.1 cells which underwent combination treatment compared to the wells infected with supernatant collected from J1.1 which were infected with MG1. These results show that at the time when the supernatants are collected to perform the plaque assay, there is more virus in the supernatants collected from J1.1 cells which were only infected with MG1 compared to cells that underwent combination therapy with MG1 and birinapant. (Figure 9).

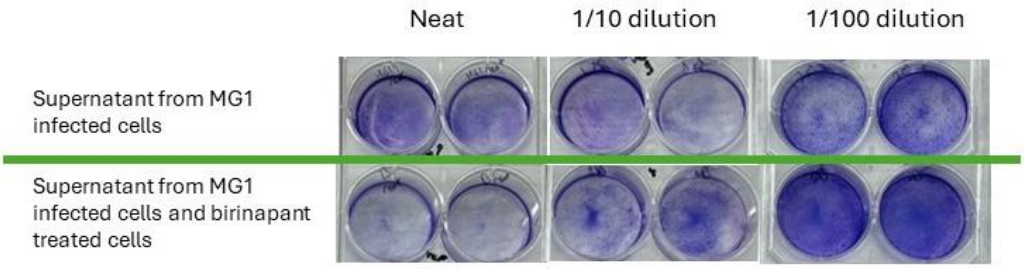
Neat
1/10 dilution
1/100 dilution
Supernatant from MG1 infected cells
Supernatant from MG1 infected cells and birinapant treated cells

Figure 9, combination treatment with MG1 and birinapant does not result in an increase in viral production. Supernatants from MG1 infected or MG1 infected and concurrently birinapant treated J1.1 cells were collected 48h post infection. The supernatants were used to infect Vero cells and perform a plaque assays. Plaques were fixed and stained 48h post infection. Experiment done n=3, above picture is a representative**.**

3.2.4 Cell surface receptor expression following SMAC mimetic treatment of HIV-infected cell lines

The expression of LDL-R, the cell surface receptors that MG1 uses for viral entry[145,162], and PD-L1, a receptor that has been shown to aid in VSV infection[263], was investigated following 48h SMAC mimetic treatment. Both J1.1 and OM10.1 cells were treated with SMAC mimetics for 48h, and then stained for LDL-R and PD-L1 receptors. In J1.1 cells there was significant increase in the cell surface expression of LDL-R, with no change in the cell surface receptor expression of PD-L1 (Figure10). Increased expression of LDL-R might correlate with increased cell death of J1.1 cells, however this does not reflect on infection percentage. Conversely, no significant changes in LDL-R or PD-L1 expression was observed in OM10.1 cells. (Figure 11).

A

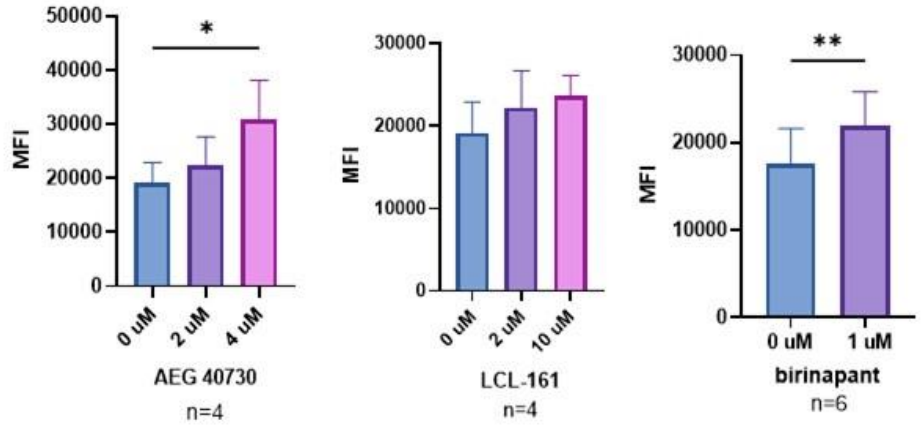

LDL-R expression

B

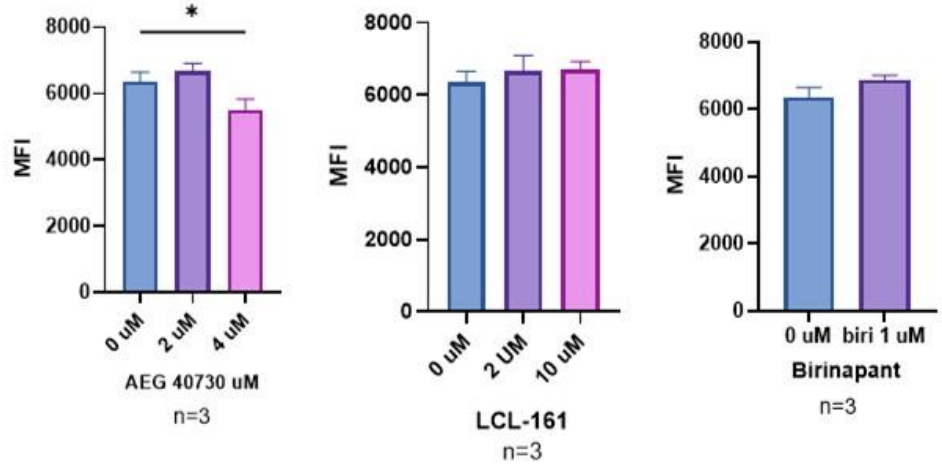

Figure 10, a slight increase in LDL-R expression is observed while PD-L1 receptor expression remains unchanged in J1.1 cells treated with SMAC mimetics. Row A) J1.1 cells were treated with SMAC mimetics AEG 40730 (2 μM, and 4 μM.), LCL 161 (2 μM and 10 μM) and birinapant (1 μM). LDL-R expression was measured 48hp treatment via flow cytometry. **Row B)** J1.1 cells were treated with SMAC mimetics AEG 40730 (2 μM, and 4 μM.), LCL 161 (2 μM and 10 μM) and birinapant (1 μM). PD-L1 expression was measured 48hp treatment via flow cytometry. (*P<.05, **P<.01, by 2-way analysis of variance with the Dunnet post hoc test for multiple comparisons between different SMAC mimetic doses. Data represent mean values ± standard deviation of the mean; n values represent separate biological replicates.)

A

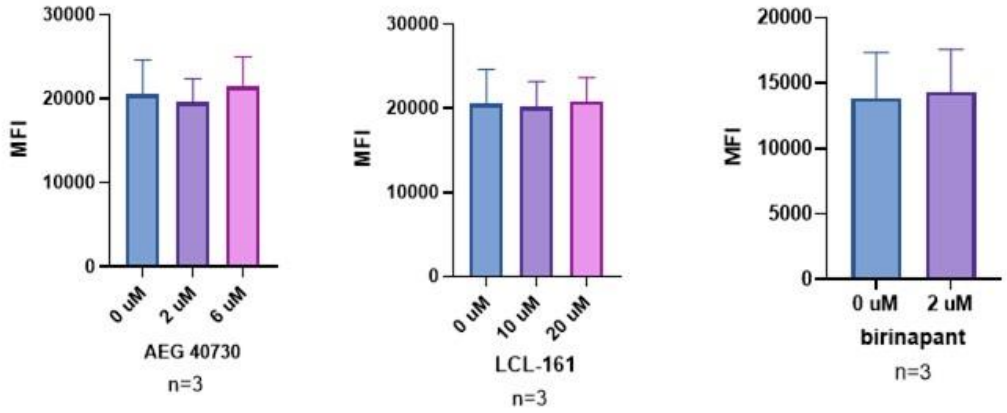

LDL-R expression

B

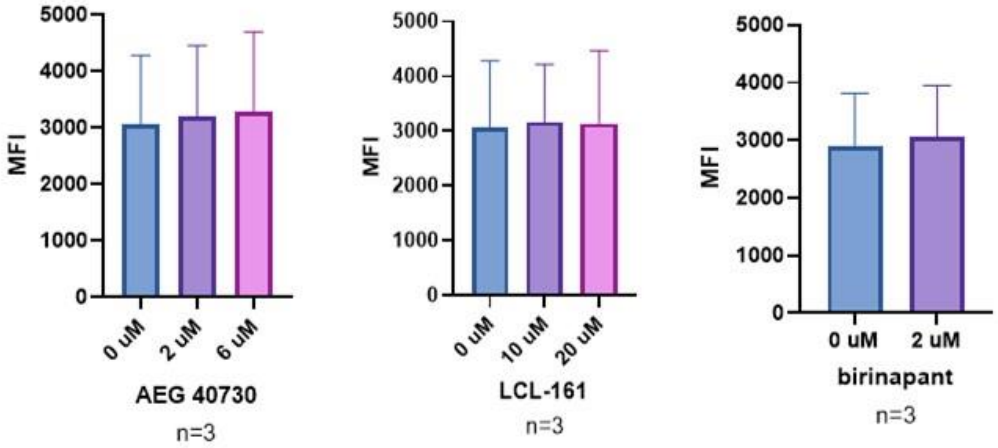

PD–L1 expression

Figure 11, no change in LDL-R and PD-L1 receptor expression is observed in OM1.1cells treated with SMAC mimetics. Row A) OM10.1 cells were treated with SMAC mimetics AEG 40730 (2 μM, and 6 μM.), LCL 161 (10 μM and 20 μM) and birinapant (2 μM). LDL-R expression was measured 48hp treatment via flow cytometry. Row B) OM01.1 cells were treated with SMAC mimetics AEG 40730 (2 μM, and 6 μM.), LCL 161 (10 μM and 20 μM) and birinapant (2 μM). PD-L1 expression was measured 48hp treatment via flow cytometry.

3.2.5 RNAseq analysis of J1.1 cells following combination treatment

J1.1 cells were infected with MG1 or treated with a combination of MG1 and birinapant, to identify potential changes induced by SMAC mimetic treatment that could sensitize cells to MG1-mediated death. Interestingly, gene ontology (GO) analysis for using the biological processes GO database demonstrated that in the presence of MG1, SMAC mimetics caused an upregulation in genes that play a role in sterol biosynthesis pathway while causing downregulation in genes that play a role in immune response regulating signaling pathway (including TNFα signaling PRR signaling, and TLR signaling), canonical NFκB transduction pathway, and lipid storage. There results suggest that SMAC mimetics may downregulate the immune response against MG1 infection, and thus sensitizing cells to MG1-mediated death (Figure 12).

A

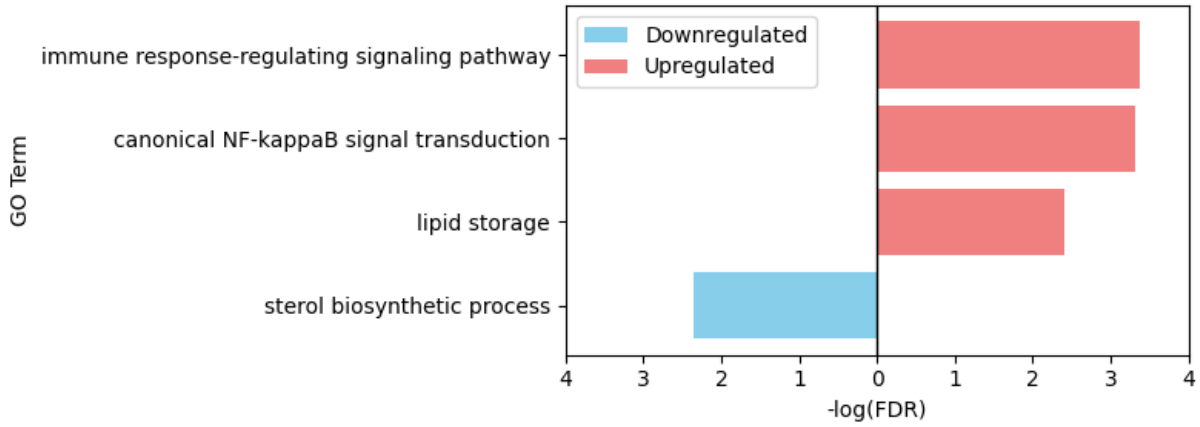
Downregulated
Upregulated
immune response-regulating signaling pathway
canonical NF-kappaB signal transduction
lipid storage
sterol biosynthetic process
GO Term
4
3
2
1
0
1
2
3
4
-log(FDR)

B

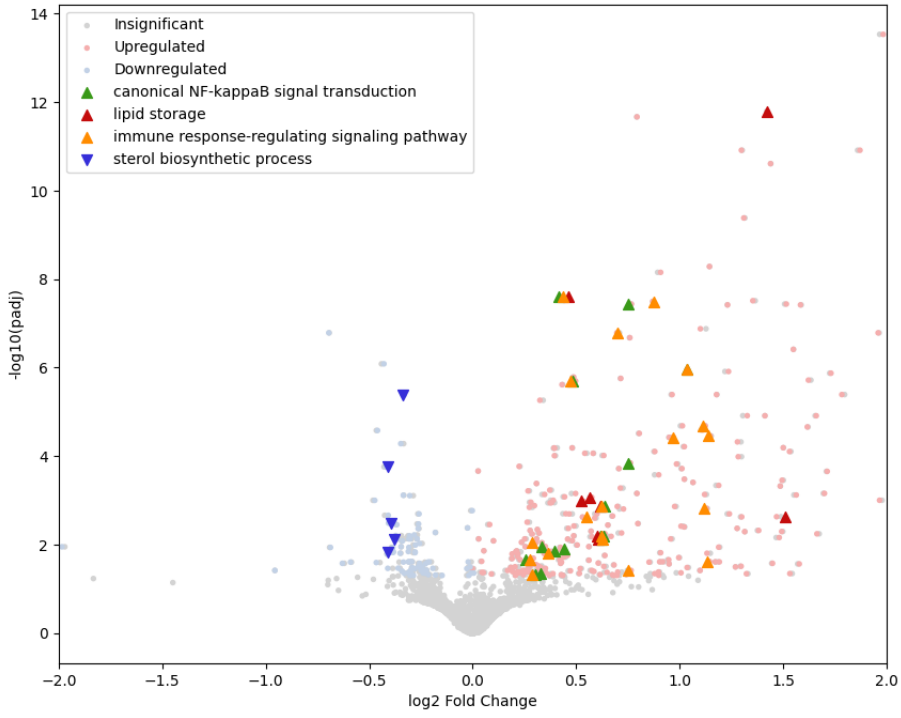
Insignificant
Upregulated
Downregulated
canonical NF-kappaB signal transduction
lipid storage
immune response-regulating signaling pathway
sterol biosynthetic process
-log10(padj)
log2 Fold Change

C

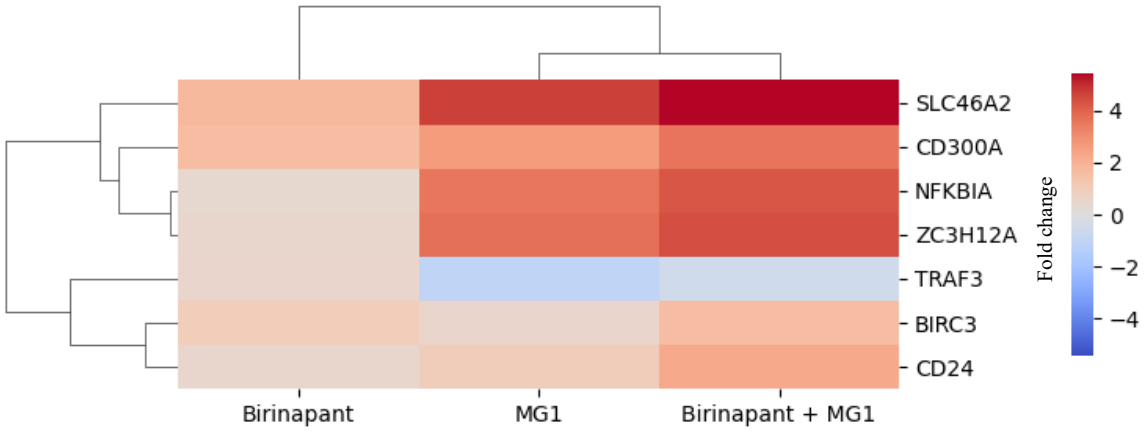
SLC46A2
CD300A
NFKBIA
ZC3H12A
TRAF3
BIRC3
CD24
Birinapant
MG1
Birinapant + MG1
Fold change
4
2
0
−2
−4

Figure 12, genes in the immune system regulating pathway are upregulated after combination treatment with MG1 and SMAC mimetics compared to MG1 infection. Top 4 significantly enriched GO terms (out of 27 terms total) are shown in both A) Volcano plot, B) Gene ontology biological process analysis and C) Heat map of the genes upregulated in the immune system regulating pathway.

3.2.6 Cytokine production following SMAC mimetic treatment of HIV-infected cell lines

SMAC mimetics can cause the degradation of cIAP1 and cIAP2 in the cytoplasm, resulting in the activation of the non-canonical NFκB pathway[168]. In both J1.1 and OM10.1 cells, there was a dose-dependent increase in non-canonical NFκB signaling as measured by the absorbance (OD) values from DNA based non-canonical NFκB ELISA measured 48h after SMAC mimetic treatment (Figure 13). Since NFκB signaling can result in production of HIV virions in latently infected cells, p24 capsid protein of HIV was measured in supernatants of cells treated with the SMAC mimetics AEG 40730 and LCL 161 for 24h. A significant increase in p24 production was not detected. (Figure 14)

A downstream effect of NFκB signaling is the production of TNFα. Hence, the amount of TNFα in the supernatants of SMAC mimetic treated or MG1 infected J1.1 and OM10.1 cells was measured via U-PLEX MSD kit and confirmed by TNFα ELISA 48h post treatment. TNFα was only detectable in the supernatants of AEG 40730 treated OM10.1 cells (Figure 15). This suggests that TNFα may not be a major player in the cell death of J1.1 treated with MG1 and SMAC mimetics, but more experiments in the future were TNFα is blocked with antibodies or TNFR1 is silenced via siRNA will give us more insight regarding the involvement of TNFα.

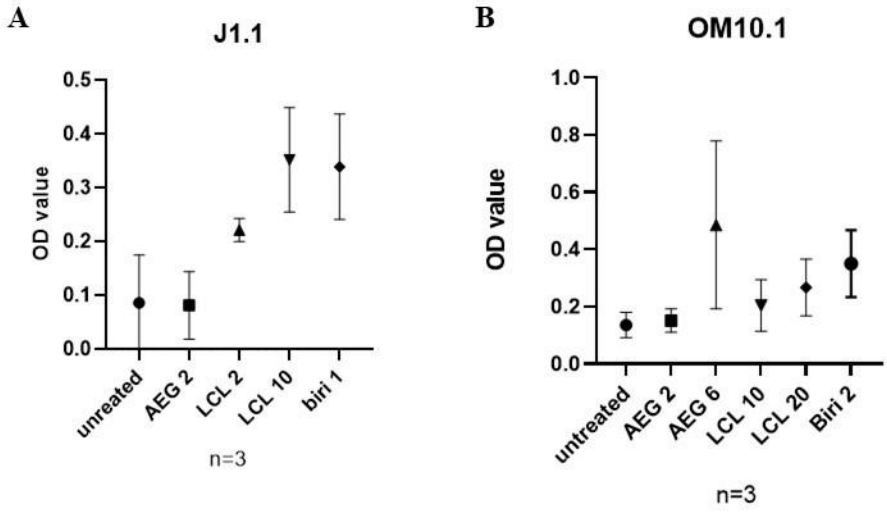
A
J1.1
OD value
0.5
0.4
0.3
0.2
0.1
0.0
unreated
AEG 2
LCL 2
LCL 10
biri 1
n=3
B
OM10.1
OD value
1.0
0.8
0.6
0.4
0.2
0.0
untreated
AEG 2
AEG 6
LCL 10
LCL 20
Biri 2
n=3

Figure 13, non-canonical NFκB activity is increased in A) J1.1 and B) OM10.1 cells treated with SMAC mimetics. J1.1 and OM10.1 cells were treated with SMAC mimetics for 48h and their non-canonical NFκB activity was measured via TransAM® NFκB Activation Assay, a DNA based ELISA. Increase in transcription factor activity is represented by increase in absorbance (OD) values.

A)

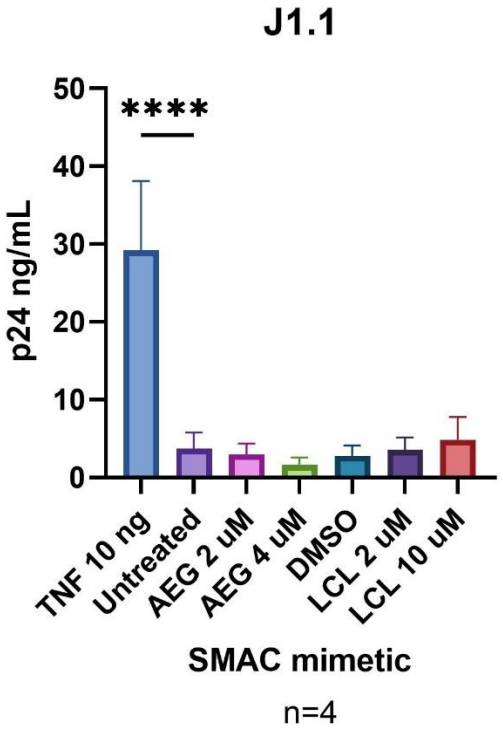
J1.1
****
p24 ng/mL
50
40
30
20
10
0
TNF 10 ng
Untreated
AEG 2 uM
AEG 4 uM
DMSO
LCL 2 uM
LCL 10 uM
SMAC mimetic
n=4

B)

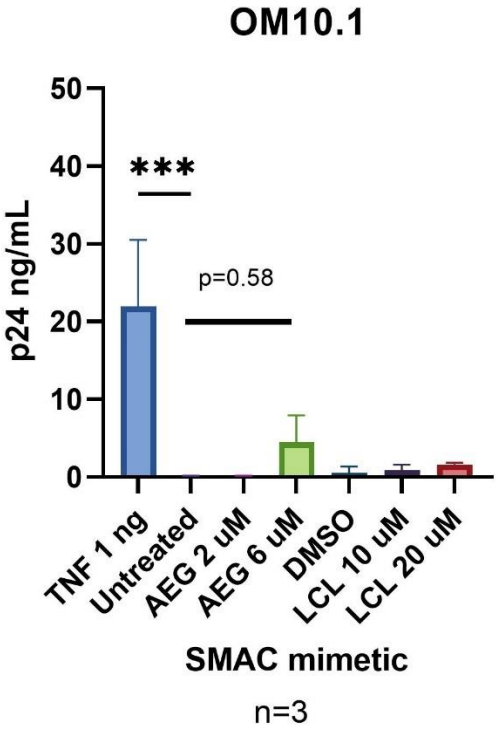
OM10.1
***
p=0.58
p24 ng/mL
50
40
30
20
10
0
TNF 1 ng
Untreated
AEG 2 uM
AEG 6 uM
DMSO
LCL 10 uM
LCL 20 uM
SMAC mimetic
n=3

Figure 14, p24 production does not increase in J1.1 and OM10.1 cells following 24h treatment with AEG 40730 and LCL-161 treatment. A) p24 detected in the supernatants of J1.1 cells treated with SMAC mimetics for 24h. **B)** p24 detected in the supernatants of OM10.1 cells treated with SMAC mimetics for 24h. (***P<.001, ****P<.0001, by 1-way analysis of variance with the Dunnet post hoc test for multiple comparisons between different SMAC mimetic doses. Data represent mean values ± standard deviation of the mean; n values represent separate biological replicates.)

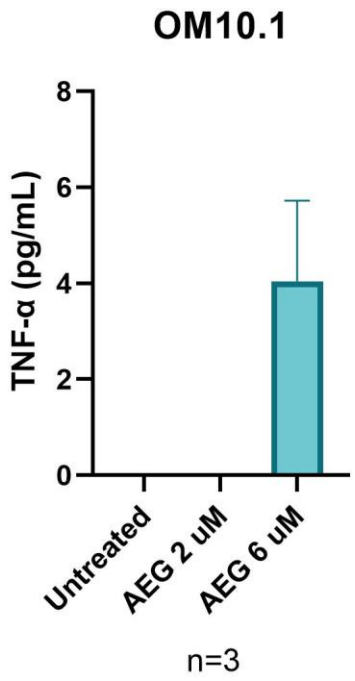
OM10.1
TNF-α (pg/mL)
8
6
4
2
0
Untreated
AEG 2 uM
AEG 6 uM
n=3

Figure 15, TNFα is detected in the supernatants of OM10.1 cells infected with MG1 or treated with SMAC mimetics OM10.1 cells were treated with SMAC mimetics for 48h and TNFα was measured in their supernatant via MSD uPLEX technology.

Chapter 4

SMAC mimetics sensitize HIV-infected monocyte derived macrophages to MG1-mediated death

4.1 Introduction and rationale

MG1 has been shown to selectively infect and kill HIV-infected monocyte-derived macrophages because of the inherent IFN signaling defects in HIV-infected MDM[155,161,162]. SMAC mimetics have also been shown to kill HIV-infected MDM both in a TNFα dependent and independent manner[223,235]. Furthermore oncolytic virus mediated killing has been shown to be enhanced via the usage of SMAC mimetics in the cancer field[186,238,239].

Since macrophages are more resistant to HIV infection compared to $CD4^+$ T-cells and that in culture, HIV infection results in a mixed population of persistently HIV-infected and bystander cells, making the interpretation of data more difficult. Hence, a reporter HIV called HIV NL4.3 BAL-IRES-HSA[158] was used to differentiate persistently HIV-infected macrophages (HSA+) from bystander cells (HSA-). In this infection model, 2-8% of cells are HSA+.

Although in previous studies MG1 was shown to be able to selectively infect and kill HIV-infected cells, the same was not true for VSVΔ51, an oncolytic virus closely related to MG1[159,161]. Since SMAC mimetics have been shown to sensitize refractory cancer cells to VSVΔ51 mediated death[239,240], this may also hold true for HIV-infected cells.

The objective of this chapter is to investigate the effect of combination treatment of MG1 and SMAC mimetics (LCL-161 and birinapant) on *ex vivo* HIV-infected monocyte derived macrophages. Moreover, cytokine production and cell surface receptor expression following SMAC mimetic treatment was assessed. Lastly, the effect of the SMAC mimetic birinapant in sensitizing HIV-infected cells to VSVΔ51 was investigated.

4.2 Results

4.2.1 Combination treatment of MG1 and SMAC mimetics kill *ex vivo* HIV-infected monocyte derived macrophages

Monocyte-derived macrophages were generated from fresh PBMC using plate adherence and M-CSF treatment. 7 days post plating, MDM were infected with the reporter virus HIV-NL4.3-BAL-IRES-HSA. 6 days post infection, HIV-infected MDM were treated with MG1 and SMAC mimetics (LCL-161 or birinapant) concurrently. 48h post infection, cells were assessed for their HIV infection status (bystander cells: HSA – and persistently infected cells: HSA+) and cell death by AnnexinV staining via flow cytometry (Figure 16). Cell death was assessed in both bulk macrophage populations and HSA- and HSA+ fractions. Gating strategy can be seen in Figure 17.

In bulk MDM, a slight increase in cell death with combination treatment with MG1 and LCL-161 was observed. Moreover, there was significant increase in cell death in the HIV-infected HSA+ population with the combination treatment when compared to either treatment alone. (Figure 18). In cells treated with MG1 and birinapant, a significant increase in cell death can be observed both in the bulk population and HSA- and HSA+ fractions. (Figure 19).

The decrease in HIV-infected cells was measured by proviral HIV DNA qPCR for SMAC only, MG1 only, and combination treatment conditions. Although there is a decreasing trend for proviral DNA, the comparison between fold change of the combination treated to MG1 infection only is not significant (Figure 20).

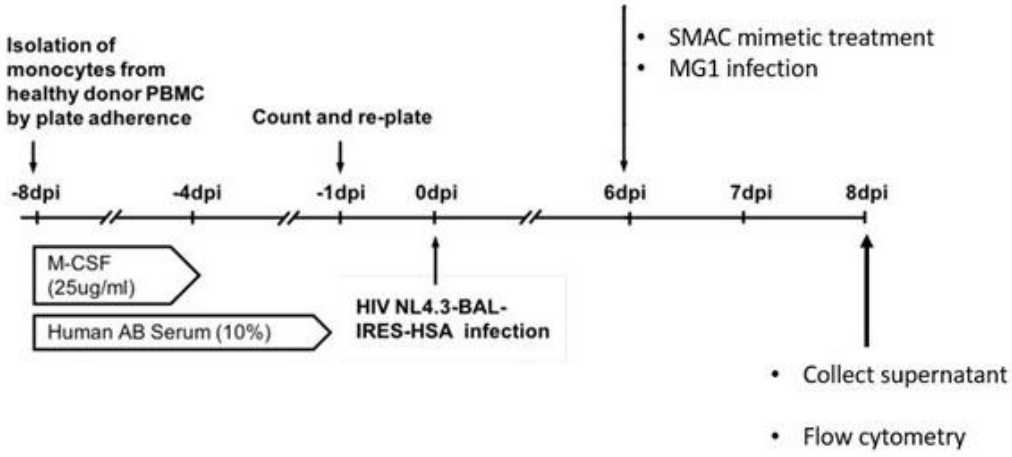
Isolation of monocytes from healthy donor PBMC by plate adherence
Count and re-plate
• SMAC mimetic treatment
• MG1 infection
-8dpi
-4dpi
-1dpi
0dpi
6dpi
7dpi
8dpi
M-CSF (25ug/ml)
Human AB Serum (10%)
HIV NL4.3-BAL-IRES-HSA infection
• Collect supernatant
• Flow cytometry

Figure 16, experimental design for the generation of monocyte-derived macrophages, subsequent HIV infection and MG1 and SMAC mimetic treatment.

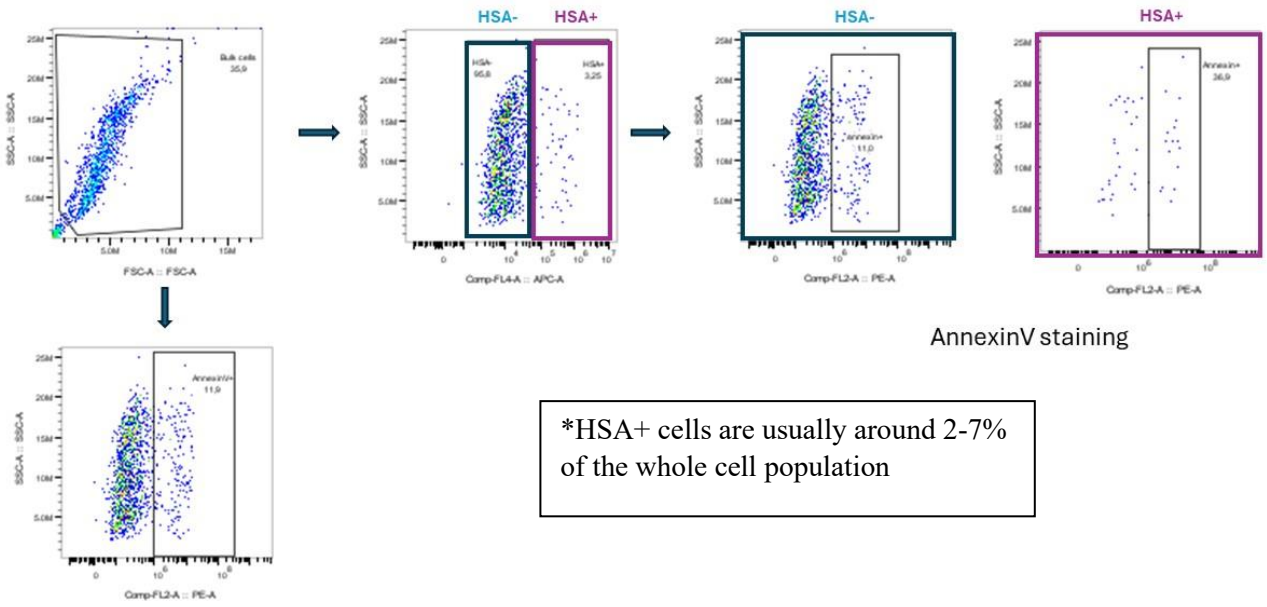

AnnexinV staining

Bulk AnnexinV staining

*HSA+ cells are usually around 2-7% of the whole cell population

Figure 17, gating strategy employed on monocyte derived macrophages to determine cell viability as determined by AnnexinV staining and HIV infection status as determined by determined by the presence of HSA on the cell surface.

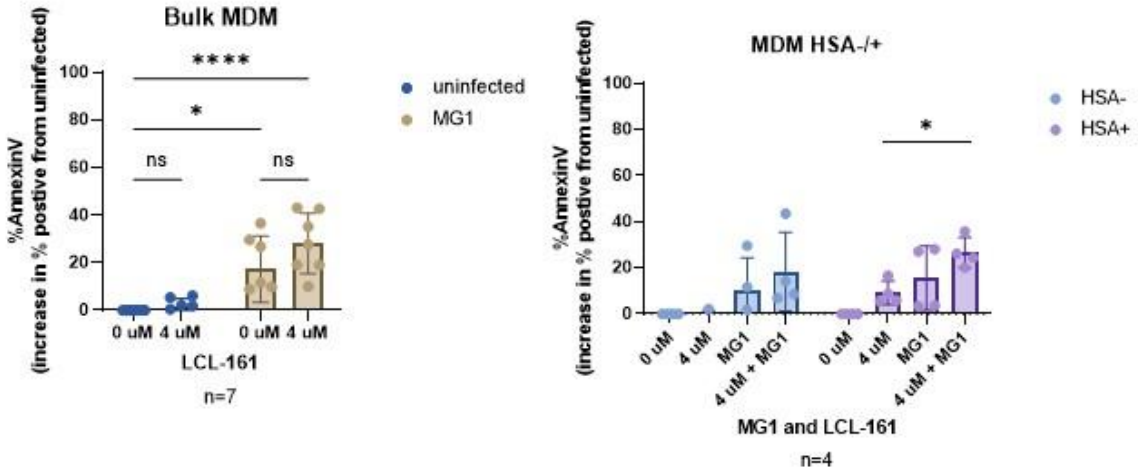
Bulk MDM
%AnnexinV
(increase in % postive from uninfected)
****
*
ns
ns
0 uM 4 uM 0 uM 4 uM
LCL-161
n=7
uninfected
MG1
MDM HSA-/+
%AnnexinV
(increase in % postive from uninfected)
*
0 uM
4 uM
MG1
4 uM + MG1
MG1 and LCL-161
n=4
HSA-
HSA+

Figure 18, cell viability of HIV-infected monocyte derived macrophages decreases after combination treatment with MG1 and LCL-161. HIV-infected MDM were infected with MG1 MOI 1 and treated with the SMAC mimetic LCL 161 (4 μM). Cell death was measured by AnnexinV staining and HIV infection status was determined by HSA staining via flow cytometry. **A)** Cell viability of bulk MDM following 48hpi concurrent treatment. . (*P<.05, ****P < .0001, by 2-way analysis of variance with the Dunnet post hoc test for multiple comparisons between different treatment conditions. Data represent mean values ± standard deviation of the mean; n values represent separate biological replicates.) **B)** Breakdown of cell viability of HSA- (bystander) and HSA+ (HIV-infected) MDM (*P < .05, 1-way analysis of variance was performed within each group with Tukey's multiple comparison's post-test for multiple comparisons. Data represent mean values ± standard deviation of the mean; n values represent separate biological replicates.)

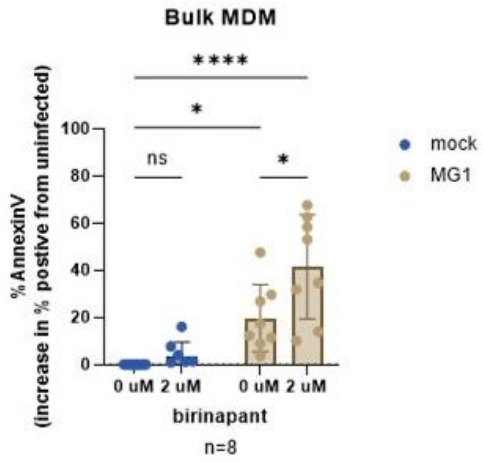
Bulk MDM
****
*
ns
*
100
80
60
40
20
0
% AnnexinV
(increase in % postive from uninfected)
0 uM 2 uM 0 uM 2 uM
birinapant
n=8
mock
MG1

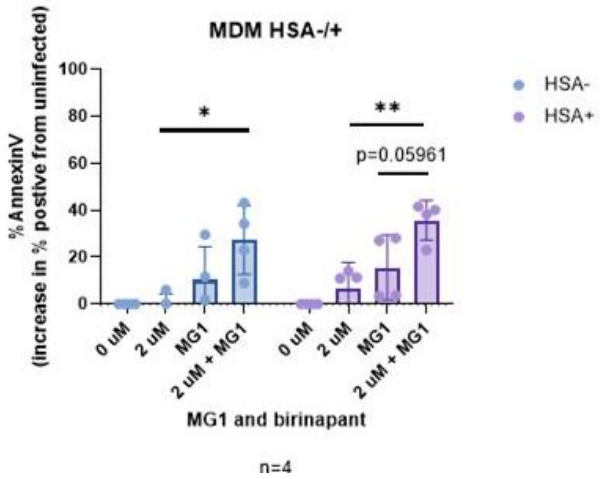
MDM HSA-/+
*
**
p=0.05961
100
80
60
40
20
0
% AnnexinV
(increase in % postive from uninfected)
0 uM
2 uM
MG1
2 uM + MG1
0 uM
2 uM
MG1
2 uM + MG1
MG1 and birinapant
n=4
HSA-
HSA+

Figure 19, cell viability of HIV-infected monocyte derived macrophages decreases after combination treatment with MG1 and birinapant. HIV-infected MDM were infected with MG1 MOI 1 and treated with the SMAC mimetic birinapant (2 μM). Cell death was measured by AnnexinV staining and HIV infection status was determined by HSA staining via flow cytometry. **A)** Cell viability of bulk MDM following 48hpi concurrent treatment. (*P<.05, ****P < .0001, by 2-way analysis of variance with the Dunnet post hoc test for multiple comparisons between different treatment conditions. Data represent mean values ± standard deviation of the mean; n values represent separate biological replicates.) **B)** Breakdown of cell viability of HSA- (bystander) and HSA+ (HIV-infected) MDM (*P <.05, **P < .01, ****P<.0001 1-way analysis of variance was performed within each group with the Tukey's multiple comparison's post-test for multiple comparisons. Data represent mean values ± standard deviation of the mean; n values represent separate biological replicates.)

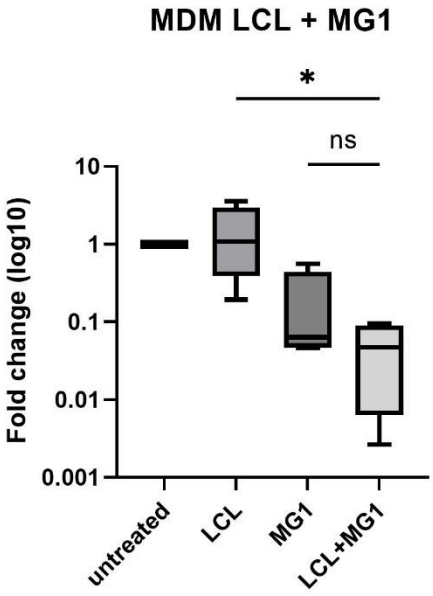
MDM LCL + MG1
*
ns
Fold change (log10)
10
1
0.1
0.01
0.001
untreated
LCL
MG1
LCL+MG1

n=4

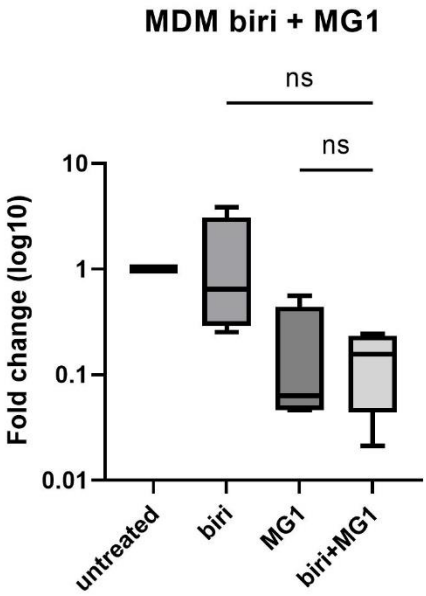
MDM biri + MG1
ns
ns
Fold change (log10)
10
1
0.1
0.01
untreated
biri
MG1
biri+MG1

n=4

Figure 20, although not significant, a decrease in proviral HIV DNA following combination treatment with MG1 relative to HIV-infected untreated cells can be seen. HIV-infected MDM were infected with MG1 MOI 1 and treated with the SMAC mimetic **A)** LCL 161 (4μM) or **B)** birinapant (2 μM). (n=4, p=0.0351 by Sidak's posttest) Data represent mean ± SEM; n values represent separate biological replicates.

4.2.2 Cell surface receptor expression and cytokine production following SMAC mimetic treatment and MG1 infection of HIV-infected MDM

LDL-R and PD-L1 expression on HIV-infected MDM was measured 48h post SMAC mimetic treatment in bulk and HSA-/HSA+ populations via flow cytometry. However, there was not a statistically significant difference between the basal level expressions, or expressions post-SMAC mimetic treatment of the two receptors in either bulk or HSA-/HSA+ fractions (Figure 21 and Figure 22).

A

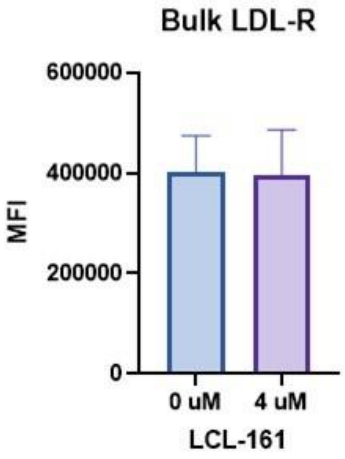
Bulk LDL-R
600000
400000
200000
0
MFI
0 uM
4 uM
LCL-161

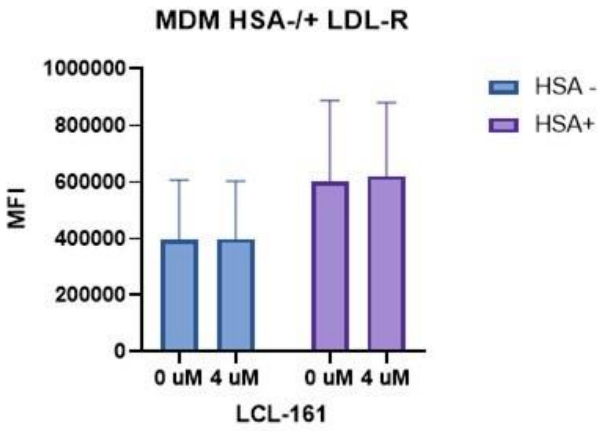
MDM HSA-/+ LDL-R
1000000
800000
600000
400000
200000
0
MFI
0 uM 4 uM
0 uM 4 uM
LCL-161
HSA -
HSA+

B

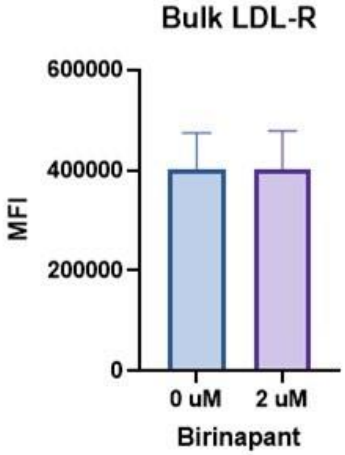
Bulk LDL-R
600000
400000
200000
0
MFI
0 uM
2 uM
Birinapant

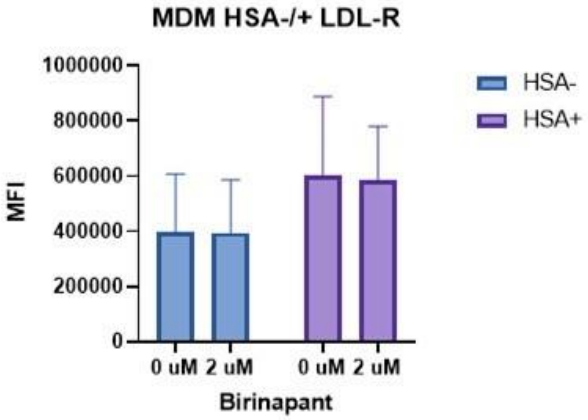
MDM HSA-/+ LDL-R
1000000
800000
600000
400000
200000
0
MFI
0 uM 2 uM
0 uM 2 uM
Birinapant
HSA-
HSA+

Figure 21, LDL-R expression remains unchanged on HIV-infected SMAC mimetic treated MDM following 48h of treatment. Row A) LDL-R expression on LCL 161 treated HIV+ MDM in bulk and HSA- (bystander) and HSA+ (HIV-infected) populations. Cell viability of bulk MDM following 48hpi concurrent treatment. **Row B)** LDL-R expression on birinapant treated HIV+ MDM in bulk and HSA- (bystander) and HSA+ (HIV-infected) populations.

A

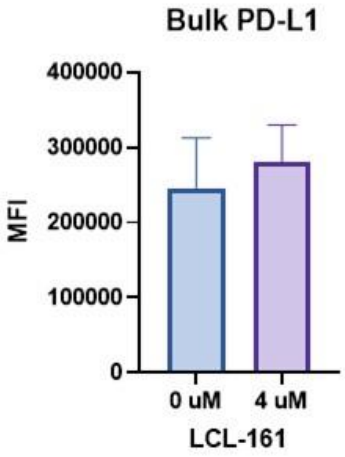
Bulk PD-L1
MFI
400000
300000
200000
100000
0
0 uM
4 uM
LCL-161

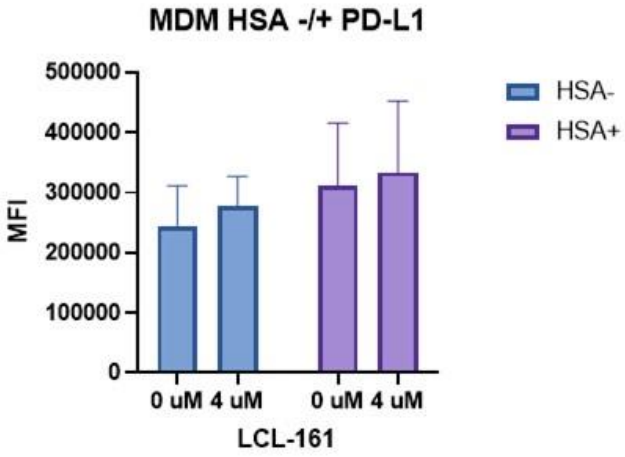
MDM HSA -/+ PD-L1
MFI
500000
400000
300000
200000
100000
0
0 uM 4 uM
0 uM 4 uM
LCL-161
HSA-
HSA+

B

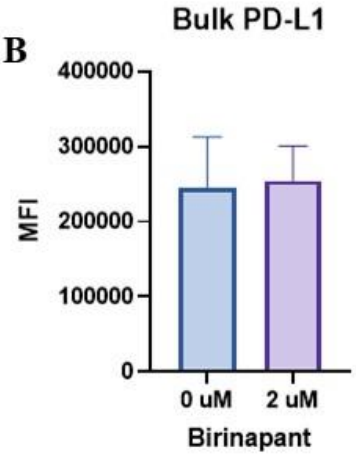
Bulk PD-L1
MFI
400000
300000
200000
100000
0
0 uM
2 uM
Birinapant

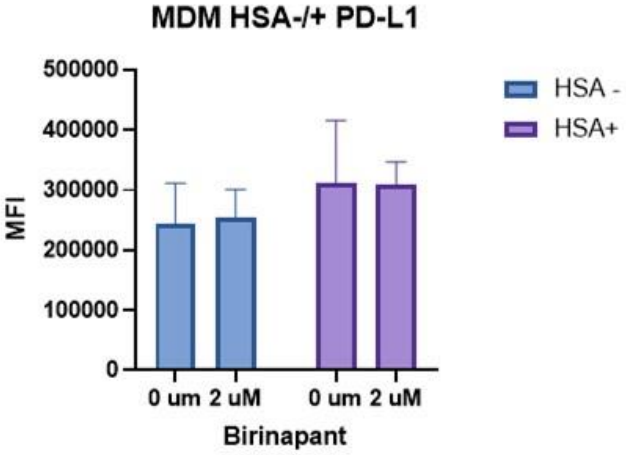
MDM HSA-/+ PD-L1
MFI
500000
400000
300000
200000
100000
0
0 um 2 uM
0 um 2 uM
Birinapant
HSA -
HSA+

Figure 22, PD-L1 expression remains unchanged on HIV-infected SMAC mimetic treated MDM following 48h of treatment. Row A) PD-L1 expression on LCL 161 treated HIV+ MDM in bulk and HSA- (bystander) and HSA+ (HIV-infected) populations. Cell viability of bulk MDM following 48hpi concurrent treatment. Row B) PD-L1 expression on birinapant treated HIV+ MDM in bulk and HSA- (bystander) and HSA+ (HIV-infected) populations.

Next, TNFα was measured in the supernatants of MG1 and SMAC mimetic treated HIV-infected MDM via ELISA. There was a significant production of TNFα in cells treated with MG1 or MG1 and SMAC mimetics (Figure 23). To investigate if cell death is dependent on TNFα, HIV-infected MDM were treated with exogenous TNFα, or TNFα and birinapant to see if exogenous TNFα can replace the effect of MG1 infection. However, no increased cell death could be seen compared to control with the combination treatment, implying that although TNFα production may be important in cell death, it is not solely dependent on it (Figure 24).

IFNα production following MG1 infection and SMAC mimetic treatment was measured via ELISA, but was not detectable (not shown).

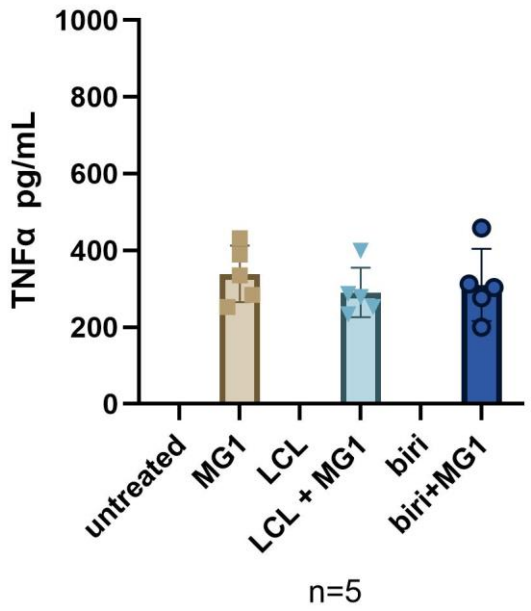
1000
800
600
400
200
0
TNFα pg/mL
untreated
MG1
LCL
LCL + MG1
biri
biri+MG1
n=5

Figure 23, TNFα is detected in the supernatants HIV+MDM treated with MG1 or MG1 and SMAC mimetics. HIV-infected MDM were infected with MG1 MOI 1 and treated with the SMAC mimetic LCL 161 (4 μM) or birinapant (2 μM). TNFα was measured 48h post treatment via TNFα ELISA.

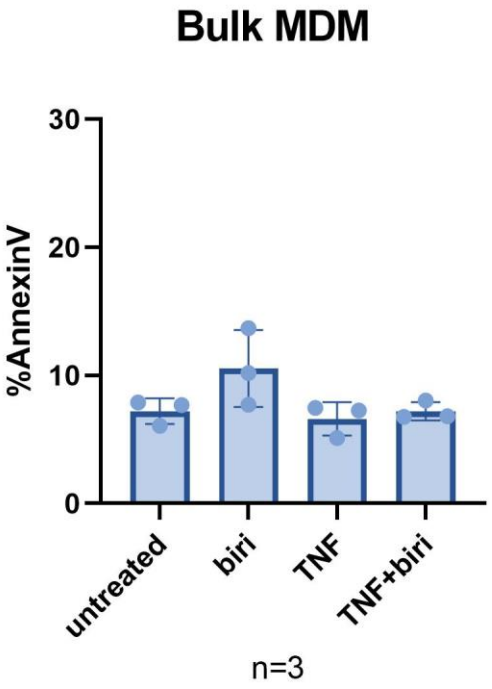
Bulk MDM
%AnnexinV
30
20
10
0
untreated
biri
TNF
TNF+biri
n=3

Figure 24, Exogenous TNFα treatment in combination with birinapant does not result in an increase in cell death. HIV-infected MDM were either left untreated, treated with 2μM birinapant, treated with 10 μg TNFα, or treated with a combination of birinapant and TNFα. Cell death was measured 48h post treatment via AnnexinV staining in bulk macrophage population by flow cytometry.

4.2.3 VSVΔ51-GFP infection and killing of HIV-infected cell lines and HIV-infected MDM in combination with SMAC mimetics

VSVΔ51 has been previously demonstrated to be not effective in killing HIV-infected cell lines or HIV-infected MDM[159,161]. Hence, the effect of SMAC mimetics to sensitize HIV-infected cells to VSVΔ51 mediated death was evaluated. Firstly, latently infected OM10.1 cells were concurrently treated with VSVΔ51 and SMAC mimetics AEG 40730, LCL-161 and birinapant for 48h. Following this, cell death was measured by PI staining and infection was measured by GFP via flow cytometry. Interestingly, LCL-161 and birinapant did not result in increased cell death of OM10.1 when combined with VSVΔ51 infection, even though this effect could not be seen with MG1. A slight but insignificant increase in GFP% also accompanied the increase in cell death (Figure 25).

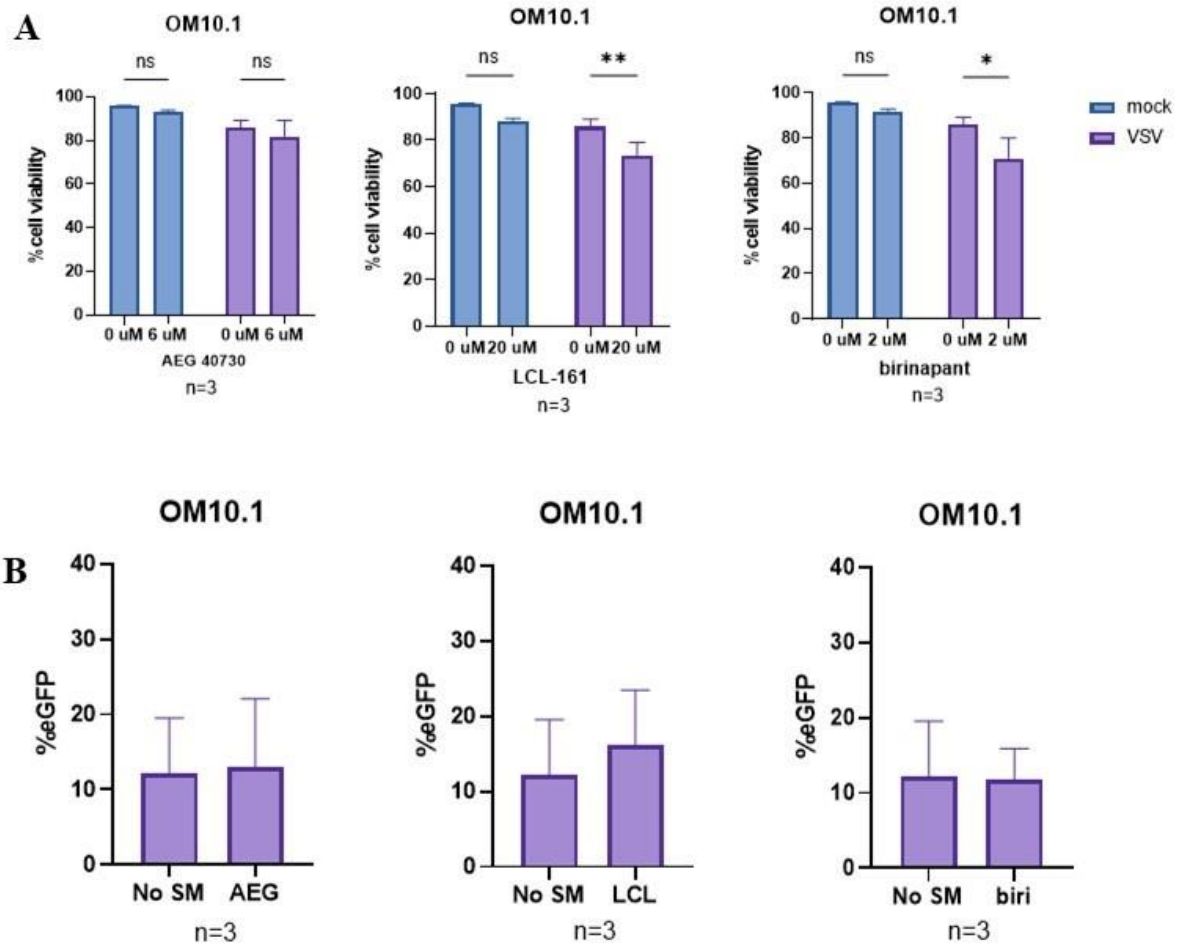
A
OM10.1
ns
ns
% cell viability
0 uM 6 uM
0 uM 6 uM
AEG 40730
n=3
OM10.1
ns
**
0 uM 20 uM
0 uM 20 uM
LCL-161
n=3
OM10.1
ns
*
0 uM 2 uM
0 uM 2 uM
birinapant
n=3
mock
VSV
B
OM10.1
%αeGFP
No SM
AEG
n=3
OM10.1
No SM
LCL
n=3
OM10.1
No SM
biri
n=3

Figure 25, cell viability of OM10.1 cells decreases after combination treatment with VSVΔ51 and SMAC mimetics but infection% remains unchanged. OM10.1 cells were infected with VSVΔ51 MOI 1 and treated with SMAC mimetics AEG 40730 (6 μM.), LCL 161 (20 μM) and birinapant (2 μM). Cell death was measured by flow cytometry via PI staining. **Row A)** Cell viability of OM10.1 cells following 48hpi concurrent treatment **Row B)** GFP% following 48h of concurrent treatment. (*P<.05, **P < .01, by 2-way analysis of variance with the Dunnet post hoc test for multiple comparisons between different SMAC mimetic doses. Data represent mean values ± standard deviation of the mean; n values represent separate biological replicates.)

Next, HIV-infected MDM were concurrently treated with VSVΔ51 and either LCL 161 or birinapant. 48h post infection cells cell death was (AnnexinV) measured in both bulk macrophages and the HSA-/HSA+ population via flow cytometry. Although VSVΔ51 alone does not kill in either bulk MDM or HSA-/+ populations, there is a significant increase in death when it is used in combination with either LCL 161 or birinapant (Figure 26 and Figure 27). Interestingly, the amount of cell death was higher compared to combination treatment with MG1 and SMAC mimetics. Furthermore, even though not significant, a decrease in proviral HIV DNA can be observed (Figure 28).

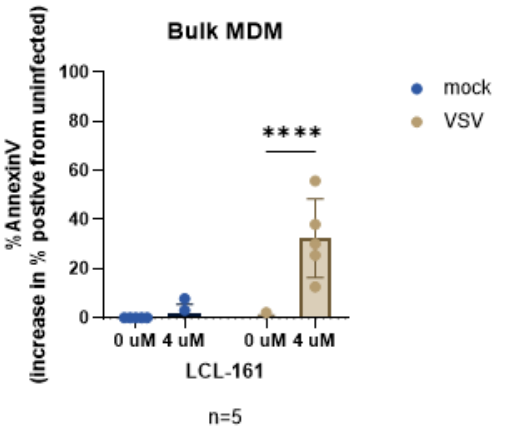
Bulk MDM
%AnnexinV
(increase in % postive from uninfected)
100
80
60
40
20
0
****
mock
VSV
0 uM 4 uM 0 uM 4 uM
LCL-161
n=5

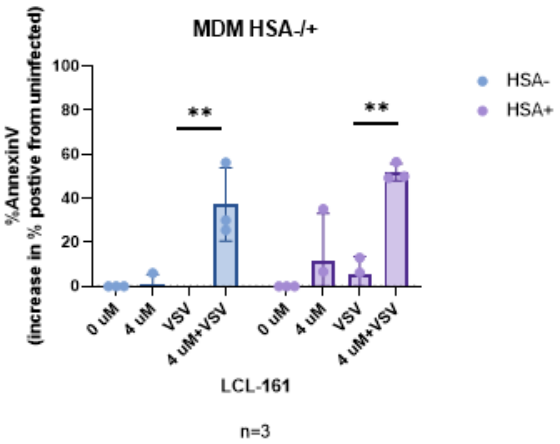
MDM HSA-/+
%AnnexinV
(increase in % postive from uninfected)
100
80
60
40
20
0
**
**
HSA-
HSA+
0 uM
4 uM
VSV
4 uM+VSV
0 uM
4 uM
VSV
4 uM+VSV
LCL-161
n=3

Figure 26, cell viability of HIV-infected monocyte-derived macrophages decreases after combination treatment with VSVΔ51 and LCL-161. HIV-infected MDM were infected with VSVΔ51 MOI 1 and treated with the SMAC mimetic LCL 161 (4 μM). Cell death was measured by AnnexinV staining and HIV infection status was determined by HSA staining via flow cytometry. **A)** Cell viability of bulk MDM following 48hpi concurrent treatment. (****P<.0001, by 2-way analysis of variance with the Dunnet post hoc test for multiple comparisons between different SMAC mimetic doses. Data represent mean values ± standard deviation of the mean; n values represent separate biological replicates.) **B)** Breakdown of cell viability of HSA- (bystander) and HSA+ (HIV-infected) MDM. (**P<.01, 1-way analysis of variance was performed within each group with Tukey's multiple comparison's post-test for multiple comparisons. Data represent mean values ± standard deviation of the mean; n values represent separate biological replicates.)

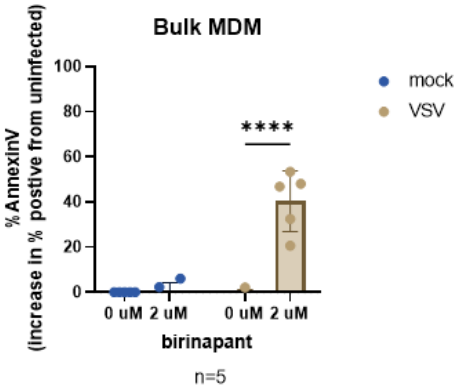
Bulk MDM
% AnnexinV
(increase in % postive from uninfected)
100
80
60
40
20
0
****
0 uM
2 uM
0 uM
2 uM
birinapant
n=5
mock
VSV

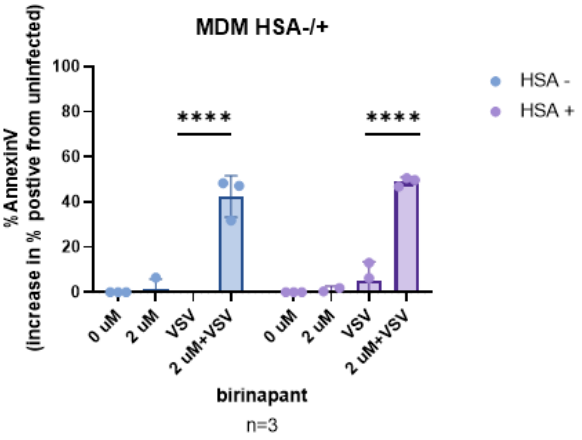
MDM HSA-/+
% AnnexinV
(increase in % postive from uninfected)
100
80
60
40
20
0
****
****
0 uM
2 uM
VSV
2 uM+VSV
0 uM
2 uM
VSV
2 uM+VSV
birinapant
n=3
HSA -
HSA +

Figure 27, cell viability of HIV-infected monocyte derived macrophages decreases after combination treatment with VSVΔ51 and birinapant. HIV-infected MDM were infected with VSVΔ51 MOI 1 and treated with the SMAC mimetic birinapant (2 μM). Cell death was measured by AnnexinV staining and HIV infection status was determined by HSA staining via flow cytometry. **A)** Cell viability of bulk MDM following 48hpi concurrent treatment. (****P<.0001, by 2-way analysis of variance with the Dunnet post hoc test for multiple comparisons between different SMAC mimetic doses. Data represent mean values ± standard deviation of the mean; n values represent separate biological replicates.) **B)** Breakdown of cell viability of HSA- (bystander) and HSA+ (HIV-infected) MDM. (****P<.0001, 1-way analysis of variance was performed within each group with Tukey's multiple comparison's post-test for multiple comparisons. Data represent mean values ± standard deviation of the mean; n values represent separate biological replicates.)

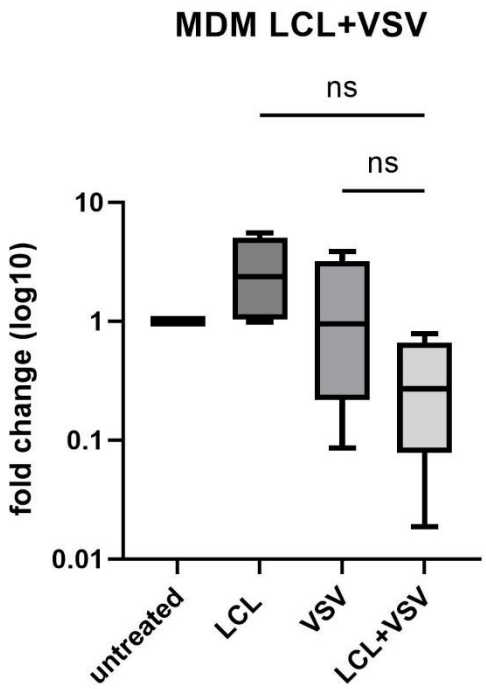
MDM LCL+VSV
ns
ns
10
1
0.1
0.01
fold change (log10)
untreated
LCL
VSV
LCL+VSV

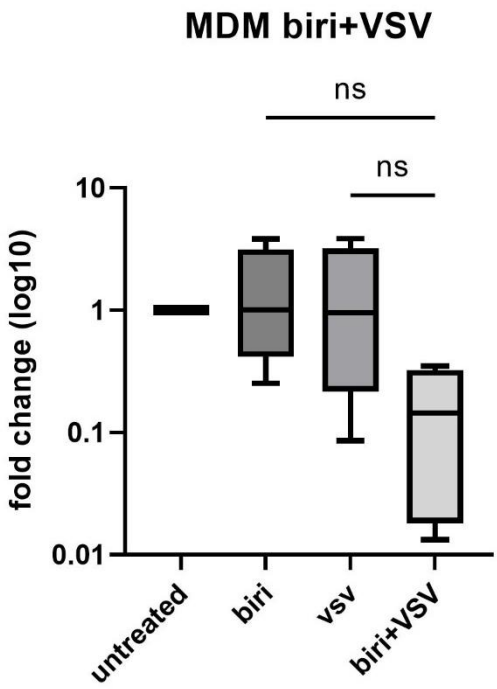
MDM biri+VSV
ns
ns
10
1
0.1
0.01
fold change (log10)
untreated
biri
vsv
biri+VSV

Figure 28 although not significant, a decrease in proviral HIV DNA following combination treatment with VSVΔ51 relative to HIV-infected untreated cells can be seen HIV-infected MDM were infected with VSVΔ51 MOI 1 and treated with the SMAC mimetic **A)** LCL 161 (4μM) or **B)** birinapant (2 μM). Proviral HIV DNA was measured by qPCR. n=4

4.2.4 Cytokine production following SMAC mimetic treatment and VSV51 infection of HIV-infected MDM

As cell death with combination treatment of VSVΔ51 and SMAC mimetics are higher than that of combination treatment with MG1 and SMAC mimetics, it was hypothesized that one of the reasons for this may be the VSVΔ51 infection resulting in a more pro-inflammatory compared to MG1 infection in terms of TNFα production. Thus, TNFα was measured in the supernatants of VSVΔ51 and SMAC mimetic treated HIV-infected MDM via ELISA. There was a significant production of TNFα in cells treated with VSVΔ51 or VSVΔ51 and SMAC mimetics (Figure 29A). The amount of TNFα produced is higher compared to TNFα produced due to MG1 infection, which may be one of the reasons why combination treatment with VSVΔ51 and SMAC mimetics result in higher percentage of cell death.

Next the production of IFNα following VSVΔ51infection and SMAC mimetic treatment was measured via ELISA. Interestingly, although not significant, there was a decrease in IFNα when VSVΔ51 was combined with SMAC mimetics (Figure 29B). One of the reasons why VSVΔ51 by itself does not kill but kills when combined with SMAC mimetics could be due to the decreased production of IFNα.

A

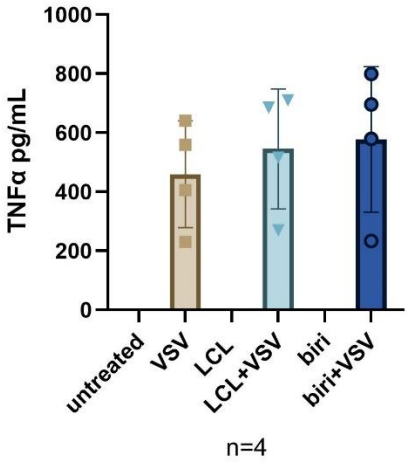
TNFα pg/mL
1000
800
600
400
200
0
untreated
VSV
LCL
LCL+VSV
biri
biri+VSV
n=4

B

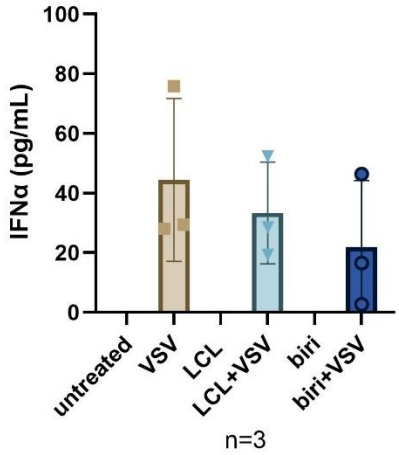
IFNα (pg/mL)
100
80
60
40
20
0
untreated
VSV
LCL
LCL+VSV
biri
biri+VSV
n=3

Figure 29, TNFα and IFNα is detected in the supernatants HIV+ MDM treated with VSVΔ51 and SMAC mimetics. HIV-infected MDM were infected with VSVΔ51 MOI 1 and treated with the SMAC mimetic LCL 161 (4 μM) or birinapant (2 μM). A) TNFα was measured 48h post treatment via TNFα ELISA.B) IFNα was measured 48h post treatment via IFNα ELISA.

Chapter 5

Pseudotyping MG1 with HIV envelope protein to enhance its ability to selectively kill HIV-infected cells.

5.1 Introduction and Rationale

MG1 is an oncolytic virus that mainly uses the LDL receptor for viral entry, granting it broad tropism[146]. Although this is beneficial for the usage of MG1 in treating different types of cancer in different tissues[150–152,154], it is important to increase MG1's inherent selectivity for latently HIV-infected cells if it is to be used in the clinic as a potential treatment for HIV infection. Enhancing MG1's selectivity can be achieved by pseudotyping MG1 with HIV envelope protein gp160, thereby effectively narrowing its tropism to cells that express the receptors required for viral entry of HIV, in this case, CD4 and CCR5.

Although pseudotyping of MG1 or Maraba virus has not been done yet, there are many studies in which VSV has been pseudotyped with HIV envelope[245,249–251,264]. The main challenge in pseudotyping with HIV gp160 is the incorporation of a functional HIV envelope protein in the VSV envelope. Studies have shown that a signal present at gp41 may prevent correct insertion into the VSV envelope, and that truncations to the CT-tail of HIV envelope, along with fusing gp120 to the CT-tail of VSV G, can increase incorporation efficiency along with viral titer upon viral rescue[250,251]. Therefore, as a proof of concept, MG1 clones containing full length HIV envelope, truncated HIV envelope, and truncated HIV envelope fused to MG1 G were developed.

5.2 Results

5.2.2 MG1 clone generation

Three versions of MG1 containing HIV envelope were made.

- Mgp160: Full length CCR5 tropic HIV envelope from p96ZM651 expression plasmid was cloned into MG1-Gless backbone via restriction enzyme cloning. Then the conserved

VSV/MG1 start stop sequence (5’ TGTATGAAAAAAACTCATCAACAGCCATC 3’)[254] was added by Q5 site directed mutagenesis kit.

- MTM_4aa: Truncated HIV envelope cut to 4 amino acids after the transmembrane region was cloned into MG1 G-less backbone via Gibson assembly. the conserved VSV/MG1 start stop sequence (5’ TGTATGAAAAAAACTCATCAACAGCCATC 3’)[254] was added by Q5 site directed mutagenesis kit.
- Mct: The truncated insert used to generate MTM_4aa was cloned into the MG1 backbone fused to the CT region of MG1 G glycoprotein using Gibson Assembly

All clones were verified using full length plasmid sequencing by Plasmidsaurus. The clone plasmids can be seen in Figure 30.

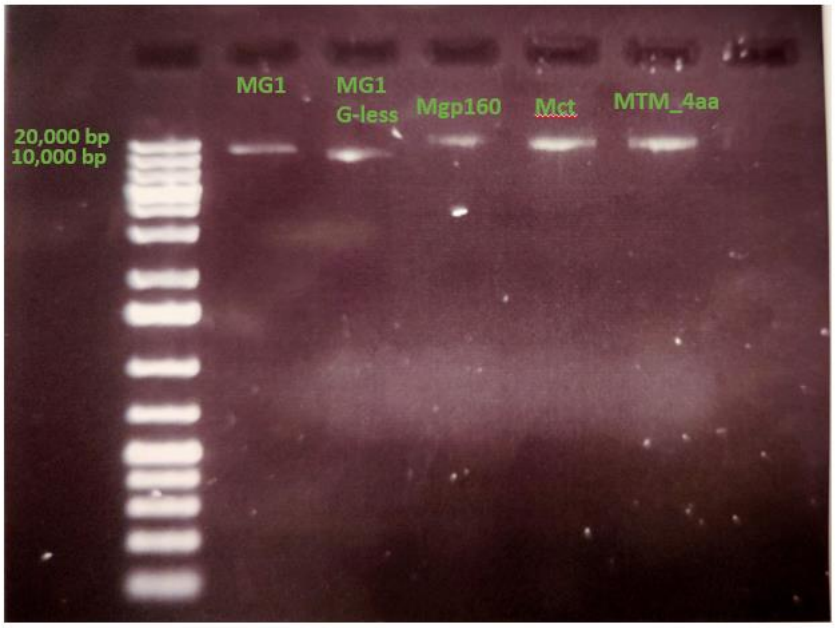
MG1
MG1
G-less
Mgp160
Mct
MTM_4aa
20,000 bp
10,000 bp

Figure 30, MG1, MG1 G-less Mgp160, Mct and MTM_4aa plasmids. Agarose gel electrophoresis image where lanes 2 contains MG1 eGFP plasmid (14,023 bp), lane 3 contains MG1 G-less plasmid (12,440 bp), lane 4 contains Mgp160 plasmid which has full length gp160 insert (15,536 bp), and lane 5 contains Mct plasmid which has gp160 insert fused to MG1 G glycoprotein (14,686 bp) and lane 6 contains MTM_4aa plasmid which has a truncated gp160 insert (14,407 bp). The DNA ladder used is Gene Ruler 1 Kb plus (Thermoscientific). All clones were verified by full length plasmid sequencing.

5.2.3 Viral rescue for MG1 pseudotyped with HIV envelope

A modified VSV rescue protocol[265] where single gene expressing plasmids, N, P, and L were switched to MG1 gene single gene plasmids, was used initially to rescue MG1 and MG1 clones. Briefly, the cells are infected with T7 polymerase expressing Vaccinia virus (T7 VV). After infection, the cells are transfected with MG1 single gene plasmids containing MG1 N, MG1 P, MG1 L and MG1 backbone using Lipofectamine 2000. As all plasmids are under the control of T7 promoter, transcription occurs from the plasmids due to the Vaccinia virus infection, after 24-48h incubation, VV is filtered out using 0.22 μm filter, and the remaining supernatant is used to amplify the rescued virus. Although the rescue of "WT" MG1 was successful, the clones were unable to be rescued by using this protocol. Hence, optimizations were made to be able to rescue the MG1 clones. These optimizations include but are not limited to:

- Using different cell lines for the rescue: Vero, GHOST, HEK 293T, TREx ™-293 cells expressing VSV G
- MOI of T7 vaccinia: MOI1, MOI 3, MOI 5
- Using extra plasmids: VSV G, HIV envelope expression plasmid p96zm651
- Increasing or decreasing the amount of time cells are infected with T7 Vaccinia
- Increasing total run time of experiment up to 3 weeks
- Using different transfection reagents: Lipofectamine 2000. Fugene, Fugene 4K, GeneJuice

A more detailed version of optimizations made can be found in Table 4. Although transfection was successful in most of the conditions, as verified by GFP expression under confocal microscopy, no infectious viral particles were obtained. The results of each optimization trial is discussed in detail in Chapter 6.

Cell line	**T7 MOI**	**T7 incubation time**	**Plasmids**	**Transfection Reagent**	**Rescue total time**
Vero	5/3/1	48h	standard	Lipofectamine 2000	7 days
Ghost	5/3/1	48h	standard	Lipofectamine 2000	7 days
Ghost	1	24h	standard	Lipofectamine 2000	7 days
Ghost	1	24h	increased concentration of N plasmid	Lipofectamine 2000	7 days
Ghost	1	24h	+HIV envelope expression plasmid	Lipofectamine 2000	7 days
Ghost	1	24h	Increased concentration of N plasmid and extra HIV envelope expression plasmid	Lipofectamine 2000	7 days
HEK 293T	1	24h	standard	Lipofectamine 2000	7 days

HEKTrex	1	48h	standard - doxycycline induction to express VSV G	Lipofectamine 2000	7 days
HEKTrex	1	24h	standard - doxycycline induction to express VSV G	Lipofectamine 2000	7 days
HEKTrex	1	48h	standard - doxycycline induction to express VSV G	Lipofectamine 2000	14 days
HEK 293T	1	24h	standard	Fugene	7/14/21 days
HEK 293T	1	24h	standard	Fugene 4K	7/14/21 days
HEK 293T	1	24h	standard	GeneJuice	7/14/21 days

Table 4, Optimization strategies to rescue MG1 clones. Standard plasmids refer to MG1 N, MG1 P, and MG1 L.

Chapter 6

Discussion

6.1 Summary

The oncolytic virus MG1 has been shown to kill latently HIV-infected cell lines, latently HIV-infected $CD4^+$ T-cells and persistently HIV-infected monocyte derived macrophages[159,161]. We have shown that pro-apoptotic SMAC mimetics can sensitize HIV-infected cells to oncolytic rhabdovirus mediated death. It is shown in Chapter 3 of this thesis that combination therapy with MG1 and SMAC mimetics result in a greater killing of the latently HIV-infected cell lines J1.1 and OM10.1 than with either treatment alone, and this depends on the order of treatment administration. It is shown in Chapter 4 of this thesis that combination therapy with MG1 and the SMAC mimetics LCL-161 and birinapant result in increased killing of HIV-infected monocyte derived macrophages and bystander cells. Furthermore, it is shown that although VSVΔ51 infection by itself is not able to kill the latently infected OM10.1 cells or persistently HIV-infected monocyte derived macrophages, combination therapy with LCL-161 or birinapant significantly increases cell death. Lastly, it is shown in Chapter 5 that while pseudotyping MG1 with HIV envelope protein gp160 might be an option to increase the specificity of MG1 to target cells of HIV, but the rescue of the pseudotyped MG1 was not successful.

6.2 SMAC mimetics sensitize HIV-infected cell lines to MG1-mediated death

As demonstrated in Chapter 3, combination therapy with MG1 and SMAC mimetics AEG 40730, LCL-161, and birinapant kill HIV-infected cell lines. Cell death was evaluated by PI staining via flow cytometry. It was shown that treatment order regarding MG1 and SMAC mimetics administration is important in the increase in cell death. Although cell death was accompanied by an increase in caspase-3/7 and caspase-1 activity, the pan-caspase blocker ZVAD-fmk and RIPK-1 inhibitor necrostatin-1s failed to increase cell viability when cells underwent

combination treatment, suggesting that more than one programmed cell death may be in play. Furthermore, SMAC mimetic treatment resulted in an increase in LDL-R expression on J1.1 cells, but this increase did not correlate with an increase in infection as measured by GFP or viral production as measured by plaque assay, indicating the relevance of this observation remains unknown. There was also no increase in the level of cell surface expression of PD-L1 following SMAC mimetic treatment. Lastly, the non-canonical NFκB pathway was activated upon SMAC mimetic treatment, but it did not necessarily result in production of TNFα, confirming that in HIV-infected cell lines, the role of TNFα in cell death is unclear.

6.2.1 Importance of the treatment order of MG1 and SMAC mimetics

As explained in the Introduction, Kim et al., has shown that in EMT6 tumor bearing mice, treatment intravenous injection of VSVΔ51 followed by LCL-161 treatment 6 hours after injection resulted in increased survival, LCL-161treatment prior to infection with VSVΔ51 resulted in a complete loss of OV infection[238]. Other studies have shown that LCL-161 treatment itself does not affect the growth kinetics of VSVΔ51[237], leading to Kim and colleagues hypothesizing that perhaps in their *in vivo* model, LCL-161 pre-treatment results in secretion of anti-viral cytokines.

Using the above studies as a guide, three different orders of treatment administration were tested in HIV-infected cell lines; (1) concurrent treatment with MG1 and SMAC mimetics, (2) MG1 infection followed by SMAC mimetics treatment, and (3) SMAC mimetics treatment followed by MG1 infection. The results show that administration order is indeed important, though this depended on the cell line model. In J1.1 cells, cell death generally increased in all three situations. However, in OM10.1 cells, only AEG 40730 pre-treatment followed by MG1 infection resulted in increased cell death. Interestingly, AEG 40730 treatment is the only condition in which

OM10.1 cells have detectable TNFα secretion, suggesting there might be a causal relationship with cell death and TNFα in the specific case of pre-treatment of OM10.1 cells with AEG 40730, but more research is required to confirm this potential relationship.

These results confirm the importance of treatment administration order, and that this should be one of the considerations when combination treatment moves on to animal models.

6.2.2 MG1 and cell death pathways

How MG1 kills cells, particularly cells latently infected with HIV, is still a point of ongoing research. VSV was shown to kill cancer cells via a 'combination of apoptosis, necroptosis, and pyroptosis, a newly identified molecular pathway called PANoptosis[266]. By using VSV cell death pathways as a guide, our group has shown that MG1 may favor different killing mechanisms of latently HIV-infected cells than their uninfected counterparts. Cell death induced by MG1 could be significantly reduced when HIV uninfected cells Jurkat and HL-60 were treated with the pan-caspase inhibitor ZVAD-fmk or the caspase-3/7 inhibitor ZDEVD-fmk, whereas both inhibitors failed to reduce cell death in latently HIV-infected cell lines J1.1 and OM10.1[260]. Similarly, in MDM infected *ex vivo* with HIV, cell death by MG1 was unable to be blocked by the ZVAD-fmk or the necroptosis inhibitor necrostatin-1.

In this study, it was shown that an increase in caspase-3/7 and caspase-1 accompanies cell death. These caspases are active in apoptosis and pyroptosis respectively. However, although cell death induced by SMAC mimetics could almost completely be inhibited by the combination of ZVAD-fmk and necrostatin-1s, cell death following MG1 infection was not blocked. These results indicate that although caspases responsible for programmed cell death pathways get activated following MG1 infection, the cells might be switching to other cell death mechanisms and

continuing to die. One of the players in MG1 induced cell death might be ER stress induced unfolded protein response pathway (UPR) due to the accumulation of unfolded or misfolded proteins in the cytoplasm). UPR results in regulation of gene expression, inhibition of protein synthesis, and in some cases, cell death[267,268].

Interestingly, in experiments done in U2OS sarcoma line, MG1 infection caused an increase in the expression of the anti-apoptotic protein Bcl-X_L at the translational level, and a significant increase in *XIAP* mRNA at 12h post infection, eliciting a somewhat anti-apoptotic response. However, in U343 glioblastoma cells, it was shown that the expression of pro-apoptotic genes in the ER stress pathway such as *CHOP* and *GADD34* were increased, confirming that depending on the cell line, MG1 may result in the UPR pathway getting activated[269].

Surprisingly, this is not the only case where the combination of SMAC mimetics and oncolytic viruses resulted in ER stress. The SMAC mimetics LCL-161 and birinapant have been shown to increase the replication of the oncolytic alphavirus M1 and cause ER-stress mediated cell death in refractory hepatocellular and colorectal cell lines, and ex vivo tumor models established by using the hepatocellular cancer cell lines. The increased protein translation as a result of increased M1 virus replication has been shown to cause ER stress, which results in UPR and ultimately cell death[236].

Considering that cell death caused by MG1 could not be inhibited by apoptosis or necroptosis inhibitors, it is most likely that more than one cell death pathway gets activated during MG1 infection of HIV-infected cells. Since this is the case, one of the pathways to be investigated moving forward should be ER stress and UPR.

6.2.3 Viral sensitizers to increase MG1 infection and killing in HIV-infected cells

As it is unlikely MG1 will be used as a monotherapy in HIV infection, we have proposed to use SMAC mimetics as a way to enhance MG1-mediated killing. Interestingly, although cell death with combination treatment increased significantly, such an increase was not reflected in the proportion of infected cells as measured by GFP expression. Furthermore, although there was increased expression of LDL-R in J1.1 cells following SMAC mimetic treatment, this did not translate to increased infection. Thus, the physiological relevance of increased LDL-R expression is not clear.

Since rhabdovirus infection can block cellular transcription by modulating eukaryotic transcription initiation factors[269] and thus possibly affect the transcription of GFP, viral output as an indication of MG1 production was measured via plaque assay. It was found that there was significantly less virus in supernatant from combination treated cells compared to cells only infected with MG1. One of the reasons for the lack of increased infection observed with SMAC mimetics treatment may be due to the greater level of cytotoxicity that occurs during combination treatment, and the resulting decrease in target cells for MG1 infection. Another reason might be that MG1 and SMAC mimetics work through different pathways to kill the cells that do not necessarily interact. As shown in the cell death inhibitor treatment experiments, ZVAD-fmk and necrostatin-1s can almost completely block cell death in SMAC mimetic treated cells whereas they do not affect the cell viability in cells infected with MG1. Thus, it may be that the cytotoxicity effect of combination treatment is additive rather than synergistic.

Drugs such as the HDACi SAHA and the PKR inhibitor C16 have been used in combination with MG1 to kill HIV-infected cells. SAHA has been previously shown to enhance the spread of VSV and dampen the type 1 interferon responses and refractory cancer cell lines,

primary tissue explants and animal models[270]. In latently HIV-infected cells OM10.1 and U1, SAHA was able to increase infection of VSVΔ51 but not cell death. However, SAHA pre-treatment was shown to increase both the percentage of cells infected by MG1 and cell death in these cell lines. The effect of SAHA stimulation was shown to be specific to HIV-infected cell lines, as the SAHA and MG1 combination treatment of uninfected parental cell lines HL60 and U937 did not result in increased infection or cell death. It was hypothesized that the reason behind this effect could be due to increased dampening of the type 1 interferon responses of HIV-infected cell lines[159]. Interestingly, SAHA pre-treatment was unable to increase infection or cell death caused by either VSVΔ51 or MG1 in HIV-infected MDM[161].

The effect of C16, a PKR inhibitor was also investigated in combination with MG1 infection in other studies. PKR is an RNA sensing antiviral protein and can induce antiviral apoptosis[271]. When HIV-infected MDM were pre-treated with C16 and then infected with MG1, it was seen that the percentage of infected cells increased significantly in both in HSA- and HSA+ fractions, but the overall reduction of HIV as measured by qPCR was not altered by C16, implying that increased infection does not necessarily result in increased cell death. These results suggest that C16 is most likely inhibiting the activity of PKR in both HSA- and HSA+ fractions, rendering them both more permissive to MG1 infection[161]. Going forward, it might be worthwhile to devise a way to deliver C16 directly to persistently HIV-infected cells, or to upregulate the ISG production in bystander cells to protect them against the activities of C16.

6.2.5 RNAseq analysis of J1.1 cells treated with SMAC mimetics and infected with MG1

To better understand the changes that occur in the cell with the addition of SMAC mimetics to MG1 infection, the cell transcriptome of cells treated with MG1 and SMAC mimetics was compared to cells infected with MG1. The genes that were upregulated were shown to mainly belong to immune response pathways and the genes that were downregulated belong to the sterol biosynthesis pathway. Although it has been previously shown that HIV infection is capable of upregulating the expression of genes that play a role in the cholesterol synthesis pathway[272], the effect of oncolytic virus infection and SMAC mimetics on cholesterol biosynthesis has on latently HIV-infected cells have not been yet shown. Interestingly, in a murine cytomegalovirus (mCMV) infection model, it has been shown that there is crosstalk between host defense mechanisms and metabolic pathways. Specifically, it was shown that IFNβ and IFNγ produced in response to viral infection results in transcriptional downregulation of the sterol biosynthesis pathway[273]. In our model, the downregulation of sterol biosynthesis pathway (and the consequent upregulation of lipid storage) may be partly explained as a consequence of the ongoing viral infection.

When the immune response regulated pathway is examined closely, it can be seen that genes that increase permissiveness to RNA viruses (*CD24*)[274], and genes that restrict viral replication (*ZC3H12A)*[275,276] are upregulated, showing that the effect that SMAC mimetics have on HIV infected cells that have been infected with MG1 and treated with SMAC mimetics is not straightforward. Going forward, more in depth analysis, including the validation of mRNA targets in the protein level will be necessary to fully elucidate the changes caused by SMAC mimetic treatment in the context of MG1 infection.

6.2.6 NFκB signaling following SMAC mimetic treatment

SMAC mimetics have been shown to activate non-canonical NFκB signaling as they result in the degradation of cIAP proteins in the cytoplasm, therefore freeing NIK, and starting the non-canonical NFκB signaling cascade[277]. It was seen that all three SMAC mimetics tested in HIV-infected cell lines resulted in an increase in non-canonical NFκB activation. Other studies in the HIV field have shown that this non-canonical NFκB activation can result in latency reversal and production of active virions[228,229]. Therefore, SMAC mimetics can be used as latency reversal agents for the 'shock and kill' approach. However, increased p24 production did not occur in SMAC mimetic treated J1.1 cells or OM10.1 cells, implying that SMAC mimetics did not increase HIV protein production and hence did not reverse HIV latency. These results confirm that the effect of the SMAC mimetics on latently HIV-infected cells are heavily dependent on the SMAC mimetic and the HIV infection model used. Lastly, the increase in non-canonical NFκB signaling did not necessarily translate to an increase in TNFα production with the exception of in OM10.1 cells treated with a high dose of AEG 40730. The role TNFα may have in combination treatment with SMAC mimetics and MG1 is further discussed below in detail in the HIV-infected macrophages section.

6.3 SMAC mimetics sensitize HIV-infected monocyte derived macrophages to MG1-mediated death

As demonstrated in Chapter 4, the SMAC mimetics LCL-161 and birinapant sensitize HIV-infected MDM to MG1-mediated death. MDM were infected with the reporter virus HIV-NL4.3-BAL-IRES-HSA to be able to differentiate between actively infected and bystander cells,

determined by the presence of mouse HSA (CD24) on the cell surface. Cell death was assessed both in bulk populations and HSA-/+ populations via AnnexinV staining.

6.3.1 SMAC mimetics can kill macrophages in different disease models

With inflammatory and anti-inflammatory properties, macrophages play a role in different diseases such as cancer[278], and tuberculosis[279], leprosy[280], and multiple sclerosis[281].Therefore, studying the effect of SMAC mimetics in killing macrophages is important in finding new treatment options. Hamza et al., has shown that although unpolarized M0 and anti-inflammatory M2 macrophages are resistant to SMAC mimetic mediated death, the inflammatory M1 macrophages are highly susceptible. Interestingly, in this model, SMAC mimetic induced death was not shown to depend on the level of expression of inhibitors apoptosis proteins, which suggest that other pathways may be important when determining the sensitivity to SMAC mimetic treatment[282].

SMAC mimetics have been used to modulate macrophage activity in disease models such as IGROV-1 human ovarian carcinoma cells and sarcoma tumor bearing mice. SMAC mimetic SM83 was able to revert the phenotype of tumor associated macrophages from M2 to M1 state, and also resulted in neutrophil recruitment, which aided in tumor clearance. In another study, Stutz et al., show that *Mycobacterium tuberculosis* infected macrophages can be killed by using the SMAC mimetics LCL-161 and birinapant, and that in mouse infection models, this results in reduction in bacterial burden in both pulmonary and extra-pulmanory sites[283].

In HIV research, previous studies have shown that treatment with the SMAC mimetic AEG 40730 of MDM infected with HIV-BAL-HSA reporter virus, results in a significant increase in cell death in the HSA+ fraction compared to HSA- cells. A similar but not significant increase was also observed in LCL-161 treated HIV-infected MDM[235]. In another study, where MDM were

infected with two different non-reporter HIV strains, $HIV_{Ba\text{-}L}$ and $HIV_{93IN905,}$ treatment with LCL-161, AT-406, or birinapant resulted in significant decreases of the inhibitors of apoptosis proteins cIAP1 and XIAP, accompanied by cell death[223]. However, it is important to consider that in that study, the percentage of MDM persistently infected with HIV was measured by p17 (HIV matrix) protein expression, and reported to be 80%, which is most likely an overestimation as (1) macrophages may be infected with HIV but might not be able to form infectious virions due to abortive replication and (2) macrophages can engulf p17 and stain positive without being infected by HIV. Thus, it is most likely that the amount of persistently infected cells is lower than what is reported. Regardless, these studies done by Caballero et al[235]., and Campbell et al[223]., suggest that there is preferential killing of HIV-infected MDM when treated with SMAC mimetics. In this thesis, it was shown that there is no increase in cell death in the bulk population of MDM treated with LCL-161 or birinapant but in the HSA- and HSA+ fractions, there was a slight but insignificant increase in SMAC mimetic treatment only condition. These results imply that SMAC mimetics may indeed selectively kill HIV-infected MDM, but demonstration of how much the population dies relies heavily on the HIV infection model used.

6.3.2 Oncolytic viruses and macrophages in different disease models

Oncolytic virus therapy in cancer can be categorized to have two main outcomes; the establishment of OV infection and direct killing of the tumor cells, or OV infection activating the other immune cells and thus aiding in the immune response against the tumor. In cancer models, OV infection polarizes macrophages to the pro-inflammatory M1 phenotype, and the infection of the tumor results in the infiltration of the macrophages in the tumor microenvironment[284,285].

In the field of HIV, MG1 has been shown to specifically infect and kill persistently HIV-infected macrophages (HSA+). Persistently HIV-infected macrophages have defects in their interferon signalling, presenting as lower expression of MHC-1 on HSA+ cells compared to HSA- cells, and HSA+ cells being less responsive to IFNα stimulation compared to HSA- cells as measured by PKR and ISG15 expression. These defects make HIV-infected macrophages more susceptible to infection by the OV MG1. It was shown that the presence of infectious virus is necessary for the killing, as conditioned media or UV inactivated MG1 failed to produce any effect[161]. It was also shown that even though MG1 infected macrophages have increased caspase 3/7 activity, inhibition by the pan-caspase inhibitor ZVAD-fmk or RIPK1 inhibitor necrostatin-1 failed to prevent MG1-mediated death. This finding is also presented in this thesis in HIV-infected cell line models, showing cell death induced by MG1 most likely occurs via more than one cell death pathway[161].

In a more physiologically relevant model, alveolar macrophages collected from people living with HIV via bronchoalveolar lavage have been shown to be somewhat permissive to MG1 infection. The patients had inter-donor variability and could be broadly categorized as 'responders' and 'non-responders', where responders showed decrease in integrated proviral HIV DNA following MG1 infection[161].

Lastly, it was shown that different oncolytic viruses differ in their abilities to infect and kill HIV-infected macrophages. VSVΔ51 was unable to show a dose dependent decrease in proviral HIV DNA, or an increase in cell death of HSA+ MDM[161,162].

6.3.3 Combination treatment with SMAC mimetics and MG1

To enhance the activity of MG1 killing, combination therapy with MG1 and SMAC mimetics was evaluated on HIV-infected monocyte derived macrophages. With the combination of SMAC mimetics LCL 161 or birinapant, it was shown that while either treatment alone does not increase cell death in bulk cell population, addition of SMAC mimetics resulted in a dramatic increase in cell death caused by MG1. When the population is broken down into HSA- and HSA+, there is significant increase in cell death in both populations, implying that combination therapy might not be as selective as monotherapies in specifically killing HIV-infected cells. However, it must also be taken into consideration that not just infection itself, but other soluble factors released upon treatment might be playing a role in the death of bystander cells.

To further confirm cell death of HIV-infected cells, a decrease in the size of the HIV-infected cell population was determined by the amount of proviral HIV DNA. SMAC mimetic treatment alone did slightly increase cell death as measured by AnnexinV expression, but it did not consistently result in a decrease in proviral HIV DNA. Moreover, while combination treatment slightly decreased proviral HIV DNA compared to single treatment alone, this decrease was not significant. This can potentially be explained by donor variability and the limited amount of biological replicates.. As the qPCR done on these samples measures the integrated amount of proviral HIV DNA, and does not measure amount of HIV transcripts, the proviral DNA measured may not directly correlate with the amount of cells that can produce infectious particles of HIV. This might explain the gap between the flow cytometry results where cell death is measured in cells that are actively producing HIV related proteins versus the decrease in integrated proviral HIV DNA which can be used as a substitute for the cell death in the HIV-infected population.

Next, the cell surface receptor expression of LDL-R or PD-L1 after SMAC mimetic treatment was evaluated to see if their expression levels might be playing a role in the increase in killing. LDL-R, the main receptor MG1 uses for viral entry, has been shown to have an elevated expression on HSA+ macrophages[161,162]. However, neither LCL-161 or birinapant treatment showed an increased expression of LDL-R. There was a slight but insignificant increase in the expression of PD-L1 in LCL-161 treated macrophages both in the bulk and HSA+ and HSA – fractions. Engagement of PD-L1 in cancer cells has been shown to increase glycolysis and thus increase lactate production. This in turn inhibits type 1 IFN responses, which results in enhanced activity of the OV VSVΔ51 in killing cancer cells[263,286]. In HIV, the PD-1 PD-L1 axis has been mainly studied in T-cells and focuses on antibody blocking of PD-L1. PD-L1 blocking has been shown to enhance proliferation of SIV specific $CD4^+$ T-cells and addition of CD28 stimulation has been shown to increase the number of HIV specific $CD4^+$ T-cells[287,288]. Moreover, blocking PD-L1 resulted in reinvigoration of exhausted T-cells and improved viral control in SIV infection in NHP[289,290]. PD-L1 levels have been shown to be increased on dendritic cells, monocytes, and B cells in PLHIV compared to HIV negative controls, and this directly correlated with increase in viral load and decrease in $CD4^+$ T-cell counts[291,292]. Moreover, PD-L1 induction on HIV-infected PBMC requires type 1 IFNs, suggesting that in PD-L1 and type 1 IFN responses may be interconnected in HIV-infected cells as well[293]. To see if this is the case in this infection model, IFNα levels were measured in the supernatants of HIV-infected MDM via ELISA following MG1 infection, SMAC mimetic treatment, or combination treatment. Under none of these conditions was there detectable amounts of IFNα. Thus, we were unable show a relationship between the PD-L1 expression levels and IFNα production, but this pathway can be further explored in the future.

Next, the role of TNFα was investigated in MG1 infected, SMAC mimetic treated, or combination treated HIV-infected MDM. It was found that while SMAC mimetic treatment alone does not result in TNFα production, MG1 infection or MG1 infection with SMAC mimetic treatment does. MG1 infection has been previously shown to result in TNFα production in HIV uninfected MDM[162]. Moreover, in another study SMAC mimetic treatment did not induce TNFα production in HIV-infected MDM and that treating HIV-infected MDM with exogenous TNFα instead of SMAC mimetics did not result in cell death[235]. Interestingly, in another HIV infection model, blocking TNFα in SMAC mimetic treated HIV-infected MDM resulted in the ablation of cell death[223]. To further investigate the role of TNFα, HIV-infected MDM were treated with SMAC mimetics alone, with exogenous TNFα alone or with a combination of the two. Interestingly, there was no increased cell death under any of these conditions, suggesting that the presence of exogenous TNFα cannot replace the effect produced by MG1 infection. These results imply that even though TNFα may be important in cell death of HIV-infected macrophages, its role is not straight-forward and that it is not the only driver of cell death.

6.3.4 Combination treatment with SMAC mimetics and VSVΔ51

Although VSVΔ51 and MG1 are genetically very similar viruses, their killing effect on HIV-infected cells are markedly different. VSVΔ51 has been shown to be able to infect latently HIV-infected cell lines, latently infected $CD4^+$ T-cell models and persistently infected macrophages. However, cell death following infection was significantly less compared to MG1 induced killing[159,161]. Hence, evaluating whether SMAC mimetics can enhance VSVΔ51 induced killing was one of the objectives of this thesis. It was seen that in the latently HIV-infected cell line OM10.1, while VSVΔ51 alone was unable to induce killing, using the SMAC mimetics LCL-

161 or birinapant alongside VSVΔ51 significantly increased cell death. This effect was not seen when VSVΔ51 was combined with AEG 40730. Differences in the outcome of combination treatment with VSVΔ51 and SMAC mimetics may be attributed to the different structures of the SMAC mimetics and their binding efficiencies to their target IAP proteins. The increase in cell death was not accompanied with an increase in infection.

Following the data from cell lines, HIV-infected MDM were treated with the combination of VSVΔ51 and the SMAC mimetics LCL-161 or birinapant. Interestingly, in the bulk cell population, and the HSA+ and HSA- fractions, while there was no cell death in VSVΔ51 infected cells, there was a significant increase in cell death when VSVΔ51 was combined with either SMAC mimetic. The percent cell death was higher than that of combination with MG1 and SMAC mimetics as well (in the case of LCL + MG1 mean cell death in the HSA+ fraction, is around 40% whereas for LCL+VSVΔ51 this was around 60%). This increase in cell death was accompanied by a trend in decrease of proviral HIV DNA. These results show that while VSVΔM51 and SMAC mimetics were unable to kill cells on their own, SMAC mimetics can be used as viral sensitizers to enhance VSVΔM51 mediated cell death.

Next, the role of TNFα was once again investigated. It was seen that VSVΔ51 infected cells or cells treated with VSVΔ51 in combination with SMAC mimetics produced TNFα at much higher levels compared to that of infection with MG1. Hence, the higher amount of TNFα present in the cell culture when cells are treated with SMAC mimetics plus VSVΔ51 may be one of the contributing factors of higher amounts of cell death compared to SMAC mimetics plus MG1. Still, the exact role of TNFα remains to be elucidated.

Lastly, the role of IFNα in combination treatment with VSVΔ51 and SMAC mimetics was evaluated. Interestingly, there was a slight but not statistically significant decrease in the amount

of IFNα produced when VSVΔ51 was used in combination with either LCL-161 or birinapant. Hence, it could be that the decrease in IFNα upon combination treatment may be one of the reasons why cell killing is not observed when cells are only infected by VSVΔ51, but is observed in combination treatment.

Overall, it was shown that SMAC mimetics can increase MG1 and VSVΔ51 mediated cell death in HIV-infected MDM. Oncolytic virus infection and combination treatment results in the production of TNFα, which is one of the drivers of cell death but is not the only mediator. Furthermore, SMAC mimetic treatment slightly dampens the IFNα production induced by VSVΔ51 infection, which may be one of the reasons why VSVΔ51 mediated killing is increased in combination treatment. These results show that using SMAC mimetics alongside oncolytic viruses to kill HIV-infected MDM is a viable option to enhance oncolytic virus mediated killing.

6.4. Pseudotyping MG1 with HIV envelope protein

MG1 mainly uses the LDL receptor for viral entry, granting it broad tropism[145]. This is a useful trait from a cancer perspective as this means MG1 can be used to target many different types of cancer[150,152,294]. Since engineering oncolytic viruses such as VSVΔ51 and MG1 are relatively straightforward and have been done extensively to change their tropism[250,251], vaccine development, and delivering agents such as cytokines and chemokines to their targets[149,239,240], it was hypothesized that the tropism of MG1 can be changed via pseudotyping it with the HIV envelope protein gp160 and modified versions of gp160.

Studies on VSV has shown that there is a signal at the gp41 portion of gp160 which prevents incorporation of gp160 to VSV virions[250] implying that this portion needs to be removed or replaced for the pseudotyping to work successfully. This finding is confirmed in another study

where VSV pseudotyped with a fusion protein composed of gp120 with the CT tail of VSV G glycoprotein to generate rhabdo-immunodeficiency virus (RhIV) has been shown to infect human osteosarcoma cells that display CD4 and CCR5 receptors, and transgenic mice that express human CD4 and CCR5 in mouse $CD4^+$ T-cells[295]. RhIV was also able to result in a significant decrease in $CD4^+$ T-cells 4 days post infection when transgenic mice that express human CD4 and CCR5 receptors and lack the IFNAR receptor were infected via intraperitoneal injection[295]. In the same study, immunocompetent transgenic mice were also able to be infected with RhIV with varying degrees.

The classical VSV rescue protocol requires infection of cells with T7 polymerase expressing vaccinia virus, then subsequent transfection of cells with VSV N. P, L single gene plasmids along with full length VSV plasmid. All of the transfected plasmids are under the control of T7 promoter, thus the vaccinia infection is required to drive the transcription of VSV plasmids[265]. Although other protocols have been established which do not require infection with T7 expressing vaccinia virus, but do require cells that have been transfected to express T7 polymerase[296,297], these protocols have not been used in this work. Following transfection, cells are incubated for 48h, until cell death can be seen, the supernatants are collected and vaccinia virus filtered out via the use of a 0.22µM syringe filter, and the supernatant is used to further infect cells and thus amplify the newly rescued virus.

Clones of MG1 containing full length gp160, truncated gp160, and gp120 fused to MG1 G CT tail were generated by either restriction enzyme cloning or the PCR based cloning technique Gibson assembly. The HIV envelope chosen was from the p96zm651 envelope expression plasmid, yielding a CCR5 tropic HIV envelope. Following the generation of clones, the plasmids were sent to full length plasmid sequencing, and the plasmids were verified to not contain any

insertions, deletions, or other mutations that might cause a frameshift in the reading frame, early termination or amino acid sequence change. To rescue the pseudotyped MG1 clones, the classical VSV reverse genetics rescue system was employed. Vero cells were infected with T7 vaccinia, and transfected with MG1 single gene plasmids along with the modified MG1 backbone. After 48h, the supernatant was collected and filtered, and passed on to GHOST cells that express CD4 and CCR5. Unfortunately, the rescue using this protocol was unsuccessful.

Next, each step of the VSV rescue protocol was changed to see if the changes would result in a pseudotyped MG1 virus. The first step that was changed was the MOI of vaccinia virus. Studies by Yang et al., show that MOI of vaccinia virus used in VSV rescues determine the efficiency of the rescue, and that MOI 5 of vaccinia virus was the most efficient in their rescue of mCherry expressing VSV vector, as measured by the detection of mCherry when using the BSR-T7 cell line[298]. However, in the MG1 rescue protocol, it was observed that MOI 5 of vaccinia virus infection was killing the cells before they had a chance to produce the virus, as Vero cells used in the MG1 rescue protocol do not produce type 1 interferons and therefore are very permissive to most viral infections[299]. Experiments using WT MG1 showed that using a lower MOI such as MOI 1 results in viral production whereas higher MOIs do not. Unfortunately, changing the vaccinia virus MOI did not result in production of psedutoyped MG1.

Following this, GHOST cells were used for the viral rescues instead of Vero cells, as it was hypothesized that perhaps the pseudotyped MG1 virions are being produced but the lack of CD4 and CCR5 receptors on Vero cells block re-infection and result in the death of any produced virion. For this protocol, MOI 1 was chosen along with 24h incubation time following transfection, as this combination proved to work for the rescue of WT MG1. When this did not work, extra single gene plasmids were added to the transfection mix rather than the standard N, P, and L. The first thing

that was considered was the total size of the MG1 clone constructs. It was hypothesized that since N nucleoprotein wrapping the genome of VSV is required for the binding of RdRp to start transcription[300], and that MG1 containing HIV envelope has a larger genome size than WT MG1, more N protein may be required to kick-start the transcription. Hence, the amount of N single gene plasmid was increased in the transfection but this change did not result in production of infectious virions. Next, extra HIV envelope expression plasmid was added to the rescue with the intent of increasing incorporation efficiency of HIV envelope into the virion, along with adding in extra HIV envelope expression plasmid with extra N single gene plasmid, which where again unsuccessful.

The next thing hypothesized was to see if increasing transfection efficiency could help in viral production. To do this, HEK 293T cells were used for transfection. Along with this, different transfection reagents such as Fugene, Fugene 4K, and GeneJuice, were used to transfect cells. Although transfection was verified by the presence of GFP under confocal microscopy, when the supernatant was transferred to GHOST cells to amplify the virus, no infectious virions could be obtained.

Lasty, a HEKTrex cell system that produces VSV G upon stimulation with doxycycline was used for the rescue to aid budding off viruses with the presence of VSV G. This cell rescue system has been shown to work in rescuing G-less MG1 virus[301]. However, similar to previous optimizations, no infectious virions were obtained.

In all these trials, although transfection could be confirmed via the presence of GFP, infectious virions did not form. This suggests that the problem steps are most likely:

1. Transcription and translation of HIV envelope protein
2. Accurate processing of HIV envelope protein

3. Budding and subsequent infection

- Transcription and translation of HIV envelope protein

Although appropriate start/stop codons were added and rhabdovirus specific start stop sequences were present in each intergenic region, it might be that the Maraba virus transcription machinery is not equipped to efficiently handle the transcription of HIV envelope protein inserts. The full length, truncated, or fused to MG1 G CT tail (869 amino acids (aa), 715 aa and 742 aa respectively) are significantly longer than the native MG1 G glycoprotein at 513 amino acids. Moreover, it has been shown that using synonymous codons to disrupt homopolymeric sequences greater than 4 nucleotides has significantly improved the genetic stability of VSV-env[245], which was not done in this study. Although there must be some translation of the HIV env since GFP was detected at the transfected cells, which lies downstream of the HIV envelope, the amount produced may not be enough for sufficient incorporation and budding.

- Accurate processing of HIV envelope protein

Upon being translated, HIV env gp160 is targeted to go to the rough endoplasmic reticulum surface by a signal in its N terminal domain. A 'stop-transfer' signal present in the CT tail of the gp41 portion of env prevents gp160 to be fully internalized into the ER lumen, which situates the gp120 portion to be inside the ER to get glycosylated with *N*- and *O*-linked oligosaccharide chains, whereas a portion of gp41 stays in the cytoplasm. Inside the ER, gp160 oligomerizes into trimers, which triggers gp160 to be trafficked to the Golgi complex[302]. Here, gp160 gets cleaved into its mature form via furin and furin-like proteases at highly conserved K/R-X-K/R-R motif[303]. This cleavage results in gp120, the surface portion of the glycoprotein and gp41, the transmembrane

portion of the glycoprotein. Following this step, gp120 and gp41 remain bound via non-covalent interactions, forming the heterotrimeric mature HIV envelope. Env is rapidly recycled after its arrival to the cellular membrane by endocytosis, and some gp120 is shed. This results in about 10 envelope particles getting incorporated per virion[304].

Since the MG1 clone containing the full length HIV envelope does have gp41, its targeting to the ER lumen might not have caused an issue. However, VSV and MG1 replication cycle is much faster than that of HIV, which means that the error prone RdRp might introduce errors to env, resulting in inaccurate targeting[295]. In case of the truncated clone and the env-MG1 G fusion clone, neither have the 'stop-tranfer' signal present in the CT tail of gp41, which might have caused the glycoprotein to fully enter the ER, preventing it from getting further processed or incorporated in to the virions.

According to The Human Protein Atlas, HEK293T cells and derivates, and GHOST cells do express furin[305]. Similarly, Vero cells express furin as well, as studies show that Vero cells can be used for a SARS-CoV-2 model, where the S protein gets cleaved into S1 and S2 subunits via furin[306]. Studies that have pseudotpyed VSV with env show that transferring the supernatant following transfection into HEK cells that overexpress furin yields higher titers of the pseudotyped VSV, and the resulting env trimers can elicit an antibody response[251]. This suggests that if env was properly targeted to the Golgi apparatus to get cleaved, the cell lines used to transfect and amplify the virus are appropriate choices as they all express furin. However, using a cell line that overexpresses furin might have helped in processing of env.

- Budding and subsequent infection

Although all research regarding pseudotyping has been done with VSV and not Maraba virus, the two are genetically similar[146], allowing us to extrapolate the information from VSV to be used to study Maraba virus. G-less rhabdoviruses can still bud off from cell, but the presence of G glycoprotein CT tail results in more efficient budding[307]. Studies using pseudotpyed VSV with env show that VSV G tail is required for incorporation of HIV env. The reason for this might be that the cytoplasmic domain of env might be too long to incorporated into the VSV virion or that there is a signal at the tail of env that directs its localization away from sites of VSV budding. It was also shown that the incorporation of env is much lower compared to VSV G to the virions which might be due to gp160 targeting to the cell surface (detected at 8h post infection) being slower than VSV G (detected at 4 hours post infection). Lastly, viral titer of pseudotyped VSV has been shown to be 10-fold lower than wildtype[249].

Taken together, these studies suggest even if HIV envelope or envelope-G fusion were properly processed, they might have localized at sites different than were MG1 would bud off, the glycoprotein might have been too long to be incorporated into MG1, and even if the virus assembly was properly achieved, it might have resulted in a lower titer of virus. Since the cell type used to amplify the virus does have intact interferon signaling, the cells might have mounted an interferon response, resulting in the eradication of pseudotyped virus.

6.4.1 An ideal world – would MG1 pseudotyped with HIV envelope be able to kill latently HIV-infected cells?

To date, MG1 has never been pseudotyped with another viral protein, so concerns raised here will be based on experiments done with VSV. VSV pseudotyped with HIV envelope has been shown to successfully target $CD4^+$ T-cells[249,295]. In the case of clones produced in this work, a CCR5 tropic HIV envelope was chosen to pseudotype MG1. Since HIV can use CCR5 and CXCR4

co-receptors and these co-receptors are differentially expressed on the target cells of HIV[308], to fully infect all cells that harbor HIV, pseudotyped viruses with different tropisms might have to be made.

Although it is hard to say what the viral production rate would be for MG1 pseudotyped with env, if it follows the same pattern as VSV and the titer is lower compared to WT, viral sensitizers that boost the viral production and aid in MG1 killing might need to be used. As shown in previous chapters in this thesis, SMAC mimetics might be a good candidate to use alongside to increase killing.

Studies done with VSV-env showed that when humanized mice wereinfected with the virus, clearance of the infection conferred protection against re-infection and even though high titers of HIV env binding antibodies were found, a B-cell response was not required for protection[295]. In another study, VSV pseudotyped with env was able to stimulate potent protective antibody responses against HIV env, including neutralizing antibodies[245]. These studies suggest that if MG1 pseudotyped with HIV env is used to kill HIV-infected cells rather than a vaccine agent, a neutralizing antibody response might be generated, decreasing the effectiveness of the virus.

6.5 Future directions

6.5.1 Increasing the specificity of MG1

Although pseudotyping a virus is one way to change its specificity, it is not the only way. MG1 can be genetically engineered to selectively replicate in cells that contain HIV proteins. For example, HIV protease cleavage site can be inserted to the intergenic or intragenic regions of the MG1 genome. Heilmann et al., have successfully introduced autocatalytically active cleavage sites

to the P gene or between the GFP and L genes of allowing the virus to have an ON/OFF switch for VSV replication. As such, virus replication can be enabled or inhibited using protease inhibitor depending on the viral construct. In the ON construct, the P gene autocatalytically gets cleaved without the protease inhibitor, and VSV cannot replicate. This construct was evaluated *in vivo* using mice with U87 tumor xenografts. When mice were injected with VSV-Pprot-GFP along with the protease inhibitors amprenavir (APV) and ritonavir (RTV) a decrease in tumor size and increased survival was observed. In another construct, the protease dimer was inserted between the reporter GFP and L, effectively fusing these genes together. With the addition of protease inhibitor, the fused GFP and L genes cannot separate and become functionally inactive, and the virus cannot replicate. In NOD-SCID mice with subcutaneous G62 glioblastoma xenografts, Prot-OFF viral injections resulted in neurotoxicity 15 days post injection. However, this neurotoxicity was less compared to mice injected with WT VSV. The addition of protease inhibitor successfully stopped viral replication, resulting in no neurotoxicity but loss of tumor control[309].

As evidenced by this study, using MG1 engineered to have autocatalytic cleavage sites may work to control its replication in tissues that carry the target cells of HIV. Using an engineered MG1 virus that could be switched on/off or that has specific tropism for certain cells along with SMAC mimetics would enhance the combination therapies effectiveness and specificity, therefore allowing for an easier transition to the clinic.

6.5.2 Testing combination therapy with MG1 and SMAC mimetics in other HIV infection models

Another important cell model that can be used to expand upon the work of this thesis is latently infected $CD4^+$ T-cells. Our research group has previously utilized the CCL19 latent infection model, where resting $CD4^+$ T-cells from healthy donors are treated with CCL19 to

enhance nuclear localization and integration of HIV, and then spinoculated with HIV[159,310]. It was shown that there was a significant decrease in integrated proviral HIV DNA upon treatment with MG1. Furthermore, the capacity of MG1 to eradicate latently infected $CD4^+$ T-cells from PLHIV on cART was demonstrated via a decrease in viral outgrowth and HIV *gag* RNA following MG1 infection of isolated $CD4^+$ T-cells.

SMAC mimetics have also been shown to selectively kill HIV-infected $CD4^+$ T-cells in several different studies[232,311]. Hence, combining SMAC mimetics with MG1 to kill latently infected $CD4^+$ T-cells would be the best next move to evaluate the effects of combination therapy in all relevant latently HIV-infected cell types.

6.5.3 Testing MG1 in animal models for HIV study

In order to translate combination therapy with MG1 from the laboratory to the clinic, its effect on *in vivo* HIV infection models must be evaluated. The two main animal models used to study HIV are humanized mice and non-human primates. Humanized mice are generally the first choice to move studies *in vivo*. Even though NHP models have a more similar physiology to humans, there are several barriers in using them such as cost, ethics, and restriction factors[312].

Humanized mice usually come from an immunocompromised background and are engrafted with human cells or tissues to form a human-like immune system. Currently, our research group is testing MG1 therapy in humanized cord blood cardiac surgery thymus (CCST) mice. This is a NOD/SCID/IL2rγ^{null} background mouse model, meaning its non-obese diabetic, lacks mature B and T cells and does not have NK cell activity, that is engrafted with cord blood derived $CD34^+$ cells and allogeneic pediatric thymus tissue. CCST mice have been shown to have 60% hCD45+ reconstitution in the blood at 5 weeks post humanization (wph). Furthermore, $hCD3^+$

cells could be detected after 2 wph at around 3.6%, which then gradually increased. The T-cell function of CCST mice were verified with allogeneic human tumor challenge and *ex vivo* PHA-dependent stimulation assay. Most importantly, CCST mice were able to support HIV infection and generate HIV-specific T-cell responses. The infection was able to be controlled with cART treatment, and upon treatment cessation, virus could be detected in the blood, showing that CCST mouse model can be used as a model for HIV persistence.

Our research group has assessed the tolerability of MG1 in HIV uninfected CCST mice. Although MG1 can be tolerated in healthy mice[144] at doses up to $1x10^8$, it is important for the safety of MG1 to be evaluated in this immunocompromised mouse model. Unfortunately, MG1 that was administered via IV at $1x10^6$ pfu showed systemic infection and poor tolerability. Hence, the intraperitoneal (IP) administration route was investigated. MG1 administered at doses $1x10^6$ pfu and $1x10^8$ pfu showed improved survival rates compared to the IV administration, with 4/6 mice reaching endpoint. The two mice that did not reach endpoint were older than their cohorts, implying that age of the CCST mice is an important factor in determining their tolerability to MG1 treatment (unpublished). Currently, the safety of multiple doses of MG1 in HIV uninfected CCST mice, as well as the effect of MG1 on HIV-infected and cART treated CCST mice are undergoing investigation. The results of this study will give us insight on MG1's distribution in the CCST mice model following infection, its tolerability in HIV-infected and cART treated CCST mice, and its ability as a potential therapy to eradicate latently HIV-infected cells, allowing us to better modify MG1 to be used in the clinic.

Combination therapy with the OV VSVΔ51 and SMAC mimetics have been shown to increase survivability and decrease tumor size in many different cancer mouse models[237–239].

Hence, the efficacy of combination therapy with MG1 and SMAC mimetics in eradicating latently HIV-infected cells in CCST mice can also be evaluated.

MG1 has already been tested in NHP models as a booster vaccine in the Ad:MG1 strategy for the MAGEA3 antigen along and has shown to be well tolerated and systemically distributed[313]. Furthermore, NHP models are already being widely used in HIV vaccine development, antiretroviral drug development, and microbicide development[314]. Moving forward, evaluating HIV reservoir size in SIV or SHIV-infected NHP models after MG1 treatment will give valuable insights with regards to MG1-based HIV cure strategy.

6.6 Conclusion

The objective of this thesis was to determine whether combination therapy with MG1 and SMAC mimetics can kill HIV-infected cells. As there is no cure for HIV , it is of utmost importance to investigate possible therapies that can eradicate the latently/persistently infected cell populations. It was shown that combination treatment with MG1 and SMAC mimetics result in enhanced killing of HIV-infected cell lines and monocyte derived macrophages. It was also shown that SMAC mimetics can be used to enhance VSVΔ51 mediated killing, which was previously shown to be unable to induce killing in HIV-infected cells. This study opens up the way to show how OV mediated killing of HIV-infected cells can be enhanced and lays the groundwork to use combination treatment in humanized mice models to increase the efficacy of MG1-mediated killing. Using SMAC mimetics to sensitize HIV-infected cells to MG1-mediated killing, provides us with another useful tool in our arsenal to fight HIV infection and hopefully will bring us one step closer to a cure for HIV.

References

1. Brennan, RobertO. & Durack, DavidT. GAY COMPROMISE SYNDROME. *The Lancet* **318**, 1338–1339 (1981).
2. Gottlieb Michael S. *et al.* Pneumocystis carinii Pneumonia and Mucosal Candidiasis in Previously Healthy Homosexual Men. *N. Engl. J. Med.* **305**, 1425–1431 (1981).
3. Barre-Sinoussi, F. *et al.* Isolation of a T-lymphotropic retrovirus from a patient at risk for acquired immune deficiency syndrome (AIDS). *Science* **220**, 868–871 (1983).
4. Gallo, R. *et al.* Isolation of human T-cell leukemia virus in acquired immune deficiency syndrome (AIDS). *Science* **220**, 865–867 (1983).
5. UNAIDS. UNAIDS Fact Sheet 2024. https://www.unaids.org/sites/default/files/media_asset/UNAIDS_FactSheet_en.pdf.
6. Sharp, P. M. & Hahn, B. H. Origins of HIV and the AIDS Pandemic. *Cold Spring Harb. Perspect. Med.* **1**, a006841 (2011).
7. Huet, T., Cheynier, R., Meyerhans, A., Roelants, G. & Wain-Hobson, S. Genetic organization of a chimpanzee lentivirus related to HIV-1. *Nature* **345**, 356–359 (1990).
8. Hirsch, V. M., Olmsted, R. A., Murphey-Corb, M., Purcell, R. H. & Johnson, P. R. An African primate lentivirus (SIVsm) closely related to HIV-2. *Nature* **339**, 389–392 (1989).
9. Vallari, A. *et al.* Confirmation of Putative HIV-1 Group P in Cameroon. *J. Virol.* **85**, 1403–1407 (2011).
10. Seitz, R. Human Immunodeficiency Virus (HIV). *Transfus. Med. Hemotherapy* **43**, 203–222 (2016).

11. Strebel, K. HIV Accessory Proteins versus Host Restriction Factors. *Curr. Opin. Virol.* **3**, 10.1016/j.coviro.2013.08.004 (2013).

12. Humans, I. W. G. on the E. of C. R. to. HUMAN IMMUNODEFICIENCY VIRUS-1. in *Biological Agents* (International Agency for Research on Cancer, 2012).

13. Gifford, L. B. & Melikyan, G. B. HIV-1 Capsid Uncoating Is a Multistep Process That Proceeds through Defect Formation Followed by Disassembly of the Capsid Lattice. *ACS Nano* **18**, 2928–2947 (2024).

14. Simon, V., Ho, D. D. & Karim, A. Q. HIV/AIDS epidemiology, pathogenesis, prevention, and treatment - PMC. https://www.ncbi.nlm.nih.gov/pmc/articles/PMC2913538/.

15. Shaw, G. M. & Hunter, E. HIV Transmission. *Cold Spring Harb. Perspect. Med.* **2**, a006965 (2012).

16. Mehandru, S. *et al.* Primary HIV-1 Infection Is Associated with Preferential Depletion of CD4+ T Lymphocytes from Effector Sites in the Gastrointestinal Tract. *J. Exp. Med.* **200**, 761–770 (2004).

17. Brenchley, J. M. *et al.* CD4+ T Cell Depletion during all Stages of HIV Disease Occurs Predominantly in the Gastrointestinal Tract. *J. Exp. Med.* **200**, 749–759 (2004).

18. Yerly, S. & Hirschel, B. Diagnosing acute HIV infection. *Expert Rev. Anti Infect. Ther.* **10**, 31–42 (2012).

19. Kelley, C. F., Barbour, J. D. & Hecht, F. M. The Relation Between Symptoms, Viral Load, and Viral Load Set Point in Primary HIV Infection. *JAIDS J. Acquir. Immune Defic. Syndr.* **45**, 445–448 (2007).

20. Muema, D. M. *et al.* Association between the cytokine storm, immune cell dynamics, and viral replicative capacity in hyperacute HIV infection. *BMC Med.* **18**, 81 (2020).

21. Demers, K. R. *et al.* Temporal Dynamics of CD8+ T Cell Effector Responses during Primary HIV Infection. *PLoS Pathog.* **12**, e1005805 (2016).

22. Magnitude and kinetics of CD8+ T cell activation during hyperacute HIV infection impacts viral set point - PMC. https://www.ncbi.nlm.nih.gov/pmc/articles/PMC4575777/.

23. Sadanand, S., Suscovich, T. J. & Alter, G. Broadly Neutralizing Antibodies Against HIV: New Insights to Inform Vaccine Design. *Annu. Rev. Med.* **67**, 185–200 (2016).

24. Dashi, A., DeVico, A. L., Lewis, G. K. & Sajadi, M. M. Broadly Neutralizing Antibodies against HIV: Back to Blood - PMC. *Trends Mol. Med.* **25**, 228–240 (2019).

25. Deng, K. *et al.* Broad CTL response is required to clear latent HIV-1 due to dominance of escape mutations. *Nature* **517**, 381–385 (2015).

26. Martínez del Río, J. *et al.* HIV-1 Reverse Transcriptase Error Rates and Transcriptional Thresholds Based on Single-strand Consensus Sequencing of Target RNA Derived From *In Vitro*-transcription and HIV-infected Cells. *J. Mol. Biol.* **436**, 168815 (2024).

27. Le Tuan *et al.* Enhanced CD4+ T-Cell Recovery with Earlier HIV-1 Antiretroviral Therapy. *N. Engl. J. Med.* **368**, 218–230 (2013).

28. Deeks, S. G., Overbaugh, J., Phillips, A. & Buchbinder, S. HIV infection. *Nat. Rev. Dis. Primer* **1**, 1–22 (2015).

29. Kumar, P. Long term non-progressor (LTNP) HIV infection. *Indian J. Med. Res.* **138**, 291–293 (2013).

30. Battistini Garcia, S. A. & Guzman, N. *Acquired Immune Deficiency Syndrome (AIDS) CD4+ Count*. *StatPearls* (2018).

31. McMichael, A. J., Borrow, P., Tomaras, G. D., Goonetilleke, N. & Haynes, B. F. The immune response during acute HIV-1 infection: clues for vaccine development. *Nat. Rev. Immunol.* **10**, 11–23 (2010).

32. Eisele, E. & Siliciano, R. F. Redefining the Viral Reservoirs that Prevent HIV-1 Eradication. *Immunity* **37**, 377–388 (2012).

33. Moar, P., Premeaux, T. A., Atkins, A. & Ndhlovu, L. C. The latent HIV reservoir: current advances in genetic sequencing approaches. *mBio* **14**, e01344-23 (2023).

34. Blankson, J. N., Persaud, D. & Siliciano, R. F. The Challenge of Viral Reservoirs in HIV-1 Infection. *Annu. Rev. Med.* **53**, 557–593 (2002).

35. Wei, X. *et al.* Viral dynamics in human immunodeficiency virus type 1 infection. *Nature* **373**, 117–122 (1995).

36. Soriano-Sarabia, N. *et al.* Quantitation of Replication-Competent HIV-1 in Populations of Resting CD4+ T Cells. *J. Virol.* **88**, 14070-14077. (2014).

37. Chomont, N. *et al.* HIV reservoir size and persistence are driven by T cell survival and homeostatic proliferation. *Nat. Med.* **15**, 893–900 (2009).

38. Simonetti, F. R., Sobolewski, M. D., Fyne, E. & Maldarelli, F. Clonally expanded CD4+ T cells can produce infectious HIV-1 in vivo. *PNAS* **113**, 1883–1888 (2016).

39. Coffin, J. M. & Hughes, S. H. Clonal Expansion of Infected CD4+ T Cells in People Living with HIV. *Viruses* **13**, 2078 (2021).

40. Eriksson, S. *et al.* Comparative Analysis of Measures of Viral Reservoirs in HIV-1 Eradication Studies. *PLoS Pathog.* **9**, (2013).

41. Crowe, S. M. & Sonza, S. HIV-1 can be recovered from a variety of cells including peripheral blood monocytes of patients receiving highly active antiretroviral therapy: a further obstacle to eradication. *J. Leukoc. Biol.* **68**, 345–350 (2000).

42. Ellery, P. J. *et al.* The CD16+ monocyte subset is more permissive to infection and preferentially harbors HIV-1 in vivo. *J. Immunol. Baltim. Md 1950* **178**, 6581–6589 (2007).

43. Veenhuis, R. T. *et al.* Monocyte-derived macrophages contain persistent latent HIV reservoirs. *Nat. Microbiol.* **8**, 833–844 (2023).

44. Shen, R. *et al.* Stromal Down-Regulation of Macrophage CD4/CCR5 Expression and NF-κB Activation Mediates HIV-1 Non-Permissiveness in Intestinal Macrophages. *PLOS Pathog.* **7**, e1002060 (2011).

45. Ganor, Y. *et al.* HIV-1 reservoirs in urethral macrophages of patients under suppressive antiretroviral therapy. *Nat. Microbiol.* **4**, 633–644 (2019).

46. Josefsson, L. *et al.* The HIV-1 reservoir in eight patients on long-term suppressive antiretroviral therapy is stable with few genetic changes over time. *Proc. Natl. Acad. Sci.* **110**, E4987–E4996 (2013).

47. Yukl, S. A. *et al.* A comparison of methods for measuring rectal HIV levels suggests that HIV DNA resides in cells other than CD4+ T cells, including myeloid cells. *AIDS* **28**, 439 (2014).

48. Ho, D. D., Rota, T. R. & Hirsch, M. S. Infection of monocyte/macrophages by human T lymphotropic virus type III. *J. Clin. Invest.* **77**, 1712–1715 (1986).

49. Le Douce, V., Herbein, G., Rohr, O. & Schwartz, C. Molecular mechanisms of HIV-1 persistence in the monocyte-macrophage lineage. *Retrovirology* **7**, 32 (2010).

50. Swingler, S., Mann, A. M., Zhou, J., Swingler, C. & Stevenson, M. Apoptotic killing of HIV-1-infected macrophages is subverted by the viral envelope glycoprotein. *PLoS Pathog.* **3**, 1281–1290 (2007).

51. Busca, A., Saxena, M., Kryworuchko, M. & Kumar, A. Anti-apoptotic genes in the survival of monocytic cells during infection. *Curr. Genomics* **10**, 306–17 (2009).

52. Lambotte, O. *et al.* Persistence of replication-competent HIV in the central nervous system despite long-term effective highly active antiretroviral therapy. *AIDS Lond. Engl.* **19**, 217–218 (2005).

53. Guadalupe, M. *et al.* Viral Suppression and Immune Restoration in the Gastrointestinal Mucosa of Human Immunodeficiency Virus Type 1-Infected Patients Initiating Therapy during Primary or Chronic Infection. *J. Virol.* **80**, 8236–8247 (2006).

54. Zalar, A. *et al.* Macrophage HIV-1 infection in duodenal tissue of patients on long term HAART - PubMed. *Antiviral Res.* **87**, 269–71 (2010).

55. Poles, M. A. *et al.* Lack of decay of HIV-1 in gut-associated lymphoid tissue reservoirs in maximally suppressed individuals. *J. Acquir. Immune Defic. Syndr. 1999* **43**, 65–68 (2006).

56. Chun, T. W. *et al.* Presence of an inducible HIV-1 latent reservoir during highly active antiretroviral therapy. *Proc. Natl. Acad. Sci. U. S. A.* **94**, 13193–13197 (1997).

57. Zhang, H. *et al.* Human immunodeficiency virus type 1 in the semen of men receiving highly active antiretroviral therapy. *N. Engl. J. Med.* **339**, 1803–1809 (1998).

58. Mayer, K. H. *et al.* Persistence of human immunodeficiency virus in semen after adding indinavir to combination antiretroviral therapy. *Clin. Infect. Dis. Off. Publ. Infect. Dis. Soc. Am.* **28**, 1252–1259 (1999).

59. Perelson, A. S. *et al.* Decay characteristics of HIV-1-infected compartments during combination therapy. *Nature* **387**, 188–191 (1997).

60. Veenhuis, R. T., Abreu, C. M., Shirk, E. N., Gama, L. & Clements, J. E. HIV replication and latency in monocytes and macrophages. *Semin. Immunol.* **51**, 101472 (2021).

61. Yuan, N. Y. & Kaul, M. Beneficial and Adverse Effects of cART Affect Neurocognitive Function in HIV-1 Infection: Balancing Viral Suppression against Neuronal Stress and Injury. *J. Neuroimmune Pharmacol. Off. J. Soc. NeuroImmune Pharmacol.* **16**, 90–112 (2021).

62. Clayton, K. L. *et al.* Resistance of HIV-infected macrophages to CD8 T lymphocyte-mediated killing drives immune activation. *Nat. Immunol.* **19**, 475–486 (2018).

63. Hufert, F. T. *et al.* Human Kupffer cells infected with HIV-1 in vivo. *J. Acquir. Immune Defic. Syndr.* **6**, 772–777 (1993).

64. Ko, A. *et al.* Macrophages but not Astrocytes Harbor HIV DNA in the Brains of HIV-1-Infected Aviremic Individuals on Suppressive Antiretroviral Therapy. *J. Neuroimmune Pharmacol.* **14**, 110–119 (2019).

65. Cosenza, M. A., Zhao, M., Si, Q. & Lee, S. C. Human Brain Parenchymal Microglia Express CD14 and CD45 and are Productively Infected by HIV-1 in HIV-1 Encephalitis. *Brain Pathol.* **12**, 442–455 (2006).

66. Fischer-Smith, T. *et al.* CNS invasion by CD14+/CD16+ peripheral blood-derived monocytes in HIV dementia: perivascular accumulation and reservoir of HIV infection. *J. Neurovirol.* **7**, 528–541 (2001).

67. Cribbs, S. K., Lennox, J., Caliendo, A. M., Brown, L. A. & Guidot, D. M. Healthy HIV-1-Infected Individuals on Highly Active Antiretroviral Therapy Harbor HIV-1 in Their Alveolar Macrophages. *AIDS Res. Hum. Retroviruses* **31**, 64–70 (2015).

68. Sierra-Madero, J. G. *et al.* Relationship between load of virus in alveolar macrophages from human immunodeficiency virus type 1-infected persons, production of cytokines, and clinical status - PubMed. *J. Infect. Dis.* **169**, 18–27.

69. Thompson, C. G., Gay, C. L. & Kashuba, A. D. M. HIV Persistence in Gut-Associated Lymphoid Tissues: Pharmacological Challenges and Opportunities - PMC. *AIDS Res. Hum. Retroviruses* **33**, 513–523 (2017).

70. Moretti, S. *et al.* HIV-1–Host Interaction in Gut-Associated Lymphoid Tissue (GALT): Effects on Local Environment and Comorbidities - PMC. *Internatinal J. Mol. Sci.* **24**, (2023).

71. Moron-Lopez, S. *et al.* Tissue-specific differences in HIV DNA levels and mechanisms that govern HIV transcription in blood, gut, genital tract and liver in ART-treated women. *J. Int. AIDS Soc.* **24**, e25738 (2021).

72. Mohammadzadeh, N., Chomont, N., Estaquier, J., Cohen, E. A. & Power, C. Is the Central Nervous System Reservoir a Hurdle for an HIV Cure? *Viruses* **15**, 2385 (2023).

73. Dufour, C. *et al.* Near full-length HIV sequencing in multiple tissues collected postmortem reveals shared clonal expansions across distinct reservoirs during ART. *Cell Rep.* **42**, (2023).

74. Andre, M., Nair, M. & Raymond, A. D. HIV Latency and Nanomedicine Strategies for Anti-HIV Treatment and Eradication. *Biomedicines* **11**, 617 (2023).

75. Zamborlini, A. *et al.* Centrosomal pre-integration latency of HIV-1 in quiescent cells. *Retrovirology* **4**, 63 (2007).

76. Alce, T. M. & Popik, W. APOBEC3G Is Incorporated into Virus-like Particles by a Direct Interaction with HIV-1 Gag Nucleocapsid Protein. *J. Biol. Chem.* **279**, 34083–34086 (2004).

77. Berger, G. *et al.* APOBEC3A Is a Specific Inhibitor of the Early Phases of HIV-1 Infection in Myeloid Cells. *PLoS Pathog.* **7**, e1002221 (2011).

78. Peng, G. *et al.* Myeloid differentiation and susceptibility to HIV-1 are linked to APOBEC3 expression. *Blood* **110**, 393–400 (2007).

79. Lahouassa, H. *et al.* SAMHD1 restricts HIV-1 by reducing the intracellular pool of deoxynucleotide triphosphates. *Nat. Immunol.* **13**, 223–228 (2012).

80. Liu, L. *et al.* A whole genome screen for HIV restriction factors. *Retrovirology* **8**, 94 (2011).

81. Goujon, C. *et al.* Human MX2 is an interferon-induced post-entry inhibitor of HIV-1 infection. *Nature* **502**, 10.1038/nature12542 (2013).

82. Kruize, Z. & Kootstra, N. A. The Role of Macrophages in HIV-1 Persistence and Pathogenesis. *Front. Microbiol.* **10**, 2828 (2019).

83. Yarchoan, R. *et al.* ADMINISTRATION OF 3'-AZIDO-3'-DEOXYTHYMIDINE, AN INHIBITOR OF HTLV-III/LAV REPLICATION, TO PATIENTS WITH AIDS OR AIDS-RELATED COMPLEX. *The Lancet* **327**, 575–580 (1986).

84. Fischl Margaret A. *et al.* The Efficacy of Azidothymidine (AZT) in the Treatment of Patients with AIDS and AIDS-Related Complex. *N. Engl. J. Med.* **317**, 185–191 (1987).

85. Larder, B. A., Darby, G. & Richman, D. D. HIV with reduced sensitivity to zidovudine (AZT) isolated during prolonged therapy. *Science* **243**, 1731–1734 (1989).

86. Volberding, P. A. & Deeks, S. G. Antiretroviral therapy and management of HIV infection. *Lancet Lond. Engl.* **376**, 49–62 (2010).

87. Autran, B. *et al.* Positive effects of combined antiretroviral therapy on CD4+ T cell homeostasis and function in advanced HIV disease. *Science* **277**, 112–116 (1997).

88. Menéndez-Arias, L. & Delgado, R. Update and latest advances in antiretroviral therapy. *Trends Pharmacol. Sci.* **43**, 16–29 (2022).

89. Colloty, J., Teixeira, M. & Hunt, R. Advances in the treatment and prevention of HIV: what you need to know. *Br. J. Hosp. Med.* **84**, 1–9 (2023).

90. Orkin, C. *et al.* Long-acting cabotegravir plus rilpivirine for treatment in adults with HIV-1 infection: 96-week results of the randomised, open-label, phase 3 FLAIR study. *Lancet HIV* **8**, e185–e196 (2021).

91. van Sighem, A. I. *et al.* Life expectancy of recently diagnosed asymptomatic HIV-infected patients approaches that of uninfected individuals. *AIDS Lond. Engl.* **24**, 1527–1535 (2010).

92. Loutfy, M. R. *et al.* Systematic Review of HIV Transmission between Heterosexual Serodiscordant Couples where the HIV-Positive Partner Is Fully Suppressed on Antiretroviral Therapy. *PLoS ONE* **8**, e55747 (2013).

93. Supervie, V., Viard, J.-P., Costagliola, D. & Breban, R. Heterosexual Risk of HIV Transmission per Sexual Act Under Combined Antiretroviral Therapy: Systematic Review and Bayesian Modeling. *Clin. Infect. Dis. Off. Publ. Infect. Dis. Soc. Am.* **59**, 115–122 (2014).

94. Eisinger, R. W., Dieffenbach, C. W. & Fauci, A. S. HIV Viral Load and Transmissibility of HIV Infection: Undetectable Equals Untransmittable. *JAMA* **321**, 451–452 (2019).

95. Hamlyn, E. *et al.* Plasma HIV Viral Rebound following Protocol-Indicated Cessation of ART Commenced in Primary and Chronic HIV Infection. *PLoS ONE* **7**, e43754 (2012).

96. Davey, R. T. *et al.* HIV-1 and T cell dynamics after interruption of highly active antiretroviral therapy (HAART) in patients with a history of sustained viral suppression. *Proc. Natl. Acad. Sci. U. S. A.* **96**, 15109–15114 (1999).

97. Finzi, D. *et al.* Latent infection of CD4+ T cells provides a mechanism for lifelong persistence of HIV-1, even in patients on effective combination therapy. *Nat. Med.* **5**, 512–517 (1999).

98. Siliciano, J. D. *et al.* Long-term follow-up studies confirm the stability of the latent reservoir for HIV-1 in resting CD4+ T cells. *Nat. Med.* **9**, 727–728 (2003).

99. Weichseldorfer, M., Reitz, M. & Latinovic, O. S. Past HIV-1 Medications and the Current Status of Combined Antiretroviral Therapy Options for HIV-1 Patients. *Pharmaceutics* **13**, 1798 (2021).

100. Landovitz, R. J., Scott, H. & Deeks, S. G. Prevention, treatment and cure of HIV infection. *Nat. Rev. Microbiol.* **21**, 657–670 (2023).

101. Dybul, M., Hidalgo, B., Chun, T.-W., Belson, M. & Fauci, A. S. Pilot Study of the Effects of Intermittent Interleukin-2 on Human Immunodeficiency Virus (HIV)–Specific Immune Responses in Patients Treated during Recently Acquired HIV Infection | The Journal of Infectious Diseases | Oxford Academic. *J. Infect. Dis.* **185**, 61 (2002).

102. Prins, J. M., Jurriaans, S., Van Praag, R. M. E., Rieneke, M. E. & Lange, J. M. A. Immuno-activation with anti-CD3 and recombinant human IL-2 in HIV-1-infected patients on potent antiretroviral therapy. *AIDS* **13**, 2405–2410 (1999).

103. Bouchat, S. *et al.* Histone methyltransferase inhibitors induce HIV-1 recovery in resting CD4+ T cells from HIV-1-infected HAART-treated patients. *AIDS* **26**, 1473–1482 (2012).

104. Desimio, M. G., Giuliani, E. & Doria, M. The histone deacetylase inhibitor SAHA simultaneously reactivates HIV-1 from latency and up-regulates NKG2D ligands sensitizing for natural killer cell cytotoxicity. *Virology* **510**, 9–21 (2017).

105. Contreras, X. *et al.* Suberoylanilide Hydroxamic Acid Reactivates HIV from Latently Infected Cells. *J. Biol. Chem.* **284**, 6782–6789 (2009).

106. Gunst, J. D. *et al.* Early intervention with 3BNC117 and romidepsin at antiretroviral treatment initiation in people with HIV-1: a phase 1b/2a, randomized trial. *Nat. Med.* **28**, 2424–2435 (2022).

107. Li, Z., Guo, J., Wu, Y. & Zhou, Q. The BET bromodomain inhibitor JQ1 activates HIV latency through antagonizing Brd4 inhibition of Tat-transactivation. *Nucleic Acids Res.* **41**, 277–287 (2013).

108. Macedo, A. B. *et al.* The HIV Latency Reversal Agent HODHBt Enhances NK Cell Effector and Memory-Like Functions by Increasing Interleukin-15-Mediated STAT Activation. *J. Virol.* **96**, e0037222 (2022).

109. Prins, H. A., Crespo, R., Lungu, C. & Rokx, C. The BAF complex inhibitor pyrimethamine reverses HIV-1 latency in people with HIV-1 on antiretroviral therapy | Science Advances. *Sci. Adv.* **9**, (2023).

110. Andrea J., Natesampillai, S. & Cummins, N. W. Reactivating latent HIV with PKC agonists induces resistance to apoptosis and is associated with phosphorylation and activation of BCL2 - PMC. *PLOS Pathog.* **16**, (2020).

111. Folks, T. M., Justement, J., Kinter, A. & Fauci, A. S. Characterization of a promonocyte clone chronically infected with HIV and inducible by 13-phorbol-12-myristate acetate. | The Journal of Immunology | American Association of Immunologists. *J. Immunol.* **140**, 1117–1122 (1998).

112. Rozman, M., Zidovec-Lepej, S., Jambrosic, K., Babić, M. & Drmić Hofman, I. Role of TLRs in HIV-1 Infection and Potential of TLR Agonists in HIV-1 Vaccine Development and Treatment Strategies. *Pathogens* **12**, 92 (2023).

113. Pasquereau, S., Kumar, A. & Herbein, G. Targeting TNF and TNF Receptor Pathway in HIV-1 Infection: from Immune Activation to Viral Reservoirs - PMC. *Viruses* **9**, 64 (2017).

114. Spina, C. A. *et al.* An In-Depth Comparison of Latent HIV-1 Reactivation in Multiple Cell Model Systems and Resting CD4+ T Cells from Aviremic Patients. *PLoS Pathog.* **9**, e1003834 (2013).

115. Abner, E. & Jordan, A. HIV "shock and kill" therapy: In need of revision. *Antiviral Res.* **166**, 19–34 (2019).

116. Kim, Y., Anderson, J. L. & Lewin, S. R. Getting the "Kill" into "Shock and Kill": Strategies to Eliminate Latent HIV. *Cell Host Microbe* **23**, 14–26 (2018).

117. Pollard, R. B. *et al.* Safety and efficacy of the peptide-based therapeutic vaccine for HIV-1, Vacc-4×: a phase 2 randomised, double-blind, placebo-controlled trial. *Lancet Infect. Dis.* **14**, 291–300 (2014).

118. Sgadari, C. *et al.* Continued Decay of HIV Proviral DNA Upon Vaccination With HIV-1 Tat of Subjects on Long-Term ART: An 8-Year Follow-Up Study. *Front. Immunol.* **10**, (2019).

119. Gay, C. L. *et al.* Immunogenicity of AGS-004 Dendritic Cell Therapy in Patients Treated During Acute HIV Infection. *AIDS Res. Hum. Retroviruses* **34**, 111–122 (2018).

120. García, F. *et al.* A Therapeutic Dendritic Cell-Based Vaccine for HIV-1 Infection. *J. Infect. Dis.* **203**, 473–478 (2011).

121. Haynes, B. F. *et al.* Strategies for HIV-1 vaccines that induce broadly neutralizing antibodies. *Nat. Rev. Immunol.* **23**, 142–158 (2023).

122. Mousseau, G. *et al.* The Tat Inhibitor Didehydro-Cortistatin A Prevents HIV-1 Reactivation from Latency. *mBio* **6**, e00465-15 (2015).

123. Debyser, Z., Vansant, G., Bruggemans, A., Janssens, J. & Christ, F. Insight in HIV Integration Site Selection Provides a Block-and-Lock Strategy for a Functional Cure of HIV Infection - PMC. *Viruses* **11**, 12 (2018).

124. Mendez, C., Ledger, S., Petoumenos, K. & Kelleher, A. D. RNA-induced epigenetic silencing inhibits HIV-1 reactivation from latency - PMC. *Retrovirology* **15**, (2018).

125. Hu, W. *et al.* RNA-directed gene editing specifically eradicates latent and prevents new HIV-1 infection. *Proc. Natl. Acad. Sci.* **111**, 11461–11466 (2014).

126. Kaminski, R. *et al.* Excision of HIV-1 DNA by Gene Editing: A Proof-of-Concept In Vivo Study. *Gene Ther.* **23**, 690–695 (2016).

127. Yin, C. *et al.* In Vivo Excision of HIV-1 Provirus by saCas9 and Multiplex Single-Guide RNAs in Animal Models. *Mol. Ther.* **25**, 1168–1186 (2017).

128. Mancuso, P. *et al.* CRISPR based editing of SIV proviral DNA in ART treated non-human primates. *Nat. Commun.* **11**, 6065 (2020).

129. Xu, L. *et al.* CRISPR-Edited Stem Cells in a Patient with HIV and Acute Lymphocytic Leukemia. *N. Engl. J. Med.* **381**, 1240–1247 (2019).

130. Khamaikawin, W. *et al.* CRISPR/Cas9 genome editing of CCR5 combined with C46 HIV-1 fusion inhibitor for cellular resistant to R5 and X4 tropic HIV-1. *Sci. Rep.* **14**, 10852 (2024).

131. Galluzzi, L., Kepp, O., Hett, E., Kroemer, G. & Marincola, F. M. Immunogenic cell death in cancer: concept and therapeutic implications | Journal of Translational Medicine | Full Text. *J. Transl. Med.* **21**, (2023).

132. Gujar, S. A. & Lee, Pa. W. K. Oncolytic Virus-Mediated Reversal of Impaired Tumor Antigen Presentation - PMC. *Front. Oncol.* **4**, (2014).

133. Yoneyama, M., Onomoto, K., Jogi, M., Akaboshi, T. & Fujita, T. Viral RNA detection by RIG-I-like receptors. *Curr. Opin. Immunol.* **32**, 48–53 (2015).

134. Gujar, S., Pol, J. G. & Kroemer, G. Heating it up: Oncolytic viruses make tumors 'hot' and suitable for checkpoint blockade immunotherapies. *Oncoimmunology* **7**, e1442169 (2018).

135. Santry, L. A. *et al.* Tumour vasculature: Friend or foe of oncolytic viruses? *Cytokine Growth Factor Rev.* **56**, 69–82 (2020).

136. Lin, D., Shen, Y. & Liang, T. Oncolytic virotherapy: basic principles, recent advances and future directions. *Signal Transduct. Target. Ther.* **8**, 156 (2023).

137. Conry, R. M., Westbrook, B., McKee, S. & Norwood, T. G. Talimogene laherparepvec: First in class oncolytic virotherapy. *Hum. Vaccines Immunother.* **14**, 839 (2018).

138. Andtbacka, R. H. I. *et al.* Final analyses of OPTiM: a randomized phase III trial of talimogene laherparepvec versus granulocyte-macrophage colony-stimulating factor in unresectable stage III–IV melanoma. *J. Immunother. Cancer* **7**, 145 (2019).

139. Shalhout, S. Z., Miller, D. M., Emerick, K. S. & Kaufman, H. L. Therapy with oncolytic viruses: progress and challenges. *Nat. Rev. Clin. Oncol.* **20**, 160–177 (2023).

140. Xu, L., Sun, H., Lemoine, N. R., Xuan, Y. & Wang, P. Oncolytic vaccinia virus and cancer immunotherapy. *Front. Immunol.* **14**, 1324744 (2024).

141. Muller, L., Berkeley, R., Barr, T., Ilett, E. & Errington-Mais, F. Past, Present and Future of Oncolytic Reovirus - PMC. *Cancers* **12**, 3219 (2020).

142. Engeland, C. E. & Ungerechts, G. Measles Virus as an Oncolytic Immunotherapy - PMC. *Cancers* **13**, 544 (2021).

143. Orzechowska, B. U., Jędryka, M., Zwolińska, K. & Matkowski, R. VSV based virotherapy in ovarian cancer: the past, the present and …future? *J. Cancer* **8**, 2369–2383 (2017).

144. Breitbach, C. J. Considerations for Clinical Translation of MG1 Maraba Virus. in 285–293 (Humana, New York, NY, 2020). doi:10.1007/978-1-4939-9794-7_19.

145. Finkelshtein, D., Werman, A., Novick, D., Barak, S. & Rubinstein, M. LDL receptor and its family members serve as the cellular receptors for vesicular stomatitis virus. *Proc. Natl. Acad. Sci. U. S. A.* **110**, 7306–11 (2013).

146. Brun, J. *et al.* Identification of genetically modified Maraba virus as an oncolytic rhabdovirus. *Mol. Ther. J. Am. Soc. Gene Ther.* **18**, 1440–9 (2010).

147. Matsui, M. *et al.* Activation of LDL Receptor (LDLR) Expression by Small RNAs Complementary to a Noncoding Transcript that Overlaps the LDLR Promoter - PMC. *Chem. Biol.* **17**, 1244–1355 (2010).

148. Hastie, E. & Grdzelishvili, V. Z. Vesicular stomatitis virus as a flexible platform for oncolytic virotherapy against cancer. *J. Gen. Virol.* **93**, 2529–2545 (2012).

149. Bishnoi, S., Tiwari, R., Gupta, S., Byrareddy, S. & Nayak, D. Oncotargeting by Vesicular Stomatitis Virus (VSV): Advances in Cancer Therapy. *Viruses* **10**, 90 (2018).

150. Le Boeuf, F. *et al.* Oncolytic Maraba Virus MG1 as a Treatment for Sarcoma. *Int. J. Cancer* **141**, 1257–1264 (2017).

151. Bourgeois-Daigneault, M.-C. *et al.* Combination of Paclitaxel and MG1 oncolytic virus as a successful strategy for breast cancer treatment. *Breast Cancer Res.* **18**, 83 (2016).

152. Zhang, J. *et al.* Maraba MG1 virus enhances natural killer cell function via conventional dendritic cells to reduce postoperative metastatic disease. in *Molecular Therapy* vol. 22 1320–1332 (Nature Publishing Group, 2014).

153. Hummel, J. *et al.* Maraba virus-vectored cancer vaccines represent a safe and novel therapeutic option for cats. *Sci. Rep. 2017 71* **7**, 1–12 (2017).

154. Jonker, D. J. *et al.* Phase I study of oncolytic virus (OV) MG1 maraba/MAGE-A3 (MG1MA3), with and without transgenic MAGE-A3 adenovirus vaccine (AdMA3) in incurable advanced/metastatic MAGE-A3-expressing solid tumours: CCTG IND.214. *https://doi.org/10.1200/JCO.2017.35.15_suppl.e14637* **35**, e14637–e14637 (2017).

155. Sandstrom, T. S., Ranganath, N. & Angel, J. B. Impairment of the type I interferon response by HIV-1: Potential targets for HIV eradication. *Cytokine Growth Factor Rev.* **37**, 1–16 (2017).

156. Ranganath, N., Sandstrom, T. S., Fadel, S., Côté, S. C. & Angel, J. B. Type I interferon responses are impaired in latently HIV infected cells. *Retrovirology* **13**, 66 (2016).

157. Brown, A., Zhang, H., Lopez, P., Pardo, C. A. & Gartner, S. In vitro modeling of the HIV-macrophage reservoir. *J. Leukoc. Biol.* **80**, 1127–1135 (2006).

158. Imbeault, M., Lodge, R., Ouellet, M. & Tremblay, M. J. Efficient magnetic bead-based separation of HIV-1-infected cells using an improved reporter virus system reveals that p53 up-regulation occurs exclusively in the virus-expressing cell population. *Virology* **393**, 160–167 (2009).

159. Ranganath, N. Oncolytic viruses as a potential approach to eliminate cells that constitute the latent HIV reservoir. (University of Ottawa, 2018). doi:http://dx.doi.org/10.20381/ruor-21627.

160. Ranganath, N., Sandstrom, T. S., Burke Schinkel, S. C., Côté, S. C. & Angel, J. B. The Oncolytic Virus MG1 Targets and Eliminates Cells Latently Infected With HIV-1: Implications for an HIV Cure. *J. Infect. Dis.* **217**, 721–730 (2018).

161. Sandstrom, T. S. Impairment of the type I interferon response in HIV-infected macrophages facilitates their infection and killing by the oncolytic virus, MG1. (University of Ottawa, 2019).

162. Sandstrom, T. S. *et al.* HIV-Infected Macrophages Are Infected and Killed by the Interferon-Sensitive Rhabdovirus MG1. *J. Virol.* **95**, (2021).

163. Jan, R. & Chaudhry, G.-S. Understanding Apoptosis and Apoptotic Pathways Targeted Cancer Therapeutics. *Adv. Pharm. Bull.* **9**, 205–218 (2019).

164. Bergsbaken, T., Fink, S. L. & Cookson, B. T. Pyroptosis: host cell death and inflammation. *Nat. Rev. Microbiol.* **7**, 99–109 (2009).

165. Yu, P. *et al.* Pyroptosis: mechanisms and diseases. *Signal Transduct. Target. Ther.* **6**, 1–21 (2021).

166. Wei, S., Feng, M. & Zhang, S. Molecular Characteristics of Cell Pyroptosis and Its Inhibitors: A Review of Activation, Regulation, and Inhibitors. *Int. J. Mol. Sci.* **23**, 16115 (2022).

167. Nikoletopoulou, V., Markaki, M., Palikaras, K. & Tavernarakis, N. Crosstalk between apoptosis, necrosis and autophagy. *Biochim. Biophys. Acta* **1833**, 3448–3459 (2013).

168. Bai, L., Smith, D. C. & Wang, S. Small-molecule SMAC mimetics as new cancer therapeutics. *Pharmacol. Ther.* **144**, 82–95 (2014).

169. Füllsack, S., Rosenthal, A., Wajant, H. & Siegmund, D. Redundant and receptor-specific activities of TRADD, RIPK1 and FADD in death receptor signaling. *Cell Death Dis.* **10**, 122 (2019).

170. Morrish, Brumatti, & Silke. Future Therapeutic Directions for Smac-Mimetics. *Cells* **9**, 406 (2020).

171. Kischkel, F. C. *et al.* Cytotoxicity-dependent APO-1 (Fas/CD95)-associated proteins form a death-inducing signaling complex (DISC) with the receptor. *EMBO J.* **14**, 5579–5588 (1995).

172. Dickens, L. S., Powley, I. R., Hughes, M. A. & MacFarlane, M. The 'complexities' of life and death: Death receptor signalling platforms. *Exp. Cell Res.* **318**, 1269–1277 (2012).

173. Beaudouin, J., Liesche, C., Aschenbrenner, S., Hörner, M. & Eils, R. Caspase-8 cleaves its substrates from the plasma membrane upon CD95-induced apoptosis. *Cell Death Differ.* **20**, 599–610 (2013).

174. Saelens, X. *et al.* Toxic proteins released from mitochondria in cell death. *Oncogene* **23**, 2861–2874 (2004).

175. Du, C., Fang, M., Li, Y., Li, L. & Wang, X. Smac, a mitochondrial protein that promotes cytochrome c-dependent caspase activation by eliminating IAP inhibition. *Cell* **102**, 33–42 (2000).

176. Estornes, Y. & Bertrand, M. J. M. IAPs, regulators of innate immunity and inflammation. *Semin. Cell Dev. Biol.* **39**, 106–114 (2015).

177. Cain, K., Brown, D. G., Langlais, C. & Cohen, G. M. Caspase activation involves the formation of the aposome, a large (~700 kDa) caspase-activating complex. *J. Biol. Chem.* **274**, 22686–22692 (1999).

178. Chen, Y.-S. *et al.* Pan-Caspase Inhibitor zVAD Induces Necroptotic and Autophagic Cell Death in TLR3/4-Stimulated Macrophages. *Mol. Cells* **45**, 257–272 (2022).

179. Li, H., Zhu, H., Xu, C. J. & Yuan, J. Cleavage of BID by caspase 8 mediates the mitochondrial damage in the Fas pathway of apoptosis. *Cell* **94**, 491–501 (1998).

180. Silke, J. & Vince, J. IAPs and cell death. in *Current Topics in Microbiology and Immunology* vol. 403 95–117 (Springer Verlag, 2017).

181. Cetraro, P., Plaza-Diaz, J., MacKenzie, A. & Abadía-Molina, F. A Review of the Current Impact of Inhibitors of Apoptosis Proteins and Their Repression in Cancer. *Cancers* **14**, 1671 (2022).

182. Gyrd-Hansen, M. *et al.* IAPs contain an evolutionarily conserved ubiquitin-binding domain that regulates NF-κB as well as cell survival and oncogenesis. *Nat. Cell Biol.* **10**, 1309–1317 (2008).

183. Yang, Y. L. & Li, X. M. The IAP family: Endogenous caspase inhibitors with multiple biological activities. *Cell Res.* **10**, 169–177 (2000).

184. Shiozaki, E. N. *et al.* Mechanism of XIAP-mediated inhibition of caspase-9. *Mol. Cell* **11**, 519–527 (2003).

185. Scott, F. L. *et al.* XIAP inhibits caspase-3 and -7 using two binding sites: Evolutionary conserved mechanism of IAPs. *EMBO J.* **24**, 645–655 (2005).

186. Beug, S. T., Cheung, H. H., LaCasse, E. C. & Korneluk, R. G. Modulation of immune signalling by inhibitors of apoptosis. *Trends Immunol.* **33**, 535–545 (2012).

187. Hu, S. & Yang, X. Cellular inhibitor of apoptosis 1 and 2 are ubiquitin ligases for the apoptosis inducer Smac/DIABLO. *J. Biol. Chem.* **278**, 10055–10060 (2003).

188. Liu, Z. *et al.* Structural basis for binding of Smac/DIABLO to the XIAP BIR3 domain. *Nature* **408**, 1004–1008 (2000).

189. Ye, K., Chen, Z. & Xu, Y. The double-edged functions of necroptosis. *Cell Death Dis.* **14**, 1–12 (2023).

190. Choi, M. E., Price, D. R., Ryter, S. W. & Choi, A. M. K. Necroptosis: a crucial pathogenic mediator of human disease. *JCI Insight* **4**, e128834.

191. Holler, N., Zaru, R., Micheau, Thome, M. & Tschopp, J. Fas triggers an alternative, caspase-8-independent cell death pathway using the kinase RIP as effector molecule - PubMed. *Nat. Immunol.* **1**, 489–495 (2000).

192. Cai, Z., Jitkaew, S., Zhao, J. & Liu, Z.-G. Plasma membrane translocation of trimerized MLKL protein is required for TNF-induced necroptosis. *Nat. Cell Biol.* **16**, 55–65 (2014).

193. Silke, J., Rickard, J. A. & Gerlic, M. The diverse role of RIP kinases in necroptosis and inflammation. *Nat. Immunol.* **16**, 689–697 (2015).

194. Degterev, A. *et al.* Identification of RIP1 kinase as a specific cellular target of necrostatins. *Nat. Chem. Biol.* **4**, 313–321 (2008).

195. Gurung, P., Anand, P. K., Subbarao Malireddi, R. K. & Kanneganti, T.-D. FADD and caspase-8 mediate priming and activation of the canonical and non-canonical Nlrp3 inflammasomes. *J. Immunol.* **192**, 1835–1846 (2014).

196. Kuriakose, T., Man, S. M. & Kanneganti, T.-D. ZBP1/DAI is an innate sensor of influenza virus triggering the NLRP3 inflammasome and programmed cell death pathways - PMC. *Sci. Immunol.* **1**, aag2045. (2016).

197. Hou, J. *et al.* PD-L1-mediated gasdermin C expression switches apoptosis to pyroptosis in cancer cells and facilitates tumour necrosis. *Nat. Cell Biol.* **22**, 1264–1275 (2020).

198. Tsuchiya, K. *et al.* Caspase-1 initiates apoptosis in the absence of gasdermin D. *Nat. Commun.* **10**, 2091 (2019).

199. Sagulenko, V., Vitak, N., Vajjhala, P. R., Vince, J. E. & Stacey, K. J. Caspase-1 Is an Apical Caspase Leading to Caspase-3 Cleavage in the AIM2 Inflammasome Response, Independent of Caspase-8. *J. Mol. Biol.* **430**, 238–247 (2018).

200. Jabea Ekabe, C., Asaba Clinton, N., Agyei, E. K. & Kehbila, J. Role of Apoptosis in HIV Pathogenesis. *Adv. Virol.* **2022**, (2022).

201. Pan, T. *et al.* Necroptosis Takes Place in Human Immunodeficiency Virus Type-1 (HIV-1)-Infected CD4+ T Lymphocytes. *PLoS ONE* **9**, e93944 (2014).

202. Doitsh, G. *et al.* Cell death by pyroptosis drives CD4 T-cell depletion in HIV-1 infection. *Nature* **505**, 509–514 (2014).

203. Bartz, S. R. & Emerman, M. Human Immunodeficiency Virus Type 1 Tat Induces Apoptosis and Increases Sensitivity to Apoptotic Signals by Up-Regulating FLICE/Caspase-8. *J. Virol.* **73**, 1956–1963 (1999).

204. Campbell, G. R., Watkins, J. D., Esquieu, D. & Spector, S. A. The C Terminus of HIV-1 Tat Modulates the Extent of CD178-mediated Apoptosis of T Cells*. *J. Biol. Chem.* **280**, 38376–38382 (2005).

205. Yang, Y. *et al.* Monocytes Treated with Human Immunodeficiency Virus Tat Kill Uninfected CD4 + Cells by a Tumor Necrosis Factor-Related Apoptosis-Induced Ligand-Mediated Mechanism. *J. Virol.* **77**, 6700–6708 (2003).

206. Ferrari, A. *et al.* Caveolae-mediated internalization of extracellular HIV-1 tat fusion proteins visualized in real time. *Mol. Ther. J. Am. Soc. Gene Ther.* **8**, 284–294 (2003).

207. López-Huertas, M. R. *et al.* The presence of HIV-1 Tat protein second exon delays fas protein-mediated apoptosis in CD4+ T lymphocytes: a potential mechanism for persistent viral production. *J. Biol. Chem.* **288**, 7626–44 (2013).

208. Sörgel, S., Fraedrich, K. & Schubert, U. Perinuclear localization of the HIV-1 regulatory protein Vpr is important for induction of G2-arrest. *Virology* **432**, 444–451 (2012).

209. Ward, J., Davis, Z., DeHart, J. & Barker, E. HIV-1 Vpr Triggers Natural Killer Cell–Mediated Lysis of Infected Cells through Activation of the ATR-Mediated DNA Damage Response - PMC. *PLOS Pathog.* **5**, (2009).

210. Guenzel, C. A., Herate, C. & Benichou, S. HIV-1 Vpr—a still "enigmatic multitasker". *Front. Microbiol.* **5**, (2014).

211. Zhu, Y., Roshal, M., Li, F., Blackett, J. & Planelles, V. Upregulation of survivin by HIV-1 Vpr. *Apoptosis* **8**, 71–79 (2003).

212. Cummins, N. W. & Badley, A. D. Mechanisms of HIV-associated lymphocyte apoptosis: 2010. *Cell Death Dis.* **1**, e99–e99 (2010).

213. Anand, A. R. & Ganju, R. K. HIV-1 gp120-mediated apoptosis of T cells is regulated by the membrane tyrosine phosphatase CD45. *J. Biol. Chem.* **281**, 12289–12299 (2006).

214. Dold, C. *et al.* Application of interferon modulators to overcome partial resistance of human ovarian cancers to VSV-GP oncolytic viral therapy. *Mol. Ther. Oncolytics* **3**, 16021 (2016).

215. Bridle, B. W. *et al.* HDAC Inhibition Suppresses Primary Immune Responses, Enhances Secondary Immune Responses, and Abrogates Autoimmunity During Tumor Immunotherapy - PMC. *Mol. Ther.* **21**, 887–894 (2013).

216. Yoo, J. Y., Hurwitz, B. S., Bolyard, C. & Kaur, B. Bortezomib-induced unfolded protein response increases oncolytic HSV-1 replication resulting in synergistic, anti-tumor effects - PMC. *Clin. Cancer Res.* (2014) doi:10.1158/1078-0432.CCR-14-0553.

217. Jha, B. K. *et al.* Inhibition of RNase L and RNA-dependent Protein Kinase (PKR) by Sunitinib Impairs Antiviral Innate Immunity. *J. Biol. Chem.* **286**, 26319–26326 (2011).

218. Rodrik-Outmezguine, V. S. *et al.* Overcoming mTOR Resistance Mutations with a New Generation mTOR Inhibitor. *Nature* **534**, 272–276 (2016).

219. Chadi, Z., Sean, P. & Alain, T. Active-site mTOR inhibitors augment HSV1-dICP0 infection in cancer cells via dysregulated eIF4E/4E-BP axis - PMC. *PLOS Pathog.* **14**, e1007264 (2018).

220. Kipp, R. A. *et al.* Molecular targeting of inhibitor of apoptosis proteins based on small molecule mimics of natural binding partners. *Biochemistry* **41**, 7344–7349 (2002).

221. Petersen, S. L. *et al.* Autocrine TNFα Signaling Renders Human Cancer Cells Susceptible to Smac-Mimetic-Induced Apoptosis. *Cancer Cell* **12**, 445–456 (2007).

222. Varfolomeev, E. *et al.* IAP Antagonists Induce Autoubiquitination of c-IAPs, NF-κB Activation, and TNFα-Dependent Apoptosis. *Cell* **131**, 669–681 (2007).

223. Campbell, G. R., To, R. K., Zhang, G. & Spector, S. A. SMAC mimetics induce autophagy-dependent apoptosis of HIV-1-infected macrophages. *Cell Death Dis.* **11**, 1–14 (2020).

224. Laukens, B. *et al.* Smac mimetic bypasses apoptosis resistance in FADD- or caspase-8-deficient cells by priming for tumor necrosis factor α-induced necroptosis. *Neoplasia* **13**, 971–979 (2011).

225. Hanahan, D. & Weinberg, R. A. Hallmarks of cancer: The next generation. *Cell* **144**, 646–674 (2011).

226. Bashyam, M. D. *et al.* Array-based comparative genomic hybridization identifies localized DNA amplifications and homozygous deletions in pancreatic cancer. *Neoplasia* **7**, 556–562 (2005).

227. Zender, L. *et al.* Identification and Validation of Oncogenes in Liver Cancer Using an Integrative Oncogenomic Approach. *Cell* **125**, 1253–1267 (2006).

228. Pache, L. *et al.* BIRC2/cIAP1 is a Negative Regulator of HIV-1 Transcription and Can Be Targeted by Smac Mimetics to Promote Reversal of Viral Latency. *Cell Host Microbe* **18**, 345–353 (2015).

229. Pache, L. *et al.* Pharmacological Activation of Non-canonical NF-κB Signaling Activates Latent HIV-1 Reservoirs In Vivo. *Cell Rep. Med.* **1**, 100037 (2020).

230. Nixon, C. C. *et al.* Systemic HIV and SIV latency reversal via non-canonical NF-κB signalling in vivo. *Nature* **578**, 160–165 (2020).

231. Dashti, A. *et al.* SMAC Mimetic Plus Triple-Combination Bispecific HIVxCD3 Retargeting Molecules in SHIV.C.CH505-Infected, Antiretroviral Therapy-Suppressed Rhesus Macaques. *J. Virol.* **94**, 2021 (2020).

232. Hattori, S. I. *et al.* Combination of a Latency-Reversing Agent With a Smac Mimetic Minimizes Secondary HIV-1 Infection in vitro. *Front. Microbiol.* **9**, 1–14 (2018).

233. Berro, R. *et al.* Identifying the Membrane Proteome of HIV-1 Latently Infected Cells. *J. Biol. Chem.* **282**, 8207–8218 (2007).

234. Campbell, G. R. & Spector, S. A. DIABLO/SMAC mimetics selectively kill HIV-1-infected resting memory CD4 + T cells: a potential role in a cure strategy for HIV-1 infection. *Autophagy* **15**, 744–746 (2019).

235. Caballero, R. E. *et al.* Role of RIPK1 in SMAC mimetics-induced apoptosis in primary human HIV-infected macrophages. *Sci. Rep. 2021 111* **11**, 1–18 (2021).

236. Cai, J. *et al.* Selective replication of oncolytic virus M1 results in a bystander killing effect that is potentiated by Smac mimetics. *Proc. Natl. Acad. Sci. U. S. A.* **114**, 6812–6817 (2017).

237. Beug, S. T. *et al.* Smac mimetics and innate immune stimuli synergize to promote tumor death. *Nat. Biotechnol.* **32**, 182–190 (2014).

238. Kim, D. S. *et al.* Smac mimetics and oncolytic viruses synergize in driving anticancer T-cell responses through complementary mechanisms. *Nat. Commun.* **8**, 1–13 (2017).

239. Beug, S. T. *et al.* Combination of IAP Antagonists and TNF-α-Armed Oncolytic Viruses Induce Tumor Vascular Shutdown and Tumor Regression. *Mol. Ther. Oncolytics* **10**, 28–39 (2018).

240. Li, W. *et al.* Overexpression of Smac by an Armed Vesicular Stomatitis Virus Overcomes Tumor Resistance. *Mol. Ther. - Oncolytics* **14**, 188–195 (2019).

241. Bentley, E. M., Mather, S. T. & Temperton, N. J. The use of pseudotypes to study viruses, virus sero-epidemiology and vaccination. *Vaccine* **33**, 2955–2962 (2015).

242. Condor Capcha, J. M. *et al.* Generation of SARS-CoV-2 Spike Pseudotyped Virus for Viral Entry and Neutralization Assays: A 1-Week Protocol. *Front. Cardiovasc. Med.* **7**, 618651 (2021).

243. Hoffmann, M. *et al.* SARS-CoV-2 Cell Entry Depends on ACE2 and TMPRSS2 and Is Blocked by a Clinically Proven Protease Inhibitor. *Cell* **181**, 271-280.e8 (2020).

244. Powell, T. J., Silk, J. D., Sharps, J., Fodor, E. & Townsend, A. R. M. Pseudotyped Influenza A Virus as a Vaccine for the Induction of Heterotypic Immunity. *J. Virol.* **86**, 13397–13406 (2012).

245. Rabinovich, S. *et al.* A Novel, Live-Attenuated Vesicular Stomatitis Virus Vector Displaying Conformationally Intact, Functional HIV-1 Envelope Trimers That Elicits Potent Cellular and Humoral Responses in Mice. *PLoS ONE* **9**, e106597 (2014).

246. Nie, J., Li, Q. & Wu, J. Quantification of SARS-CoV-2 neutralizing antibody by a pseudotyped virus-based assay. *Nat. Protoc.* **15**, 3699–3715 (2020).

247. Cruz-Cardenas, J. A., Gutierrez, M., Lopez-Arredodo, A. & Brunck, M. E. G. A pseudovirus-based platform to measure neutralizing antibodies in Mexico using SARS-CoV-2 as proof-of-concept |. *Sci. Rep.* **12**, (2022).

248. Cronin, J., Zhang, X.-Y. & Reiser, J. Altering the Tropism of Lentiviral Vectors through Pseudotyping. *Curr. Gene Ther.* **5**, 387–398.

249. Johnson, J. E., Schnell, M. J., Buonocore, L. & Rose, J. K. Specific targeting to CD4+ cells of recombinant vesicular stomatitis viruses encoding human immunodeficiency virus envelope proteins. *J. Virol.* **71**, 5060–8 (1997).

250. Johnson, J. E., Rodgers, W. & Rose, J. K. A Plasma Membrane Localization Signal in the HIV-1 Envelope Cytoplasmic Domain Prevents Localization at Sites of Vesicular Stomatitis Virus Budding and Incorporation into VSV Virions. *Virology* **251**, 244–252 (1998).

251. Jia, M. *et al.* VSV-Displayed HIV-1 Envelope Identifies Broadly Neutralizing Antibodies Class-Switched to IgG and IgA. *Cell Host Microbe* **27**, 963-975.e5 (2020).

252. Perez, V. L., Rowe, T., Justement, J. S., Butera, S. T., June, C. H., & Folks, T. M. An HIV-1-infected T cell clone defective in IL-2 production and Ca2+ mobilization after CD3 stimulation - PubMed. *J. Immunol. Baltim. Md 1950* **147**, 3145–3148 (1991).

253. Butera, S. T. *et al.* Extrachromosomal human immunodeficiency virus type-1 DNA can initiate a spreading infection of HL-60 cells. *J. Cell. Biochem.* **45**, 366–373 (1991).

254. Hwang, L. N., Englund, N. & Pattnaik, A. K. Polyadenylation of Vesicular Stomatitis Virus mRNA Dictates Efficient Transcription Termination at the Intercistronic Gene Junctions. *J. Virol.* **72**, 1805–1813 (1998).

255. Frankish, A., Diekhans, M., Jungreis, I., Tress, M. L. & Flicek, P. GENCODE 2021. *Nucleic Acids Res.* D916-D923. (2021) doi:10.1093/nar/gkaa1087.

256. Ewels, P. A. *et al.* The nf-core framework for community-curated bioinformatics pipelines. *Nat. Biotechnol.* **38**, 276–278 (2020).

257. Love, M., Huber, W. & Anders, S. Moderated estimation of fold change and dispersion for RNA-seq data with DESeq2. *Genome Biol.* **15**, (2014).

258. Zhu, A., Ibrahim, J. G. & Love, M. Heavy-tailed prior distributions for sequence count data: removing the noise and preserving large differences | Bioinformatics | Oxford Academic. *Bioinformatics* **35**, 2084–2092 (2019).

259. Busca, A., Saxena, M. & Kumar, A. Critical role for antiapoptotic Bcl-xL and Mcl-1 in human macrophage survival and cellular IAP1/2 (cIAP1/2) in resistance to HIV-Vpr-induced apoptosis. *J. Biol. Chem.* **287**, 15118–15133 (2012).

260. Magro, M. Programmed cell death in the eradication of HIV-1 infected cells by the oncolytic Maraba virus MG.

261. Bertheloot, D., Latz, E. & Franklin, B. S. Necroptosis, pyroptosis and apoptosis: an intricate game of cell death. *Cell. Mol. Immunol.* **18**, 1106–1121 (2021).

262. Cary, Z. D., Willingham, M. C. & Lyles, D. S. Oncolytic Vesicular Stomatitis Virus Induces Apoptosis in U87 Glioblastoma Cells by a Type II Death Receptor Mechanism and Induces Cell Death and Tumor Clearance In Vivo. *J. Virol.* **85**, 5708 (2011).

263. Hodgins, J. J. *et al.* More than a ligand: PD-L1 promotes oncolytic virus infection via a metabolic shift that inhibits the type I interferon pathway. Preprint at https://doi.org/10.1101/2022.08.31.506095 (2022).

264. Racine, T., Kobinger, G. P. & Arts, E. J. Development of an HIV vaccine using a vesicular stomatitis virus vector expressing designer HIV-1 envelope glycoproteins to enhance humoral responses. *AIDS Res. Ther.* **14**, 55 (2017).

265. Whelan, S. P., Ball, L. A., Barr, J. N. & Wertz, G. T. Efficient recovery of infectious vesicular stomatitis virus entirely from cDNA clones. *Proc. Natl. Acad. Sci. U. S. A.* **92**, 8388–8392 (1995).

266. Christgen, S. *et al.* Identification of the PANoptosome: A Molecular Platform Triggering Pyroptosis, Apoptosis, and Necroptosis (PANoptosis). *Front. Cell. Infect. Microbiol.* **10**, 237 (2020).

267. Harding, H. P. *et al.* Regulated translation initiation controls stress-induced gene expression in mammalian cells. *Mol. Cell* **6**, 1099–1108 (2000).

268. Lin, J. H. *et al.* IRE1 signaling affects cell fate during the unfolded protein response. *Science* **318**, 944–949 (2007).

269. Hassanzadeh, G. *et al.* Characterizing cellular responses during oncolytic maraba virus infection. *Int. J. Mol. Sci.* **20**, (2019).

270. Nguyên, T. L.-A. *et al.* Chemical targeting of the innate antiviral response by histone deacetylase inhibitors renders refractory cancers sensitive to viral oncolysis. *Proc. Natl. Acad. Sci. U. S. A.* **105**, 14981–14986 (2008).

271. Zuo, W., Wakimoto, M., Kozaiwa, N., Kato, H. & Fujita, T. PKR and TLR3 trigger distinct signals that coordinate the induction of antiviral apoptosis. *Cell Death Dis.* **13**, (2022).

272. van ′t Wout, A. B. *et al.* Nef Induces Multiple Genes Involved in Cholesterol Synthesis and Uptake in Human Immunodeficiency Virus Type 1-Infected T Cells. *J. Virol.* **79**, 10053–10058 (2005).

273. Blanc, M. *et al.* Host Defense against Viral Infection Involves Interferon Mediated Down-Regulation of Sterol Biosynthesis. *PLOS Biol.* **9**, e1000598 (2011).

274. Mazar, J. *et al.* Zika virus as an oncolytic treatment of human neuroblastoma cells requires CD24. *PLoS ONE* **13**, e0200358 (2018).

275. Qian, Y. *et al.* Selective degradation of plasmid-derived mRNAs by MCPIP1 RNase. *Biochem. J.* **476**, 2927 (2019).

276. Li, M. *et al.* MCPIP1 inhibits coxsackievirus B3 replication by targeting viral RNA and negatively regulates virus-induced inflammation. *Med. Microbiol. Immunol. (Berl.)* **207**, 27–38 (2018).

277. Molyer, B., Kumar, A. & Angel, J. B. SMAC Mimetics as Therapeutic Agents in HIV Infection. *Front. Immunol.* **12**, (2021).

278. Mantovani, A., Allavena, P., Marchesi, F. & Garlanda, C. Macrophages as tools and targets in cancer therapy. *Nat. Rev. Drug Discov.* **21**, 799–820 (2022).

279. Balasubramanian, V., Wiegeshaus, E. H., Taylor, B. T. & Smith, D. W. Pathogenesis of tuberculosis: pathway to apical localization. *Tuber. Lung Dis.* **75**, 168–178 (1994).

280. Fallows, D., Peixoto, B., Kaplan, G. & Manca, C. Mycobacterium leprae alters classical activation of human monocytes in vitro. *J. Inflamm.* **18**, (2016).

281. Radandish, M., Khalilian, P. & Esmaeil, N. The Role of Distinct Subsets of Macrophages in the Pathogenesis of MS and the Impact of Different Therapeutic Agents on These Populations. *Front. Immunol.* **12**, (2021).

282. Lecis, D. *et al.* Smac mimetics induce inflammation and necrotic tumour cell death by modulating macrophage activity. *Cell Death Dis.* **4**, e920 (2013).

283. Stutz, M. D. *et al.* Macrophage and neutrophil death programs differentially confer resistance to tuberculosis. *Immunity* **54**, 1758-1771.e7 (2021).

284. Nakatsumi, H., Matsumoto, M. & Nakayama, K. Noncanonical Pathway for Regulation of CCL2 Expression by an mTORC1-FOXK1 Axis Promotes Recruitment of Tumor-Associated Macrophages: *Cell Rep.* **21**, 2471–2486 (2017).

285. Miller, G. C. & Fraser, N. W. Role of the immune response during neuro-attenuated herpes simplex virus-mediated tumor destruction in a murine intracranial melanoma model. *Cancer Res.* **60**, 5714–5722 (2000).

286. Hodgins, J. J. *et al.* PD-L1 promotes oncolytic virus infection via a metabolic shift that inhibits the type I IFN pathway. *J. Exp. Med.* **221**, e20221721 (2024).

287. Porichis, F. *et al.* Responsiveness of HIV-specific CD4 T cells to PD-1 blockade. *Blood* **118**, 965–974 (2011).

288. Kaufmann, D. E., Kavanagh, D. G., Pereyra, F. & Walker, B. D. Upregulation of CTLA-4 by HIV-specific CD4+ T cells correlates with disease progression and defines a reversible immune dysfunction. *Nat. Immunol.* **8**, 1246–1244 (2007).

289. Velu, V. *et al.* Enhancing SIV-Specific Immunity In Vivo by PD-1 Blockade. *Nature* **458**, 206–210 (2009).

290. Finnefrock, A. C. *et al.* PD-1 blockade in rhesus macaques: impact on chronic infection and prophylactic vaccination. *J. Immunol. Baltim. Md 1950* **182**, 980–987 (2009).

291. Trabattoni, D. *et al.* B7-H1 is up-regulated in HIV infection and is a novel surrogate marker of disease progression. *Blood* **101**, 2514–2520 (2003).

292. Said, E. A. *et al.* Programmed death-1–induced interleukin-10 production by monocytes impairs CD4+ T cell activation during HIV infection. *Nat. Med.* **16**, 452–459 (2010).

293. Boasso, A. *et al.* PDL-1 upregulation on monocytes and T cells by HIV via type I interferon: restricted expression of type I interferon receptor by CCR5-expressing leukocytes. *Clin. Immunol. Orlando Fla* **129**, 132–144 (2008).

294. Tong, J. G. *et al.* Spatial and temporal epithelial ovarian cancer cell heterogeneity impacts Maraba virus oncolytic potential. *BMC Cancer* **17**, 594 (2017).

295. Liberatore, R. A. *et al.* Rhabdo-immunodeficiency virus, a murine model of acute HIV-1 infection. *eLife* **8**, (2019).

296. Harty, R. N., Brown, M. E., Hayes, F. P., Wright, N. T. & Schnell, M. J. Vaccinia virus-free recovery of vesicular stomatitis virus. *J. Mol. Microbiol. Biotechnol.* **3**, 513–517 (2001).

297. Garbutt, M. *et al.* Properties of Replication-Competent Vesicular Stomatitis Virus Vectors Expressing Glycoproteins of Filoviruses and Arenaviruses. *J. Virol.* **78**, 5458–5465 (2004).

298. Yang, F. *et al.* The Multiplicity of Infection of Recombinant Vaccinia Virus Expressing the T7 RNA Polymerase Determines the Rescue Efficiency of Vesicular Stomatitis Virus. *Front. Microbiol.* **13**, 846426 (2022).

299. Emeny, J. M. & Morgan, M. J. Regulation of the Interferon System: Evidence that Vero Cells have a Genetic Defect in Interferon Production | Microbiology Society. *J. Gen. Virol.* **43**, 247–252 (1979).

300. Green, T. J. *et al.* Study of the Assembly of Vesicular Stomatitis Virus N Protein: Role of the P Protein. *J. Virol.* **74**, 9515–9524 (2000).

301. Wedge, M.-E. *et al.* Virally programmed extracellular vesicles sensitize cancer cells to oncolytic virus and small molecule therapy. *Nat. Commun.* **13**, 1898 (2022).

302. Checkley, M. A., Luttge, B. G. & Freed, E. O. HIV-1 envelope glycoprotein biosynthesis, trafficking, and incorporation. *J. Mol. Biol.* **410**, 582–608 (2011).

303. Freed, E. O., Myers, D. J. & Risser, R. Mutational analysis of the cleavage sequence of the human immunodeficiency virus type 1 envelope glycoprotein precursor gp160. *J. Virol.* **63**, 4670–4675 (1989).

304. Zhu, P. *et al.* Electron tomography analysis of envelope glycoprotein trimers on HIV and simian immunodeficiency virus virions. *Proc. Natl. Acad. Sci. U. S. A.* **100**, 15812–15817 (2003).

305. Cell line - FURIN - The Human Protein Atlas. https://www.proteinatlas.org/ENSG00000140564-FURIN/cell+line.

306. Minami, S. *et al.* Vero cell-adapted SARS-CoV-2 strain shows increased viral growth through furin-mediated efficient spike cleavage. *Microbiol. Spectr.* **12**, e02859-23 (2024).

307. Robison, C. S. & Whitt, M. A. The Membrane-Proximal Stem Region of Vesicular Stomatitis Virus G Protein Confers Efficient Virus Assembly. *J. Virol.* **74**, 2239–2246 (2000).

308. Bleul, C. C., Wu, L., Hoxie, J. A., Springer, T. A. & Mackay, C. R. The HIV coreceptors CXCR4 and CCR5 are differentially expressed and regulated on human T lymphocytes. *Proc. Natl. Acad. Sci.* **94**, 1925–1930 (1997).

309. Heilmann, E. *et al.* Chemogenetic ON and OFF switches for RNA virus replication. *Nat. Commun.* **12**, 1362 (2021).

310. Cameron, P. U. *et al.* Establishment of HIV-1 latency in resting CD4+ T cells depends on chemokine-induced changes in the actin cytoskeleton. *Proc. Natl. Acad. Sci. U. S. A.* **107**, 16934 (2010).

311. Campbell, G. R., Bruckman, R. S., Chu, Y. L., Trout, R. N. & Spector, S. A. SMAC Mimetics Induce Autophagy-Dependent Apoptosis of HIV-1-Infected Resting Memory CD4+ T Cells. *Cell Host Microbe* **24**, 689-702.e7 (2018).

312. Gillgrass, A., Wessels, J. M., Yang, J. X. & Kaushic, C. Advances in Humanized Mouse Models to Improve Understanding of HIV-1 Pathogenesis and Immune Responses. *Front. Immunol.* **11**, (2021).

313. Pol, J. G. *et al.* Preclinical evaluation of a MAGE-A3 vaccination utilizing the oncolytic Maraba virus currently in first-in-human trials. *Oncoimmunology* **8**, (2019).

314. Van Rompay & A, K. K. Tackling HIV and AIDS: contributions by non-human primate models. *Lab Anim.* **46**, 259–270 (2017).